

**DEVELOPMENT OF PEDOT-PSS/ZEOLITE COMPOSITE  
AS A GAS SENSOR**

Pojjawan Chanthaanont

A Dissertation Submitted in Partial Fulfilment of the Requirements  
for the Degree of Doctor of Philosophy  
The Petroleum and Petrochemical College, Chulalongkorn University  
in Academic Partnership with  
The University of Michigan, The University of Oklahoma,  
and Case Western Reserve University  
2017

บทคัดย่อและแฟ้มข้อมูลฉบับเต็มของวิทยานิพนธ์ตั้งแต่ปีการศึกษา 2554 ที่ให้บริการในคลังปัญญาจุฬาฯ (CUIR)  
เป็นแฟ้มข้อมูลของนิสิตเจ้าของวิทยานิพนธ์ที่ส่งผ่านทางบัณฑิตวิทยาลัย

The abstract and full text of theses from the academic year 2011 in Chulalongkorn University Intellectual Repository (CUIR)  
are the thesis authors' files submitted through the Graduate School.

**Thesis Title:** Development of PEDOT-PSS/Zeolite Composite as a Gas Sensor  
**By:** Pojjawan Chanthaanont  
**Program:** Polymer Science  
**Thesis Advisor:** Prof. Anuvat Sirivat

---

Accepted by The Petroleum and Petrochemical College, Chulalongkorn University, in partial fulfilment of the requirements for the Degree of Doctor of Philosophy.

..... College Dean  
(Asst. Prof. Pomthong Malakul)

**Thesis Committee:**

..... (Asst. Prof. Pomthong Malakul)	..... (Prof. Anuvat Sirivat)
..... (Assoc. Prof. Ratana Rujiravanit)	..... (Asst. Prof. Kitipat Siemanond)

.....  
(Dr. Sumonman Niamlang)

## ABSTRACT

4982008063: Polymer Science Program

Pojjawan Chanthaanont: Development of PEDOT-PSS/Zeolite Composites as a Gas Sensor.

Thesis Advisors: Prof. Anuvat Sirivat, 114 pp.

Keywords: Poly(3,4-ethylenedioxythiophene) poly(styrenesulfonate) / PEDOT-PSS/ Zeolite/ Gas Sensor

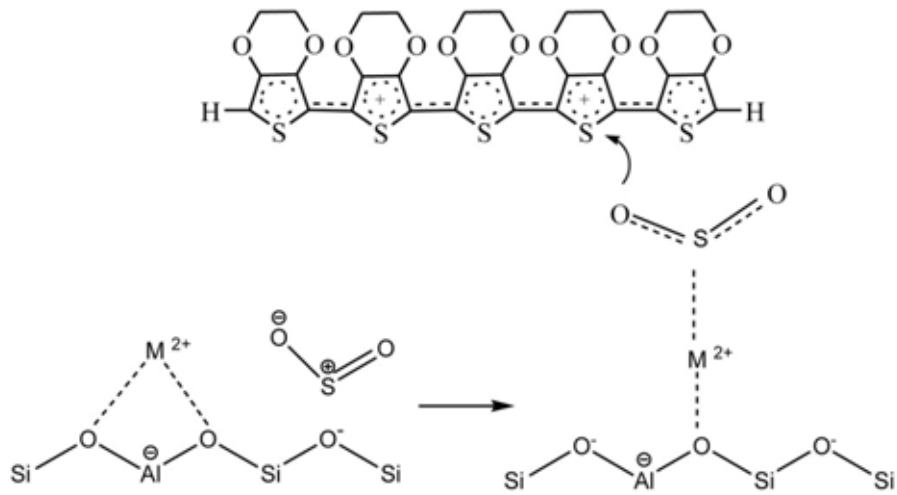
Composites with Poly(3,4-ethylenedioxythiophene) doped with poly(styrene sulfonic acid), PEDOT-PSS, as the matrix containing zeolites of various Si/Al ratios in the range of 23–280 were fabricated to investigate the effect of Si/Al ratios on electrical conductivity sensitivity responses towards the target gas. The electrical conductivity responses of PEDOT-PSS/Zeolite composites were altered due to the available adsorption sites for gas molecules. The addition of zeolites to the pristine PEDOT-PSS improves the electrical conductivity sensitivity of the composites by enhancing the interaction between PEDOT-PSS and target gas. Composites with PEDOT-PSS matrix containing faujasite zeolites type Y were fabricated to investigate the effects of cation type of faujasite zeolite type Y on the electrical conductivity response when exposed to the target gas. The types of cation in zeolite Y micropores can tuning adsorption-desorption properties of zeolite Y, which influence the electrical sensitivity of the composite. Responses and the interaction mechanism of conductive polymer/zeolite composites sensor were investigated. The results obtained can be attributed to the electronegativity of the transition metal cations exchanged into the zeolite Y micropores, which critically affects the adsorption properties of the zeolite Y, and which in turn influences the electrical sensitivity of the composites. The effect of metal exchanged zeolite Y cover layer and the thickness of cover layers on electrical conductivity response of PEDOT-PSS and their sulfur dioxide sensing properties have been investigated. Their gas sensing response; sensitivity, response time, recovering time and complication of fabrication were compared with PEDOT-PSS/MY zeolite composites in powder mixing compress form.

## บทคัดย่อ

พจนานุกรม : การพัฒนาคอมโพสิตของพอลิเอทิลีนไดออกไซด์/โพลีไพร์โรลและซีโอไลต์ เพื่อประยุกต์ใช้เป็นวัสดุตรวจวัดก๊าซ (Development of PEDOT-PSS/Zeolite Composite as a Gas Sensor) อ. ที่ปรึกษา : ศ. ดร. อนุวัฒน์ ศิริวัฒน์ 114 หน้า

พอลิเอทิลีนไดออกไซด์/โพลีไพร์โรลเป็นพอลิเมอร์นำไฟฟ้าชนิดหนึ่งที่มีความสามารถใช้เป็นวัสดุที่ใช้สำหรับงานตรวจวัดก๊าซได้เนื่องจากสามารถเปลี่ยนแปลงคุณสมบัติทางไฟฟ้าได้เมื่ออยู่ภายใต้สภาวะของก๊าซชนิดพิเศษ พอลิเอทิลีนไดออกไซด์/โพลีไพร์โรลถูกสังเคราะห์โดยวิธีพอลิเมอร์ไรเซชันแบบออกซิเดชันและเพิ่มความสามารถทางการนำไฟฟ้าด้วยพอลิสไตรีนซัลโฟเนต และเพื่อเพิ่มความไวทางคุณสมบัติการนำไฟฟ้าจึงผสมซีโอไลต์เข้ากับเมทริกซ์ของพอลิเอทิลีนไดออกไซด์/โพลีไพร์โรล จากนั้นได้ศึกษาการตอบสนองทางคุณสมบัติการนำไฟฟ้าของคอมโพสิตของพอลิเอทิลีนไดออกไซด์/โพลีไพร์โรลและซีโอไลต์ ที่มีต่อก๊าซชนิดพิเศษ โดยได้ศึกษาปัจจัยต่างๆที่เกิดจากการเปลี่ยนแปลงคุณสมบัติทางเคมีของซีโอไลต์ว่ามีผลต่อคุณสมบัติการนำไฟฟ้าของคอมโพสิตอย่างไรเมื่ออยู่ภายใต้สภาวะของก๊าซชนิดพิเศษ คุณสมบัติที่ได้ทำการศึกษาดังกล่าวได้แก่ อัตราส่วนของซิลิกาต่ออลูมิเนียมของซีโอไลต์ซีเอสเอ็มไฟต์ ที่มีผลต่อคุณสมบัติการนำไฟฟ้าของคอมโพสิตต่อก๊าซคาร์บอนมอนอกไซด์ และศึกษาปัจจัยของชนิดของแคตไอออนในซีโอไลต์วายซึ่งประกอบด้วย ไอออนของโลหะหมู่ที่หนึ่งและหมู่ที่สองตามตารางธาตุและไอออนของโลหะทรานซิชัน ที่มีผลต่อคุณสมบัติการนำไฟฟ้าของคอมโพสิตต่อก๊าซซัลเฟอร์ไดออกไซด์ และทำการศึกษาค่าคุณสมบัติทางไฟฟ้าของพอลิเอทิลีนไดออกไซด์/โพลีไพร์โรลเมื่อถูกปกคลุมด้วยชั้นของซีโอไลต์ เปรียบเทียบกับการผสมซีโอไลต์ลงไปเมทริกซ์ของพอลิเอทิลีนไดออกไซด์/โพลีไพร์โรล

## GRAPHICAL ABSTRACT



A schematic diagram indicates possibility of electrostatic interactions between  $\text{SO}_2$ , Zeolite Y and PEDOT-PSS.

## ACKNOWLEDGEMENTS

Appreciation is expressed to those who have made contributions to this dissertation. First the author gratefully acknowledges his advisors, Prof. Anuvat Sirivat from the Petroleum and Petrochemical College, Chulalongkorn University, for giving her invaluable knowledge, meaningful guidance and encouragement all along the way.

She gratefully acknowledges all faculty members and staffs at The Petroleum and Petrochemical College, Chulalongkorn University for their knowledge and assistance. Moreover, she would like to give her special thanks to all members in her research group and all of her friends for their kind assistance, continual encouragement and wonderful friendship.

Asst. Prof. Pomthong Malakul, Prof. Anuvat Sirivat, Assoc. Prof. Ratana Rujiravanit and Dr. Sumonman Niamlang are further acknowledged for being her dissertation committees, making valuable comments and suggestions.

She wishes to express her deep gratitude to her family for their unconditioned love, understanding and very supportive during all these years spent for her Ph.D. study.

Finally, she is grateful for the financial support provided by the Center of Excellence on Petrochemicals and Materials Technology, Thailand; the Conductive and Electroactive Polymers Research Unit of Chulalongkorn University; the Petroleum and Petrochemical College, Chulalongkorn University; the 90<sup>th</sup> Anniversary of Chulalongkorn University Fund (Ratchadaphiseksomphot Endowment Fund); the Thailand Research Fund (TRF-RGJ grant no.PHD/0082/2550); and the Royal Thai Government. This work would not be carried out successfully without all financial supports.

## TABLE OF CONTENTS

	<b>PAGE</b>
Title Page	i
Abstract (in English)	iii
Abstract (in Thai)	iv
Acknowledgements	v
Table of Contents	vi
List of Tables	ix
List of Figures	xi
Abbreviations	xvi
List of Symbols	xvii
 <b>CHAPTER</b>	
<b>I INTRODUCTION</b>	1
 <b>II THEORITICAL BACKGROUND AND LITERATURE SURVEY</b>	
2.1 Conductive Polymer	4
2.2 Semiconductor Model	5
2.3 Concept of Doping	7
2.4 Zeolite	8
2.5 Application of Zeolites	10
2.5.1 Adsorption and Separation	10
2.5.2 Catalysis	10
2.5.3 Ion Exchanged	11
2.6 Sensors Based on Conductive Polymers	11
2.7 Sensors Based on Zeolites	15
2.8 Sensors Based on Conductive Polymer/Zeolite Composites	17
2.9 Points of the Research	14

<b>CHAPTER</b>	<b>PAGE</b>
<b>III INTERACTION OF CARBON MONOXIDE WITH PEDOT-PSS/ZEOLITE COMPOSITE: EFFECT OF SILICA TO ALUMINA RATIO OF ZSM-5 ZEOLITE</b>	<b>20</b>
3.1 Abstract	20
3.2 Introduction	21
3.3 Experimental	22
3.4 Results and Discussion	24
3.5 Conclusions	29
3.6 Acknowledgements	30
3.7 References	30
<b>IV EFFECT OF ALKALINE AND ALKALINE EARTH ION-EXCHANGED ZEOLITES Y ON ELECTRICAL CONDUCTIVITY AND RESPONSE OF PEDOT-PSS/ ZEOLITE Y COMPOSITES TOWARD SULFUR DIOXIDE</b>	<b>43</b>
4.1 Abstract	43
4.2 Introduction	44
4.3 Experimental	45
4.4 Results and Discussion	48
4.5 Conclusions	53
4.6 Acknowledgements	54
4.7 References	54
<b>V EFFECT OF TRANSITION METAL ION-EXCHANGED ZEOLITES Y ON ELECTRICAL CONDUCTIVITY AND RESPONSE OF PEDOT-PSS/ ZEOLITE Y COMPOSITES TOWARD SULFUR DIOXIDE</b>	<b>65</b>
5.1 Abstract	65
5.2 Introduction	66
5.3 Experimental	67
5.4 Results and Discussion	69



<b>CHAPTER</b>	<b>PAGE</b>
5.5 Conclusions	74
5.6 Acknowledgements	75
5.7 References	75
<b>VI EFFECT OF METAL EXCHANGED ZEOLITE Y COVER LAYER ON ELECTRICAL CONDUCTIVITY RESPONSE OF PEDOT-PSS AND THEIR SULFUR DIOXIDE SENSING PROPERTIES</b>	<b>82</b>
6.1 Abstract	82
6.2 Introduction	83
6.3 Experimental	84
6.4 Results and Discussion	87
6.5 Conclusions	92
6.6 Acknowledgements	92
6.7 References	93
<b>VII CONCLUSIONS AND RECOMMENDATIONS</b>	<b>101</b>
<b>REFERENCES</b>	<b>104</b>
<b>CURRICULUM VITAE</b>	<b>112</b>

## LIST OF TABLES

<b>TABLE</b>		<b>PAGE</b>
<b>CHAPTER III</b>		
3.1	The specific surface areas, the pore width, and the pore volume of ZSM-5 (Si/Al = 23, 50, 80 and 280)	34
3.2	The specific conductivity (S/cm) of PEDOT-PSS, zeolites ZSM-5, and PEDOT-PSS_1:1/ZSM-5 composites when exposed to air under chamber temperature ( $T_c$ ) of $27 \pm 1$ °C	35
3.3	Electrical sensitivity of PEDOT-PSS_1:1 and its composites when exposed to CO under chamber temperature ( $T_c$ ) of $27 \pm 1$ °C, asnd at 1 atm, $K$ = correction factor = $3.625 \times 10^{-4}$ (probe no. 1) and $7.759 \times 10^{-4}$ (probe no. 2)	39
<b>CHAPTER IV</b>		
4.1	Physicochemical properties of zeolite Y	58
<b>CHAPTER V</b>		
5.1	Physicochemical properties of zeolite Y	78
<b>CHAPTER VI</b>		
6.1	Physicochemical properties of zeolite Y	96
6.2	Response time and Recovery time of PEDOT-PSS, PEDOT-PSS with MY zeolite cover layer and PEDOT-PSS/MY composite (20% v/v zeolite content) when exposed to SO <sub>2</sub> at $27 \pm 1$ °C and 1 atm.	97

## LIST OF FIGURES

FIGURE	PAGE
<b>CHAPTER II</b>	
2.1	Intrinsically Conducting Polymers. <span style="float: right;">4</span>
2.2	Schematic diagram of the band structure of metals, semiconductors, and insulators. <span style="float: right;">6</span>
2.3	Schematic diagram neutral, polaron, bipolaron state. <span style="float: right;">6</span>
2.4	Zeolite framework structure as the tetrahedral. <span style="float: right;">10</span>
<b>CHAPTER III</b>	
3.1	Morphology of PEDOT-PSS_1:1 particles, ZSM-5 powders, and PEDOT-PSS_1:1/zeolite composites. <span style="float: right;">37</span>
3.2	The specific electrical conductivity (S/cm) of: (a) PEDOT-PSS; (b) ZSM-5 and PEDOT-PSS_1:1/ZSM-5 when exposed to air at temperature ( $T_c$ ) of $27 \pm 1$ °C <span style="float: right;">38</span>
3.3	Electrical conductivity sensitivity values of PEDOT-PSS_1:1 and PEDOT-PSS_1:1/ZSM-5 composites when exposed to CO (1000 ppm) at temperature ( $T_c$ ) of $27 \pm 1$ °C, and at 1 atm. <span style="float: right;">39</span>
3.4	Proposed mechanism of CO-PEDOT interaction <span style="float: right;">40</span>
3.5	FTIR spectra of PEDOT-PSS: before, during and after exposed to CO <span style="float: right;">41</span>
3.6	CO-TPD thermograms of HZSM-5 of various Si/Al ratios <span style="float: right;">42</span>
<b>CHAPTER IV</b>	
4.1	Morphology of PEDOT-PSS particles, Zeolite Y powders and PEDOT-PSS/Zeolite Y composites: a) PEDOT-PSS at 1000x; b) Zeolite NaY at 10000x; c) Zeolite LiY at 10000x; and c) PEDOT-PSS/NaY at 2000x. <span style="float: right;">59</span>

<b>FIGURE</b>	<b>PAGE</b>
4.2 X-ray diffraction patterns of Zeolite LiY, NaY, KY, MgY, CaY and BaY.	60
4.3 The electrical conductivity sensitivity of PEDOT-PSS_1:1 and PEDOT-PSS_1:1/Zeolite NaY composites at various contents: 0, 10, 20, 30, 40 and 50% (v/v) when exposed to SO <sub>2</sub> at 27±1 °C and 1 atm.	61
4.4 The electrical conductivity sensitivity of PEDOT-PSS and PEDOT-PSS/Zeolite Y composites with various cation type: H <sup>+</sup> , Li <sup>+</sup> , Na <sup>+</sup> , K <sup>+</sup> Mg <sup>2+</sup> , Ca <sup>2+</sup> and Ba <sup>2+</sup> (20%v/v) when exposed to SO <sub>2</sub> at 27±1 °C and 1 atm.	62
4.5 Responses of PEDOT-PSS/KY composite when exposed to N <sub>2</sub> (recovery) and SO <sub>2</sub> (sensing) at 27±1 °C and 1 atm.	63

## **CHAPTER V**

5.1 Morphology of PEDOT-PSS particles, Zeolite Y powders and PEDOT-PSS/Zeolite Y composites: a) PEDOT-PSS at 1000x; b) Zeolite MnY at 10000x; c) Zeolite CuY at 10000x; and c) PEDOT-PSS/MnY at 1000x.	79
5.2 X-ray diffraction patterns of zeolites NaY and MnY.	80
5.3 The electrical conductivity sensitivity of PEDOT-PSS_1:1 and PEDOT-PSS_1:1/Zeolite NaY composites at various contents: 0, 10, 20, 30, 40 and 50% (v/v) when exposed to SO <sub>2</sub> at 27±1 °C and 1 atm.	81
5.4 The electrical conductivity sensitivity of PEDOT-PSS and PEDOT-PSS/Zeolite Y composites with various transition metal cation type: Mn <sup>2+</sup> , Fe <sup>2+</sup> , Co <sup>2+</sup> , Ni <sup>2+</sup> , Cu <sup>2+</sup> and Zn <sup>2+</sup> (20%v/v) when exposed to SO <sub>2</sub> at 27±1 °C and 1 atm.	82

<b>FIGURE</b>		<b>PAGE</b>
5.5	Responses of PEDOT-PSS/MnY composite when exposed to N <sub>2</sub> (recovery) and SO <sub>2</sub> (sensing) at 27±1 °C and 1 atm.	83
5.6	A schematic diagram indicates possibility of electrostatic interactions between SO <sub>2</sub> , Zeolite Y and PEDOT-PSS.	84

## **CHAPTER VI**

6.1	Dependence of conductivity change on SO <sub>2</sub> concentration of PEDOT-PSS with NaY zeolite cover layer and PEDOT-PSS/NaY composite (20% v/v zeolite content) at temperature (T <sub>c</sub> ) of 27 ± 1 °C, and at 1 atm.	98
6.2	The electrical conductivity sensitivity of PEDOT-PSS and PEDOT-PSS with MY zeolite cover layer at various zeolite cover layer thickness when exposed to SO <sub>2</sub> at 27±1 °C and 1 atm.	99
6.3	A schematic diagram indicates possibility of electrostatic interactions between SO <sub>2</sub> , Zeolite Y and PEDOT-PSS.	100

**ABBREVIATIONS**

CB	Conduction band
CNFs	Carbon nanofiber
CPs	Conducting polymer
DPN	Dip-pen nanolithography
DC	Direct current
EDOT	3,4-ethylenedioxythiophene
FTIR	Fourier transform infrared spectrometer
ICPs	Intrinsically conducting polymer
P3HTH	Poly(3-octyl-thiophene)
PA	Polyacetylene
P(Ac)	Polyacrylic acid
PANI	Polyaniline
PEDOT	Poly(3,4-ethylenedioxythiophene)
PEDOT-PSS	Poly(3,4-ethylenedioxythiophene) doped with poly(styrene sulfonic acid)
PMMA	Poly(methylmethacrylate)
PP	Polyphenylene
PPV	Poly(p-phenylene vinylene)
PPy	Polypyrroles
PSS	Poly(styrene sulfonic acid)
PTH	Polythiophene
QCM	Quartz crystal microbalance
SEM	Scanning electron microscopy
TGA	Thermogravimetric analyzer
TPD	Temperature programmed desorption
VB	Valance band
XRD	X-ray diffraction

## LIST OF SYMBOLS

A	Ampere unit
V	Applied voltage
V	Voltage unit
I	Resultant current
K	Correction factor
R	Resistance
$\Omega$	Ohm unit
S	Siemens unit
$\sigma$	Specific conductivity
$\Delta\sigma$	Electrical conductivity response
$\Delta\sigma_r$	Electrical conductivity response
$\Delta\sigma / \sigma_{N_2 \text{ initial}}$	Sensitivity
S	Sensitivity
$t_i$	Induction time
$t_r$	Recovery time
cm	Centimeter unit
nm	Nanometer unit
$\mu\text{m}$	Micrometer unit
ppm	Part per million unit
v/v %	Volume by volume percent concentration
$^{\circ}\text{C}$	Degree Celsius
$\text{\AA}$	Armstrong

## CHAPTER I

### INTRODUCTION

The industrial safety requirements and environmental protection become more and more stringent. There are many circumstances in which a gas sensor is desired for detecting a specific gas or gases in an environment; for instance, the emission of toxic gaseous pollutants from spills and industrial leaks, in laboratory and the leakage of anesthetic gases in hospital. The demands for accurate and dedicated sensors to monitor and control the leakage of toxic gas and also to provide precise process control and automation in manufacturing process have accelerated the development of new sensing materials and sensor technology over last decade (Wang *et al.*, 2002).

Several gas sensing materials have been developed. The gas sensor systems are required to offer high sensitivity and selectivity, rapid detection, low manufacturing costs, long life times (Densakulprasert *et al.*, 2005), robust, reproducible, small, and simple (Sasaki *et al.*, 2002). For such sensors to be incorporated into practical instruments, the dimensions and the operating temperatures need to be reduced (Currie *et al.*, 1999). The major difficulty in gas identification is the fabrication of stable sensors with high sensitivity and very good selectivity of the substance to be detected.

There are several types of gas sensors: electrochemical, infrared, catalytic bead, photoionization and solid-state. The most widely used gas sensor devices are produced from metallic oxides such as SnO<sub>2</sub> (Srivastava *et al.*, 2006), ZnO (Wagh *et al.*, 2006), WO<sub>3</sub> (Stankova *et al.*, 2006), TiO<sub>3</sub> (Zhu *et al.*, 2000), In<sub>2</sub>O<sub>3</sub> (Niu *et al.*, 2006), etc. Its electrical conductivity changes when gas molecules are adsorbed onto its surface. Even though its low selectivity has been improved (Pijolat *et al.*, 1999), its operating temperature needs to be as high as 300 – 400 °C which remains a problem. Therefore, the improvement of sensor characteristic becomes one of the principal factors that have to be achieved

Recently, there have been interests in using conductive polymers in gas sensing materials, as an alternatives to metal or metal oxide sensing films. Conductive polymers contain a conjugated system with  $\pi$ -electrons delocalized along



the polymer backbone, thus they possess the electrical and magnetic properties of metal, while retaining the mechanical properties of polymers. Due to their unique electronic, chemical and physical properties, they are potentially suitable as sensing materials. Conductive polymers offer other advantages: lightweight, flexibility, corrosion-resistivity, high chemical inertness, electrical insulation, the ease of processing and can be operated at room temperature. Furthermore, conducting polymers can respond to a wide range of gases and in particular toxic gases. Nevertheless, no commercial systems have been developed because of the remaining problems of poor reversibility and selectivity to particular gases at low concentrations of these materials. Therefore, the improvement of sensor selectivity becomes one of the principal factors that have to be achieved in order to recognize different specific chemicals. Many conductive polymers have been used as gas sensing materials (Prissanaroon *et al.*, 2000). Poly(3,4-ethylenedioxythiophene), PEDOT is one of the most interested amongst conductive polymers due to its high electrical conductivity, relatively high environmental stability, and the ease of synthesis.

Due to increasing environmental and economic concerns, the need for inexpensive selective gas sensors is of interest, and zeolite-based materials used in gas sensing have received a great deal of attention. Zeolites nanometric sized channel system providing a size and shape-selective matrix for absorbed molecule while maintaining a high surface-to-mass ratio (Dyer, 1988). Zeolite is not constructed from only silicate tetrahedral ( $\text{SiO}_4$ ), but also aluminate tetrahedral ( $\text{AlO}_4$ ); therefore, the aluminum zeolite framework requires the necessary presence of cations. The selective adsorption mechanisms of zeolite can be summed up into two main mechanisms. First, the nanometric size of pores can be utilized to process the molecular sieve property. Second, the zeolite chemical composition, the Si/Al ratio, is the main factor controlling the hydrophilic/ hydrophobic properties of materials. The introduction of specific cations, by using the cation exchange method, can alter gas adsorption properties. Zeolites are attractive candidates for numerous applications as chemical sensing materials.

In our work, we propose to develop reliable toxic gas sensing materials which can be operated at room temperature, inexpensive and easy to integrate into a

system capable of detecting an individual gas in a gas mixture at a low concentration level and with a fast response. A novel strategy in our work is based on the association of a conductive polymer and a zeolite framework. Poly(3,4-ethylenedioxythiophene), PEDOT was used as a semiconductor, where its electrical conductivity can be altered when exposed to various gases; the electrical conductivity response depends on the adsorption properties of zeolite microporous material.

## CHAPTER II

### THEORETICAL BACKGROUND AND LITERATURE SURVEY

#### 2.1 Conductive Polymer

Since the discovery of conductivity in polymer in 1961 by Hatano and coworkers (Hatano *et al.*, 1961), the so-called Intrinsically Conducting Polymer (ICPs) has been investigated extensively. Hatano *et al.* discovered that a polyacetylene sample had conductivity of the order of  $10^{-5}$  S/cm. A very important result was obtained in 1977, when Shirakawa, MacDiarmid, Heeger and coworkers reported that the conductivity of freestanding polyacetylene films increased up to 12 orders of magnitude upon exposure to halogen vapors (Shirakawa *et al.*, 1977; Chiang *et al.*, 1977; Chaing *et al.*, 1978). This can be attributed to the formation of free charge carriers in the polymer chain upon reduction or oxidation of the ICP and this process is called doping. But polyacetylene has drawbacks because of its processing difficulty and the rapid decrease in conductivity upon exposure to air. Therefore other ICPs that are more environmentally stable and that can be polymerized in an electrochemical synthesis have been developed. Thus new ICPs has been synthesized and investigated: polyacetylene, polypyrrole (PPy), polyaniline (PANI), polythiophene (PTH), and polyphenylene vinylene (PPV).

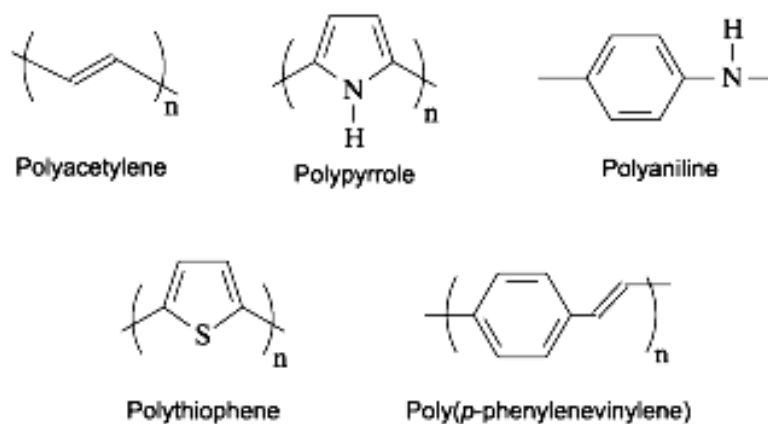


**Figure 2.1** Intrinsically Conducting Polymers.

Generally, conductive polymers are organic material which comprised of C, H and simple heteroatom such as N and S and consisting of unique  $\pi$ -conjugation electrons. Conjugation is important characteristic because it provides a pathway for electrons to migrate along a polymer chain and to jump from one chain to another chain. So, conjugated polymers have the ability to conduct electricity by the delocalization of  $\pi$ -bonded electrons over the polymeric backbone, exhibiting unusual electronic properties, such as low energy optical transitions, low ionization potentials and high electron affinities (De Paoli and Gazotti, 2002). These phenomena present electric, electronic, magnetic and optical properties inherent to metals or semiconductors, while retain the mechanical properties of conventional polymers. Those properties are intrinsic to the doped materials: they are completely different from those originated from a physical mixture of a non-conductive polymer with a conducting material, such as metal or carbon powder (Patil *et al.*, 1988). Furthermore it has several advantages: low density and cost, ease of processing, relative robustness, and lightweight, so it is widely used in many applications such as gas sensing, light-emitting cells and diodes, rechargeable batteries, electronic cells, controlled-release applications, actuators, and polymeric electronics such as transistors (Van Vught *et al.*, 2000).

## 2.2 Semiconductor Model

Materials in the world can be classified into three categories according to their room temperature conductivity properties: Insulators, Semiconductors and Conductor. These materials contain two electronic band, valence and conduction band that occur by overlapping of molecular electronic states. Each material has different electric model that illustrate in Figure 2.2

If the gap between conduction (CB) and valence band (VB) is large, electrons are difficult excited from valence to the conduction band which is characteristic of insulator. In case semiconductor has small gap, electrons are easily excited into the conduction band by thermal excitation, vibrational excitation, or excitation by photons. Conductive polymers have different electronic state after

doping, solitons, polarons or bipolarons. These defects or the charge carriers generate localized electronic states in the middle of the energy gap between the valence band and the conduction band. This effectively reduces the energy gap and the charge carriers can jump into conduction band and electrical conductivity is enhanced (Kumar and Sharma, 1998; Chandrasekhar, 1999; Van Vught *et al.*, 2000).

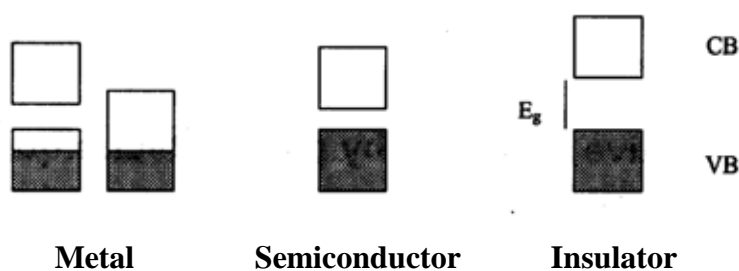


**Figure 2.2** Schematic diagram of the band structure of metals, semiconductors, and insulators ( $E_g$  is the energy gap between the valence band (VB) and the conduction band (CB)).

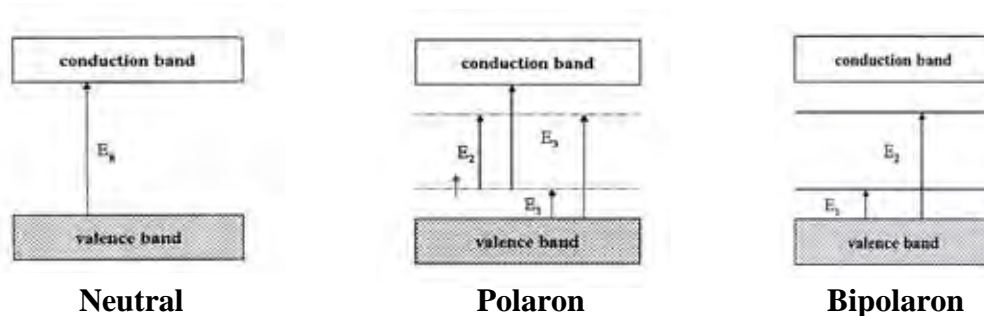


**Figure 2.3** Schematic diagram neutral, polaron, bipolaron state.

The polaron has form of radical cation (one unpaired electron), which is locally associated with a structural distortion in conductive polymer and conduction band remains empty and the valence band remain full. Therefore, electrical conduction can only take place when electron is removed from valence band into the

conduction band. If the second electron is removed from the polaron itself, bipolaron will be achieved (Chandrasekhar, 1999).

### 2.3 Concept of Doping

In intrinsic conducting polymers, also known as conjugated polymers, they are distinguished by alternating single and double bonds between carbon atoms on the polymer backbone or the main chain contains  $\pi$ -conjugation. The naturally  $\pi$ -conjugated electrons systems on conductive polymer backbone are not sufficient to render them highly conductivity; trans-polyacetylene possesses only  $10^{-6}$  S.cm<sup>-1</sup>. The high electrical conductivity is achieved by the process called the “doping process”. This process was firstly discovered by Shirakawa and Ikeda by doping of polyacetylene (PA) with iodine, and conductivity increases by 9-13 orders of magnitude (Kumar and Sharma, 1998).

The concept of doping distinguishes conducting polymers from all other kinds of polymers. The controlled addition of known, small (< 10 %) non-stoichiometric amounts of chemical species results in dramatic changes in the electronic, electrical, magnetic, optical and structural properties of the polymer (De Paoli and Gazotti, 2002). Doping of pristine conductive polymer can be accomplished by using chemical and electrochemical method via oxidation or reduction reaction. In chemical method, conjugate polymer is directly exposed with a solution or vapor of the dopant. If the oxidation in the polymer occurs, it extracts electrons from the valence band (electrons from the polymer to the dopant), creating “holes” in the valence band, which is then known as “p-doping”. It generates a positively charged conductive polymer and an associated anion. When the reduction on the polymer occurs, it adds electrons to the conduction band (electrons from the dopants to the polymer), increasing conducting electrons in this band, which is known as the “n-doping”. This generates a negatively charged conductive polymer with an associated cation (Chandrasekhar, 1999).

Doping processes are summarized in the next schematic, where M and A are the cation and the anion, respectively:

*Anionic doping (p-doping):*



*Cationic doping (n-doping):*



Dopants are generally incorporated into the conductive polymer at the time or later of synthesis. Usually, dopants are small anions or cations, eg.  $\text{ClO}_4^-$  or  $\text{Na}^+$ , or large polymeric species, such as the “polyelectrolytes” poly(styrene sulfonic acid) and poly(vinyl sulfonic acid). These counter-ions neutralizing charge on conductive polymer can influence the mobility of the charge carriers (Van Vught *et al.*, 2000). If counter-ions are large so the degree of charge delocalization is stronger. That means the stability of the conductivity can be affected by the size of the counter-ions. Moreover, conductivity can be increased via creation of more mobile charges by increasing doping level or using different dopants.

The doping with n-type dopants, anion conductive polymer is formed which is highly unstable in air and water. So, the conductivity which is generated by n-type dopants e.g. Na, Li is less stable than by p-type dopants e.g.  $\text{I}_2$ ,  $\text{AsF}_5$ ,  $\text{FeCl}_3$ ,  $\text{HClO}_4$ . Therefore p-type dopants are more frequently used (Kumar and Sharma, 1998; Chandrasekhar, 1999; Van Vught *et al.*, 2000).

## 2.4 Zeolite

Zeolites are aluminosilicates built up with  $\text{SiO}_4$  and  $\text{AlO}_4$  tetrahedra building blocks that form a ring structure. They form 3-dimensional (3D) frameworks with linked channel systems and well-defined micropores, and mesopores and provide an open porosity that gives rise to an exceptionally high surface area. Aluminum ions replacing silicon ions introduce a negative charge into the framework. This charge needs to be compensated for by an exchangeable cation, such as an alkaline or alkaline-earth cation and, thus, the ion exchange property is

provided. These cations are bound to the host framework but are mobile along the channels. Aluminum ions act as acidic sites to catalyze the chemical reaction.

Zeolites were discovered in 1756 by the Swedish mineralogist Axel Fredrick Cronstedt. He named the class of materials zeolites from the classical Greek words meaning 'boiling stones' which describe the escape of water molecules from the cavities of zeolites (Tomlinson, 1998).

R. Barrer and J. Sameshima worked extensively on zeolite synthesis that zeolites were first synthesized during the 1930's. In 1948, Richard Barrer first produced a synthetic zeolite that did not have a natural counterpart. At approximately the same time, Milton made the first materials that had no natural counterpart such as zeolite A.

Zeolites are porous crystalline aluminosilicate solids with well-defined structures. Most occur naturally as minerals, and are extensively used in many parts of the world. Others are synthetic, and are made commercially for specific uses. Generally they contain silicon, aluminium and oxygen in their framework and cations, water and/or other molecules within their pores. Their frameworks based on an extensive three-dimensional network of oxygen ions that are made up of 4-connected networks of atoms with a silicon atom in the middle and oxygen atoms at the corners. This framework liked tetrahedral that can link together by their corners to form a variety of structures. The  $\text{AlO}_2$  tetrahedra in the structure determine the framework charge. It attracts the positive cations inside within and may contain linked cages, cavities or channels, which are of the right size to allow small molecules to enter. The framework charge is balanced by cations that occupy nonframework positions (Szostak, 1989).

The vacant spaces or cages in their structures can accommodate large cations such as sodium, potassium, barium and calcium and even relatively large molecules and cation groups such as water, ammonia, carbonate ions and nitrate ions. These channels permit the easy movement of the resident ions and molecules into and out of the structure (Amerthyst Galleries, Inc, 1999, 2000).



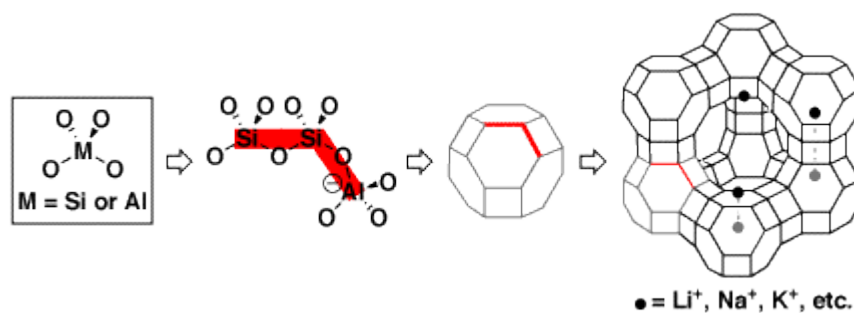


**Figure 2.4** Zeolite framework structure as the tetrahedral.

Zeolites are used in a variety of applications such as petrochemical cracking, ion-exchange (water softening and purification), and in the separation and removal of gases and solvents. Other applications are in agriculture, animal husbandry and construction. They are often also referred to as molecular sieves.

## 2.5 Applications of Zeolites

### 2.5.1 Adsorption and Separation

The shape-selective properties of zeolites are the basis for their use in molecular adsorption. The ability to adsorb certain molecules causes several of molecular sieving applications. The size and shape of pores controlling different types of molecule enter the zeolite. Some molecules diffuse through the channels more quickly.

Cation-containing zeolites are extensively used as desiccants due to their high affinity for water, and also find application in gas separation of gases as ammonia, hydrogen sulfide, carbon monoxide, carbon dioxide, sulfur dioxide, water vapor, oxygen, nitrogen, formaldehyde, and others. Molecules are separated on the basis of their electrostatic interactions with the metal ions. So Zeolites can separate molecules based on differences of size, shape and polarity.

### 2.5.2 Catalysis

Zeolites act as catalysts for chemical reactions which take place inside the cavities. An important class of reactions is that catalyzed by hydrogen-exchanged

zeolites. The framework-bound protons give rise to very high acidity. This is exploited in many organic reactions, including crude oil cracking, isomerisation and fuel synthesis. Zeolites can serve as oxidation or reduction catalysts by introducing metals into the framework.

The unique structure has a steric influence on the reaction, controlling the access of reactants and products. Increasingly, attention has focused on the properties of zeolite catalysts in order to carry out very specific syntheses of high-value chemicals e.g. pharmaceuticals and cosmetics.

### 2.5.3 Ion Exchange

The loosely-bound nature of extra-framework metal ions (such as in zeolite NaA, right) means that they are often exchanged for other types of metal when in aqueous solution. This is exploited in a major way in water softening, where alkali metals such as sodium or potassium prefer to exchange out of the zeolite, being replaced by the "hard" calcium and magnesium ions from the water. Many commercial washing powders contain substantial amounts of zeolite. Commercial waste water containing heavy metals and nuclear effluents containing radioactive isotopes can also be cleaned up using such zeolites.

Recently, zeolite is interested to use for gas sensor applications by mixing with conductive polymer such as polyaniline, polyphenylene vinylene and polythiophene. Because the well-define structure of zeolite can separate the desire gas molecules and the efficiency of gas sensor can measure by electrical conductivity changing of conductive polymer.

## 2.6 **Sensors Based on Conductive Polymers**

Shirakawa *et al.* (1977) discovered that electrical conductivity of polyacetylene can reach high values. Other conductive polymers consisting of alternative single and double bonds and the broad  $\pi$ -electron conjugated structure have been synthesized. The conductivity of these polymers can be tuned by the chemical modification, or by doping.

Among the numerous electrically conductive polymers that have been studied and developed over the past three decades, polyanilines (PANI), polypyrroles (PPy), polythiophenes (PT), polyphenylenes (PP), and poly(p-phenylene vinylene)s (PPV) have attracted the most attention. Of these, the polyaniline family stands out for high electrical conductivity, relatively high environmental stability, relatively low cost and the ease of being doped under various dopants. Polythiophenes and its derivatives belong to an important representative class of conductive polymers as the most environmentally and thermally stable materials. Applications are, for example, iodine doped polythiophene battery, electro-optical display devices, humidity sensors, radiation detectors, gas sensor, and etc.

Sensors made of conductive polymers have many important characteristics. They have high sensitivities and short response times at room temperature. Furthermore, conducting polymers have good mechanical properties, which allow a facile fabrication of sensors. Polypyrrole, polyaniline, polythiophene and their derivatives have been used as the active layers of gas sensors since early 1980s.

The electrical conductivity sensitivity of conductive polymers when they are exposed to various chemicals has been a subject of many studies towards sensing applications. Gases interacting with conductive polymers can be divided in two main classes: gases which chemically react with conductive polymers and gases which physically adsorb onto conductive polymers. Chemical reactions lead to changes in the doping level of conductive polymers and the charge carrier mobility.

Electron-accepting gases like  $\text{NO}_2$ ,  $\text{I}_2$ ,  $\text{O}_3$ ,  $\text{O}_2$  withdraw electrons from polymer chains. If the conductive polymer is a p-type-doped polymer which have positive charges as the charge carriers, doping with  $\text{NO}_2$  will increase the number of charge carriers in PANI and P3HTH through the oxidative doping with  $\text{NO}_2^-$  ions and therefore decrease the resistance.

Electron-donating gases like  $\text{H}_2\text{S}$ ,  $\text{NH}_3$  and  $\text{N}_2\text{H}_4$  reduce the amount of positive charges in p-type-doped polymer chains and hence decrease the electrical conductivity. Ammonia and  $\text{H}_2\text{S}$  will decrease the electrical conductivity of PTHs. A mechanism for the dedoping of conductive polymers by ammonia has been proposed. The polymer reduction reaction by an analyte is the reason for increasing PPy resistance upon exposed to hydrogen.

For certain gases, a partial charge transfer rather than a pure redox reaction is suggested. Interacting with PANI, CO is assumed to withdraw a lone pair electron from the amine nitrogen through the positive charge at the carbon atom. Therefore the positive charge at the carbon atom is transferred to the amine nitrogen, resulting in an increase of the amount of positive charge carriers along the PANI backbone. Another explanation suggests that CO interaction with PANI enhances charge transfer between polymer grains.

Jang and Bae (2006) fabricated PPy-coated carbon nanofiber (CNFs) for irritant gas detection. NH<sub>3</sub> and HCl caused the decrease and the increase in the electrical conductivity due to the dedoping and the oxidizing of the conductive layer, respectively. The sensors exhibited an enhanced response signal due to its thinness and uniformity, and more active sites of PPy layers on the CNF surface. The responses of the sensors after interaction with NH<sub>3</sub> and HCl were reversible, reproducible, and dependent on the thickness of the PPy layers.

Rosa *et al.* (2005) prepared poly(2-bromo-5-hexyloxy-p phenylenevinylene), BHPPV. Synthesized gas sensors were made from thin films of 10-camphorsulfonic acid doped BHPPV, deposited on interdigitated electrodes. They responded to five different solvents: acetone, hexane, water, methanol and ethanol. The sensors exhibited quite different responses to the tested vapors. In cases of acetone and hexane, the resistance increased, for the other solvents it decreased. Plots of relative response versus relative recovery showed a good discrimination between the five solvents.

Watcharaphalakorn *et al.* (2005) blended PANI with polyimide (PI) to improve mechanical, thermal behaviours of the conductive polymer. The addition of PI also enhanced the sensitivity response of the blends towards CO gas. The target gas such CO acted as an electron withdrawer and the interaction of gas and polymer phase was proposed to occur at the –NH– attack site which contained the lone pair of electron; the proposed interaction caused the increase in the conductivity of doped PANI due to the increase of the number of charge carriers on the polymer chain.

Reemts *et al.* (2004) prepared and characterized conductive layers of emeraldine base polyaniline (PANI) and tested them as a transducer for gas/organic vapor sensors. Ethanol and acetone were chosen as model compounds to be studied

on the PANI films while ammonia was used as the reference. The change in the doping level of PANI provided a significantly more sensitive signal. The films tested possessed a good sensitivity against  $\text{NH}_3$ , with a linear dependence of the signal on concentration in the PPM ranges.

Hong *et al.* (2004) prepared an ammonia gas sensor by polymerizing aniline on the surface of nylon 6 fabrics and doped with various acids. The fabricated polyaniline (PANI)–nylon 6 composite fabrics showed a high sensitivity and a fast response for  $\text{NH}_3$  gas compared to those of CO and  $\text{C}_3\text{H}_8$ . The electrical resistance of the PANI–nylon 6 composite fabrics increased when exposed to an ammonia environment but reversibly recovered after flushing with fresh air. In particular, the PANI–nylon 6 composite fabrics doped by monocarboxylic acids (such as formic acid, acrylic acid, and trichloroacetic acid) displayed an excellent sensitivity and fast responses.

Bhat *et al.* (2003) prepared polypyrrole–poly(methylmethacrylate) (PMMA+PPy) blend films. The mechanical properties of the conducting PMMA+PPy films were improved relative to the PPy films. The electrical conductivity of the films depended on the pyrrole content. These conducting composites were further used as gas sensors by observing the change in the current when exposed to ammonia gas. The film gave a fast and reproducible response towards ammonia gas.

Gangopadhyay and De (2001) prepared a polypyrrole (PPy)-based conducting composite within crosslinked matrix of poly(vinyl alcohol) (PVA). The blend was found to possess a significant  $\text{NH}_3$  sensing capacity.  $\text{NH}_3$  being an electron donating gas, resulted in an enhancement of the resistance of the PPy film. With increasing  $\text{NH}_3$  concentration, more obvious changes were observed but an  $\text{NH}_3$  concentration above 10% resulted in almost irreversible change in resistance; the mechanism of  $\text{NH}_3$  sensing response was not identified.

Qian Tang *et al.* (2008) developed doped polypyrrole to be gas sensor by ip-pen nanolithography (DPN). The DPN-generated microsized pattern was used as a gas sensor. They found the resistance of sensor increased when exposed to  $\text{CO}_2$ , because of the reduced localization of the lone pair electrons. They showed that sensor can use for  $\text{CO}_2$  sensing.

## 2.7 Sensors Based on Zeolites

Zeolites are a family of inorganic and crystalline materials. They are composed of a framework of tetrahedral  $\text{TO}_4$  building units ( $\text{T}=\text{Si}$ ,  $\text{Al}$ , or etc.). The tetrahedral  $\text{TO}_4$  units link with each other by sharing oxygen atoms to form 3-dimensional (3D) frameworks with linked channel systems and well-defined micro- and mesopores. The T-O-T links result in a variety of rings, which are responsible for the zeolite cages and channels of varying window sizes. Within the framework structure, the  $\text{Al}^{3+}$  atom at the center of an  $\text{AlO}_4$  tetrahedron connects to a neighboring  $\text{AlO}_4$  tetrahedron by sharing an O atom, and thus generates a negative framework charge which is balanced by an exchangeable cation, such as an alkaline or alkaline-earth cation, thus the property of ion exchange is derived. By means of ion-exchange with different cations, the pore size, the ion conductivity, the adsorption and catalytic selectivity of zeolites can obviously be modified. The Si/Al ratio in a zeolite framework can usually be effectively adjusted, and by changing the framework Si/Al ratio of the zeolite, the ion-exchange capacity and conductivity, the interaction between the zeolite and the adsorbed molecules, and the modification of hydrophilic or hydrophobic properties can all be changed. The zeolites with low silica contents are hydrophilic, and are usually used as drying agents for absorbing steam, whereas hydrophobic high siliceous zeolites are used for absorbing organic molecules from humid air or water. In principle, varying the framework Si/Al ratio of zeolites greatly changes the adsorption selectivity towards molecules with different polarity. Due to this unique property, zeolites are of high potential in gas sensing.

Schaf *et al.* (2006) investigated the shape-selective resistivity of gas sensors of polar molecules by using the stilbite zeolite. The interaction between zeolite and incoming molecules can be described by the Langmuir-type adsorption. The electrical conductivity change due to an exposure to a gas was interpreted mainly by the difficulty of exchangeable cation mobility, due to sterical interactions in the zeolite channels, the size, and the dipole moment of the molecule.

Vilaseca *et al.* (2006) developed and tested a new type of sensor, namely a quartz crystal microbalance (QCM) modified by a layer of  $\text{AlPO}_4\text{-18}$  crystals. The characteristics of the sensor were compared to that of other QCM devices modified

by different zeolite materials (zeolite A and silicalite). The  $\text{AlPO}_4\text{-18}$  modified sensors were sensitive to water and other polar molecules of small sizes. On the other hand, their affinity towards non-polar molecules was low, thus enabling the sensing of water in the presence of hydrocarbons.

Sahner *et al.* (2006) modified electrodes by using ZSM-5 zeolite as a cover layer of the electrodes in order to enhance response ability to hydrocarbons. The ZSM-5 cover layer caused the sensor to detect propane or butane better than the films without the ZSM-5 layer.

Huang *et al.* (2004) modified QCM with  $\text{Ag}^+$ -ZSM-5 zeolite to diagnose diabetes. Such sensor was utilized in detecting acetone in nitrogen and the concentration of acetone in diabetics' breath. The QCM coated with  $\text{Ag}^+$ -ZSM-5 zeolite had a high sensitivity and selectivity with good repeatability. A test for minimum detectable concentration of acetone vapor went as low as 1.2 ppm, and the lower detection limit of acetone vapor was conceived to be much lower. 0.26 ppm was identified in the diagnosis of diabetes. The breath between diabetics and healthy persons were well distinguished. An average of 90s response time was observed. The frequency shift of QCM along with temperature was also studied.

Rauch and Liu (2003) reported a zeolite A film coated on sensors can selectively sense a particular gas. The sensor without a zeolite layer exhibited a strong response to both oxygen and carbondioxide in the mixture of these gases. With the zeolite film coated, the sensor was able to discriminate the responses between the two gases. The modified sensor showed a response only to oxygen; the oxygen diffusion through the zeolite was preferential to  $\text{CO}_2$  diffusion.

Zhou *et al.* (2003) developed a novel freon gas sensor of piezoelectric microcantilever coated with zeolite in order to control indoor air quality. The microcantilever was employed to detect the concentration of sample freon-12 gas ranging from 0 to 100 ppm through the effect of the specific MFI zeolite modification. High selectivity and sensitivity combined with excellent repeatable and reversible performances were demonstrated. The minimum mass changing of  $3.5 \times 10^{-9}$  g and the sensitivity of  $-0.0024\%/ppm$  were found.

Vilaseca *et al.* (2003) developed semiconductor (Pd-doped  $\text{SnO}_2$ ) gas sensors covered with zeolitic films (MFI or LTA) for use as a gas phase sensing of

different species (methane, propane, and ethanol) at different humidity levels. The dynamic responses obtained with these sensors were compared with the response of a reference sensor without a zeolitic layer. A suitable zeolite layer strongly reduced, and in some cases suppressed, the response of the sensor to paraffins, thereby increasing the sensor selectivity to the alcohol, while the reference sensor could not discriminate between these molecules. This clearly showed the potential of zeolite-based sensors to achieve a higher selectivity/sensitivity in gas sensing applications.

Limtrakul *et al.* (2001) examined the interaction of CO with H-ZSM5 and Li-ZSM5 zeolites using the quantum cluster and embedded cluster models. For the H-ZSM5 and Li-ZSM5 zeolites, the C-bound complex was found to be more stable than the O-bound complex. Increase in acidity of the Bronsted acid site increased the number CO-binding sites of these complexes.

## **2.8 Sensors based on Conductive Polymer/Zeolite Composites**

Current research in gas sensor technology has been focused on the development of sensors that can provide low-cost, rapid and high sensing information due to the increasing demand for fast, continuous and trace detection (Saxena *et al.*, 2007). Nearly all the widely studied conducting polymers such as Polypyrrole, Polythiophene and Polyaniline have been used as the active materials in sensors. The methods of adjusting the sensing materials include modifying the polymer molecular structures, changing dopants and incorporating second component into conducting polymers. An advantage of using conducting polymer as the active material is that the chain structure of conducting polymer can be easily modified (Hua Bai *et al.*, 2007).

With their excellent chemical and thermal stability, zeolites can be used as a substrate to prepare compounds and devices with desirable physical and chemical properties. Some applications of zeolite materials in gas sensors have been developed based on their characteristics. Example, placing zeolites onto sensors as filter materials for enhancing the selectivity to a certain gaseous molecule; immersing zeolites into some materials or supports forming composites for making sensors,



such as the conductivity of polyaniline/zeolite composites responsive to CO, SnO<sub>2</sub>/zeolite composites responsive to H<sub>2</sub> and CO.

Soontornworajit *et al.* investigated the electrical conductivity sensitivity and interaction mechanisms between mechanically mixed polypyrrole (PPy)/13X composites and CO<sub>2</sub>, CO, and SO<sub>2</sub>. There were negligible negative responses of PPy when exposed to CO<sub>2</sub>, and CO in contrast to definite positive responses towards SO<sub>2</sub> in which the interaction was irreversible. Undoped PPy and doped PPy composites containing 10% (v/v) of 13X had the highest sensitivity to SO<sub>2</sub>. Adding fully Na<sup>+</sup> exchanged zeolite into a PPy matrix provided the highest electrical conductivity sensitivity toward SO<sub>2</sub>. The sensitivity of Ppy/13X composite to SO<sub>2</sub> diminished as the cation Na<sup>+</sup> was exchanged to other alkali cations in this decreasing order: Cs<sup>+</sup>, K<sup>+</sup>, and Li<sup>+</sup>, in the opposite order to the binding energy between the gas and the cations. The sensitivity and interaction were also reduced with increasing amount of Li<sup>+</sup>.

Densakulprasert *et al.* (2005) studied the effects of zeolite content, pore size, and ion exchange capacity on electrical conductivity response to CO of PANI/zeolite composites. Zeolite Y, 13X, and synthesized AIMCM41, all having the common cation Cu<sup>2+</sup>, were dry mixed with synthesized maleic acid doped PANI and compressed to form PANI/zeolite pellet composites. The addition of 13X zeolite to pristine PANI, increased the electrical conductivity sensitivity to CO/N<sub>2</sub>, depending on zeolite content. For the effect of zeolite type, the highest electrical conductivity sensitivity was obtained with the 13X zeolite, followed by Y zeolite, and AIMCM41, respectively. Poor sensitivity of AIMCM41 was probably due to its very large pore size and its lowest Cu<sup>2+</sup> exchange capacity. Y zeolite and 13X zeolite have comparable pore sizes but the latter had a greater free pore volume and a more favorable location distribution of the Cu<sup>2+</sup> ions within the pore. The temporal response time increased with the amount of zeolite in the composites and it was inversely related to the amount of ion exchange capacity.

Chuapradit *et al.* (2005) utilized LTA zeolites mixing with PANI for acting as CO sensor. The improvement of electrical sensitivity of PANI towards CO was accomplished by adding zeolite 4A up to 40% w/w. Zeolite 5A was the most effective mesoporous material in promoting interaction between CO and polyaniline

because of its largest pore size of 5 Å, relative to the zeolite 3A and 4A which have the pore sizes of 4 and 3 Å, respectively. The reversible interaction between CO and PANI occurred at amine nitrogen or at the polaron species.

Enzel and Bein (1998) designed a model system via an encapsulation of polymeric chain conductor in low-dimensional, ordered lattice of a zeolite in order to reduce the size of electronic circuitry to molecular dimension. Polyaniline was synthesized in the channel of mordenite (one-dimension) and zeolite Y (three-dimension). The polyaniline chains in the mordenite channels appeared to be more highly oxidized than in zeolite Y. The electrical conductivity of polymer/zeolite sample was lower than the bulk electrical conductivity of undoped polyaniline. The level of intrazeolite reaction or the nature of the channel system controlled the degree of polymer oxidation.

Wu and Bein (1994) prepared a conducting polymer, polyaniline, in a three-nanometer wide hexagonal channel system of MCM-41. The oxidative polymerization occurred by an adsorption of aniline vapor into the dehydrate host. Spectroscopic data showed that the filaments were in the protonated emeraldine salt form, and chromatography indicated a chain length about 190 aniline rings. The significant low-field conductivity of the polymer filaments as measured by microwave absorption at 26 GHz demonstrated that the conjugated polymer could be encapsulated in nanometer channels and still supported mobile charge carrier. This demonstration represented a step toward the design of nanometer electronic devices.

## **2.9 Points of the Research**

Conducting polymers are of special to gas sensor industry where arrays of polymer composites may be used to detect gases and odors. Incorporating second component into conducting polymer films is one of the most important methods to develop new sensors. As mentioned above, the main reason for blending a conductive polymer with a zeolite is to combine the advantages of the two materials, towards gas sensing applications. We propose to combine a conductive polymer with a zeolite be used as selective gas sensors with high sensitivity, good reversibility, and improved stability.

**CHAPTER III**  
**INTERACTION OF CARBON MONOXIDE WITH PEDOT-PSS/ZEOLITE**  
**COMPOSITE: EFFECT OF SILICA TO ALUMINA RATIO OF ZSM-5**  
**ZEOLITE**

**3.1 Abstract**

Composites with Poly(3,4-ethylenedioxythiophene) doped with poly(styrene sulfonic acid), PEDOT-PSS, as the matrix containing ZSM-5 zeolites of various Si/Al ratios in the range of 23–280 at 20% (v/v) were fabricated to investigate the effect of Si/Al ratios on electrical conductivity sensitivity responses towards carbon monoxide (CO). The electrical conductivity responses of PEDOT-PSS/ZSM-5 composites were altered due to the available adsorption sites for CO molecules. The electrical conductivity sensitivity to CO increases with decreasing Si/Al ratios. The composites produce irreversible responses when replacing CO with nitrogen. The addition of ZSM-5 zeolites to the pristine PEDOT-PSS improves the electrical conductivity sensitivity of the composites by enhancing the interaction between PEDOT-PSS and CO gas. The composite of ZSM-5 zeolites with a Si/Al ratio equal to 23 gives the highest electrical conductivity sensitivity toward CO.

**Keywords:** Conducting polymers; Poly (3,4-ethylenedioxythiophene); Zeolite ZSM-5; Carbon Monoxide; Gas Sensor

### 3.2 Introduction

For environmental and safety concerns, the development of sensors to detect the presence and the concentration of toxic or otherwise dangerous gases from spills and industrial leaks is needed. The fabrication of stable sensors with high sensitivity and very good selectivity towards the substance to be detected has been pursued.

CO is a very dangerous gas emitted from automobiles and industrial plants. Various materials have been employed in detecting CO at intermediate and low levels. Commercial CO gas sensors, typically based on semiconducting metal oxide sensors (e.g. tin oxide) and operating on the basis of catalytic reactions between the semiconductor and contact gases, produces a change in semiconductor conductance (Adhikari *et. al.*, 2004) The metal oxide sensor provides rapid response, but it needs to operate at high temperature (Watcharaphalakorn *et. al.*, 2005). Various polymeric materials have been investigated as CO gas sensing materials due to their acid-base or oxidizing characteristics. The unique doping process of a conductive polymer makes it favorable towards the sensing characteristics, but the conductive polymer still has poor selectivity towards gaseous analyzes (Densakulprasert *et. al.*, 2005). The ultimate desired characteristics of gas sensors are: accuracy, reliability, selectivity, sensitivity, rapid responsibility, miniaturization capability, stability and low cost.

Currently, research on new gas sensing materials to be used as matrices on the sensor device is still being pursued. Conductive polymers have received increasing attention in the field of gas sensing materials (Saxena *et. al.*, 2003). The combination of conductive polymers with other materials such as metals or metaloxide nanoparticles (Ram *et. al.*, 2005), carbon nanotubes , and insulating polymers (Hosseini *et. al.*, 2003) have been developed and studied.

Conductive polymers offer various advantages in sensor applications over their metallic counterparts: they are relatively low cost, their fabrication techniques are simple, they can be deposited on various types of substrates, they offer a wide choice of chemical structures, and their sensors can operate at near room temperature (Prissanaroon *et. al.*, 2000). Poly(3,4-ethylenedioxythiophene), or PEDOT, possesses excellent properties: ease of synthesis, excellent stability, and wet processability

when doped with poly(styrene sulfonic acid) (PSS) (Groenendaal *et. al.*, 2000). Because of these properties, PEDOT-PSS or PSS-doped PEDOT are potential candidates as new and unique sensory materials.

Recently, zeolites have been used in gas sensor applications in combination with conductive polymers (Chuapradit *et. al.*, 2005). Because of the well-defined structure of a zeolite, it can separate the desired gas molecule from others and the presence of a cation in the cavity also facilitates gas interactions. The main reason for mixing a conductive polymer with a zeolite is to combine the advantages of the two materials. In our work, we propose to combine a conductive polymer, PEDOT, with ZSM-5 zeolites to investigate the potential of the composites for use as CO sensing materials. The effect of Si/Al ratios of the zeolite on electrical sensitivity responses of the composites are investigated and reported here.

### **3.3 Experimental**

#### **3.3.1 Materials**

As the monomer, 3,4-ethylenedioxythiophene, EDOT (AR grade, Aldrich), was used. Poly(styrene sulfonic acid), PSS, was used as the dopant. Sodium persulfate,  $\text{Na}_2\text{S}_2\text{O}_8$  (AR grade, Aldrich), was used as the oxidant. Zeolite ZSM-5 samples (Si/Al: 23, 50, 80, and 280) in powder form were purchased from Zeolyst International and used in this experiment. Carbon monoxide gas (TIG, 1000 ppm) and nitrogen gas (TIG, 99% purity) were used to investigate the electrical conductivity sensitivity responses of the composites.

#### **3.3.2 Polymerization of Poly(3,4-ethylenedioxythiophene)**

PEDOT-PSS at various EDOT:PSS mole ratios in the range of 1:1 to 1:10 were prepared by mixing 3,4-ethylenedioxythiophene, the PSS solution, and  $\text{Na}_2\text{S}_2\text{O}_8$  in water. After initial stirring at room temperature for 10 minutes,  $\text{Fe}_2(\text{SO}_4)_3$  was added and the mixture was stirred vigorously for 24 hrs. The obtained dark, aqueous PEDOT-PSS mixture was purified by ion exchange with Lewatit M600 and Lewatit S100, resulting in dark blue, aqueous PEDOT-PSS solution. A transparent

film of PEDOT-PSS was obtained by casting the aqueous PEDOT-PSS solution at 100°C for 24 hrs in a vacuum oven.

### 3.3.3 Composite Preparation

PEDOT-PSS powder was ground, sieved with a 38  $\mu\text{m}$  sieve, and then dried prior to mechanically mixing with dried zeolite powders at a zeolite amount of 20 % (v/v). The mixtures were obtained by compressing with a hydraulic press machine at a pressure of 6 kN into a thin disc with a diameter of 10 mm and a nominal thickness of 1 mm.

### 3.3.4 Characterization

A Fourier transform infrared spectrometer (FTIR Nicolet, Nexus 670) with a resolution of 4  $\text{cm}^{-1}$  and the number at scans of 32 was used to characterize the functional groups and the frequency changes before, during, and after CO exposure. The thermal stability of the PEDOT-PSS was investigated by using a thermogravimetric analyzer (Dupont, TGA 2950) with a heating rate of 10  $^{\circ}\text{C}/\text{min}$  under  $\text{O}_2$  atmosphere. A scanning electron microscope (SEM JEOL, JSM 5200) was used to observe the morphology of the PEDOT-PSS, zeolites, and PEDOT-PSS/zeolite composites in powder form. An X-ray diffractometer (XRD Phillips, Rigaku) was used to examine the degree of crystallinity of the PEDOT-PSS and the crystal order of the zeolites. The surface area, pore width and pore volume of the ZSM-5 zeolite were measured using a surface area analyzer (Sorptomatic-1990). Temperature programmed desorption (Micromeritics, TPD/TPR 2900) was conducted and the HZSM-5 zeolite was pretreated at 500  $^{\circ}\text{C}$ . CO was adsorbed at room temperature and subsequently flushed with He. The TPD was started by increasing the temperature up to 600 $^{\circ}\text{C}$  with 10 $^{\circ}\text{C}/\text{min}$  ramp.

### 3.3.5 Electrical Conductivity Measurement and Gas Detection

The electrical conductivity values of the PEDOT-PSS, ZSM-5 zeolites, and its composites under exposure to air,  $\text{N}_2$ , and, CO were measured in a special gas cell. It consisted of two stainless steel chambers connected in series. The first chamber and the second chamber were called mixing and measurement

chambers, respectively. Temperature controllers connected to both chambers were used to monitor and control the temperature within the gas chambers. The second chamber contained two custom-built two-point probe meters connected to a voltage supply (Keithley, 6517A) for applying the constant voltage source (S/cm) values of  $\sigma$  and recording the resultant current. The specific conductivity of the pellets were obtained by measuring the bulk pellet resistance  $R$  ( $\Omega$ ). The relationship  $\sigma = (1/Rt)(1/K) = (I/Vt)(1/K)$  was used to calculate specific conductivity, where  $t$  is the pellet thickness (cm),  $I$  is the resultant current (A),  $V$  is the applied voltage (V), and  $K$  is the geometric correction factor, which is equal to the ratio  $w/l$ , where  $w$  and  $l$  are the probe width and the length, respectively. The geometrical correction factor ( $K$ ) was determined by calibrating the custom-built two-point probe with semi-conducting silicon sheets of known resistivity values. Electrical conductivity values of several samples were first measured at various applied DC voltages to identify their linear Ohmic regimes. The electrical conductivity response and sensitivity of the composites were determined from following the equations:  $\Delta\sigma = \sigma_{CO} - \sigma_{N_2\ initial}$  and  $\Delta\sigma / \sigma_{N_2\ initial}$ , respectively.

### 3.4 Results and Discussion

#### 3.4.1 Characterization of Poly(3,4-ethylenedioxythiophene)

PEDOT-PSS was synthesized by the polymerization of 3,4-ethylenedioxythiophene (EDOT) in an aqueous solution of PSS using  $S_2O_8^{2-}$  as the oxidant. From the FTIR spectrum of the PEDOT-PSS, the peaks at 1520 and 1339  $cm^{-1}$  can be assigned to the C=C and the C-C stretchings in the thiophene ring (Han *et. al.*, 2007) and the peaks at 929  $cm^{-1}$  and 834  $cm^{-1}$  correspond to the symmetric vibration of C-S bond in the thiophene ring (Chun *et. al.*, 2004). The peaks at 1127 and 1039  $cm^{-1}$  are assigned to the stretching mode of the ethylenedioxy group (Han *et. al.*, 2007), and the peaks at 1198 and 929  $cm^{-1}$  correspond to the  $-SO_3^-$  and the S-OH stretchings of the PSS molecule (Martin *et. al.*, 2004). The vibration of the bending mode of the C-H bond in EDOT monomer ( $\sim 892\ cm^{-1}$ ) is not present. This result confirms the formation of PEDOT molecular chains. The absorption peak at

1645  $\text{cm}^{-1}$  can be assigned to the oxidation state of PEDOT which indicates the successful doping of the PEDOT polymer with PSS. In summary, the FTIR spectrum data indicate the successful formation of PEDOT molecular chains doped with PSS counterion. Four transitions were observed in the PEDOT-PSS thermograms: 30-110  $^{\circ}\text{C}$ , 160-380  $^{\circ}\text{C}$ , 380-550  $^{\circ}\text{C}$ , and 560-900  $^{\circ}\text{C}$ ; they can be referred to as the loss of water, the side chain degradation, and the polymer backbone degradations of PSS and PEDOT, respectively. From the XRD patterns of the PEDOT-PSS, there is no characteristic peak observed by X-ray diffraction, the broad scattering background indicates the amorphous nature of the materials (Wichiansee *et. al.*, 2009). The mean particle diameter of PEDOT-PSS\_1:1 was determined to be approximately  $34 \pm 0.22 \mu\text{m}$ . The micrograph in Figure 3.1 of PEDOT-PSS particles shows rough surfaces and irregular shapes; they are moderately dispersed. The density of PEDOT-PSS\_1:1 is  $1.4750 \pm 0.0003 \text{ g/cm}^3$ .

#### 3.4.2 Characterization of Zeolite ZSM-5 and Composites

The mean particle diameters of ZSM-5 with Si/Al mole ratios of 23, 50, 80, and 280 are  $5.61 \pm 0.04$ ,  $5.69 \pm 0.21$ ,  $5.78 \pm 0.04$  and  $5.94 \pm 0.19 \mu\text{m}$ , respectively. The morphology of the zeolites and the composites is shown in Figure 3.1. Zeolite ZSM-5 particles possess irregular crystal shapes and appear to be inhomogeneously dispersed in the conductive polymer matrix of the composites. The specific surface areas, pore width, and pore volume of ZSM-5 (Si/Al = 23, 50, 80 and 280) of the H-form are tabulated in Table 3.1. The pore size of zeolites ZSM-5 (Si/Al = 23, 50, 80, and 280) are  $5.85 \pm 0.013$ ,  $5.91 \pm 0.021$ ,  $6.08 \pm 0.017$ , and  $6.21 \pm 0.048 \text{ \AA}$ , respectively. The corresponding surface areas are  $329 \pm 4.7$ ,  $336 \pm 5.1$ ,  $347 \pm 8.6$  and  $355 \pm 2.8, \text{ m}^2/\text{g}$ , respectively. Zeolites ZSM-5 (Si/Al = 23, 50, 80 and 280) have comparable surface areas and pore sizes but zeolites ZSM-5 (23) has a greater pore free volume, and more cations are contained within the pores.

#### 3.4.3 Electrical Conductivity under Air and Nitrogen Exposure

The specific electrical conductivity measurements of PEDOT-PSS, zeolite ZSM-5, and composites under air were carried out at  $27 \pm 1 \text{ }^{\circ}\text{C}$  at 1 atm. The



specific electrical conductivity of the PEDOT-PSS at various EDOT:PSS mole ratios under air exposure is shown in Figure 3.2. It varies from  $(1.169 \pm 0.003) \times 10^1$  S/cm to  $(1.802 \pm 0.612) \times 10^{-3}$  S/cm as the EDOT:PSS mole ratio is varied from 1:1 to 1:10. The specific electrical conductivity of the PEDOT-PSS increases with EDOT:PSS mole ratio due to the reduction of the insulating PSS shell surrounding the conducting PEDOT-PSS grains, which improves the pathways for charge transport (Vacca *et. al.*, 2008). Concerning the influence of the framework Si/Al ratio, we studied a series of zeolites having in common the same structure and charge-balancing cation, but differing in the framework Si/Al ratio in the range of 23-280. The specific electrical conductivity of the zeolites ZSM-5 (Figure 3.2) decreases with increasing Si/Al mole ratio. It varies from  $(1.257 \pm 0.028) \times 10^{-1}$  S/cm to  $(3.957 \pm 1.592) \times 10^{-4}$  S/cm as the Si/Al mole ratio is varied from 23 to 280. This is due to the increase in the number of cations present with decreasing Si/Al ratio. Therefore, the ion migration increases which enhances the apparent electrical conductivity (Álvaro *et. al.*, 2006). For the composites of PEDOT-PSS\_1:1 with zeolite ZSM-5, the same result occurs for the specific electrical conductivity (Figure 3.2); it varies from  $(7.415 \pm 0.466) \times 10^{-1}$  S/cm to  $(8.853 \pm 0.509) \times 10^{-2}$  S/cm as Si/Al mole ratio is varied from 23 to 280. The specific electrical conductivity values of the composites are lower than the pure PEDOT-PSS\_1:1, but are higher than those of the pure zeolites. The electrical conductivity measurement of PEDOT-PSS\_1:1 under air exposure is greater than the electrical conductivity value under N<sub>2</sub> exposure; this can be related to the interaction of oxygen and moisture in the air with the active sites (Chuapradit *et. al.*, 2005).

#### 3.4.4 Electrical Conductivity Response to Carbon monoxide

The effect of Si/Al ratios of zeolite on the electrical sensitivity responses of the composites was investigated. PEDOT-PSS, with EDOT:PSS mole ratios of 1:1, was chosen and blended with ZSM-5 zeolites (Si/Al = 23, 50, 80 and 280) to form PEDOT-PSS\_1:1/ZSM-5 at a zeolite amount of 20% (v/v). The electrical conductivity response  $(\Delta\sigma = \sigma_{CO} - \sigma_{N_2})$  is identified as the difference in the steady state electrical conductivity value when exposed to the target gas (CO) and the

steady state electrical conductivity value when exposed to N<sub>2</sub> at the same pressure and temperature, namely 1 atm at 27 ± 1 °C. Due to the differences in initial electrical conductivity values of the various composites, the interaction between the target gas and the sensing materials can be compared through the electrical conductivity sensitivity ( $\Delta\sigma/\sigma_{N_2}$ ), which is defined as the ratio of the electrical conductivity response and the electrical conductivity value under pure N<sub>2</sub> exposure at the same pressure and temperature.

The electrical sensitivity values of PEDOT-PSS\_1:1 and its composites with zeolites when exposed to air, N<sub>2</sub>, and CO were measured under a chamber temperature (T<sub>c</sub>) of 27 ± 1 °C at 1 atm (Figure 3.3). The electrical conductivity sensitivity of PEDOT-PSS\_1:1/zeolite ZSM-5 composites toward CO negatively increases with decreasing the Si/Al mole ratio of the ZSM-5 zeolites. PEDOT-PSS\_1:1/ZSM-5(Si/Al = 23) has the highest electrical conductivity sensitivity value,  $(-9.47 \pm 0.10) \times 10^{-1}$  S/cm. For PEDOT-PSS\_1:1/ZSM-5(Si/Al = 50), PEDOT-PSS\_1:1/ZSM-5(Si/Al = 80), PEDOT-PSS\_1:1/ZSM-5(Si/Al = 280), and PEDOT-PSS\_1:1, the sensitivity values are  $(-8.03 \pm 0.12) \times 10^{-1}$  S/cm,  $(-5.98 \pm 0.14) \times 10^{-1}$  S/cm,  $(-8.45 \pm 0.14) \times 10^{-2}$  S/cm, and  $(-5.72 \pm 0.14) \times 10^{-2}$  S/cm, respectively. This result can be related to fact that the amount of cations increases with decreasing Si/Al ratio. ZSM-5(Si/Al = 23) has the highest aluminum content and thus the highest cation content in its zeolite framework; this leads to a higher number and strength of active sites available on the surface for the target gas molecules to diffuse deeper into the composites, and this enhances the interaction between the conductive polymer and the target gas; and the sensitivity increases. Further evidence is that we find that the recoverable response of PEDOT-PSS\_1:1/ZSM-5(Si/Al = 23) is  $(-1.04 \pm 0.81) \times 10^{-4}$  whereas the initial response is  $(-5.92 \pm 4.05) \times 10^{-3}$ ; thus a great difference in response is observed. This suggests that the electrical conductivity response is irreversible when CO is replaced by N<sub>2</sub>. The irreversibility of conductive polymers has been reported in some literature. However, the irreversibility mechanism is still not clear. In a previous work, the researchers used a Ni-containing polymer, poly(ethylene oxide), as the active sensing material to detect the presence of carbon monoxide gas. In small concentrations, the sensor was

fully recoverable; however, for very large concentrations, irreversible chemical changes in the polymeric sensing material occurred (Kooser *et. al.*, 2004).

The temporal response time ( $t_r$ ) is the time required for the electrical conductivity value to rise from its initial value in  $N_2$  towards the equilibrium value when exposed to CO. The temporal response times of PEDOT-PSS\_1:1, PEDOT-PSS\_1:1/ZSM-5(Si/Al = 23), PEDOT-PSS\_1:1/ZSM-5(Si/Al = 50), PEDOT-PSS\_1:1/ZSM-5(Si/Al = 80), and PEDOT-PSS\_1:1/ZSM-5(Si/Al = 280) are 37, 87, 60, 52, and 46 minutes, respectively. By adding ZSM-5, a longer response time is observed, and the response time increases with decreasing Si/Al mole ratios of the ZSM-5. The response time of PEDOT-PSS\_1:1/ZSM-5(Si/Al = 23) is longer than PEDOT-PSS\_1:1 and that of the other composites, corresponding to the higher density of the adsorption sites available for CO molecules. The addition of ZSM-5 zeolites can thus enhance the interaction between PEDOT-PSS\_1:1 and CO molecules; thus the zeolites can improve the sensitivity of the pristine PEDOT-PSS\_1:1, but at the expense of a longer response time.

#### 3.4.5 Investigation of Interactions of Adsorbed CO

The interaction of CO and PEDOT-PSS was further investigated via FTIR spectroscopy under 1 atm at  $27 \pm 1$  °C. The FTIR spectra of PEDOT-PSS before, during, and after the CO exposure are shown in Figure 3.5. The adsorption peak that indicates the doping level of the polymer at  $1645\text{ cm}^{-1}$  shifts to a lower wave-number position ( $1635\text{ cm}^{-1}$ ) after exposing to CO gas. This result is evidently related to the observed decrease in electrical conductivity of PEDOT-PSS when exposed to CO (Yang *et. al.*, 2007). When the PEDOT-PSS is exposed to CO, the negative charge at the carbon atom of  $^-\text{C}\equiv\text{O}^+$  is incorporated into the polymer backbone of the PEDOT (Figure 4). The positive charge of the polymer backbone becomes neutral and the transport of charge carriers is hindered, thus accounting for the decrease in electrical conductivity of the PEDOT-PSS under CO exposure. When CO is removed, the adsorption peak at  $1635\text{ cm}^{-1}$  remains observable. This indicates that the interaction between CO and PEDOT-PSS is irreversible, corresponding to the irreversible conductivity response observed when replacing CO by  $N_2$ .

The temperature programmed desorption experiment (TPD) was carried out, after the saturation of adsorption of CO and flushing with He. TPD thermograms of ZSM-5 zeolites of various Si/Al ratios are shown in Figure 6. Adsorbed CO was desorbed during TPD starting from about 27 °C and ending at about 600 °C. This suggests that the adsorbed CO on HZSM-5 is also present as the chemisorbed species (or irreversibly adsorbed), with the exception of HZSM-5 with Si/Al= 280 where no CO desorption can be detected during the TPD experiment. This observation indicates that chemisorption of CO on ZSM-5(280) does not occur. Thus, the TPD thermograms are consistent with the results obtained from FTIR and electrical conductivity sensitivity responses; this is due to the weak base properties of the CO molecule. The TPD thermograms suggest a weak chemical interaction between H<sup>+</sup> and CO. The TPD thermograms of ZSM-5 show two desorption peaks: the low-temperature peak and the high-temperature peak; this result can be related to the weak active site and the strong active site, respectively. The thermogram peak of HZSM-5(23) is greater than the others, which indicates that more active sites are available for CO adsorption relative to the other HZSM-5 samples (Auerbach *et. al.*, 2001)

### 3.5 Conclusions

Poly(3,4-ethylenedioxythiophene) doped with poly(styrene sulfonic acid), PEDOT-PSS, was successfully synthesized via oxidative polymerization at various EDOT to PSS mole ratios. The composites with PEDOT-PSS as the matrix containing ZSM-5 zeolites of various Si/Al ratios at 20% (v/v) were used to investigate the electrical conductivity sensitivity responses towards CO. The specific electrical conductivity of the PEDOT-PSS increases with increasing EDOT-to-PSS mole ratios and the specific electrical conductivity of ZSM-5 increases with decreasing Si/Al mole ratios. The electrical conductivity sensitivity of PEDOT-PSS\_1:1/zeolite ZSM-5 composites towards CO negatively increases with decreasing Si/Al mole ratio of the ZSM-5 zeolite. PEDOT-PSS\_1:1/ZSM-5(Si/Al = 23) has the highest electrical conductivity sensitivity response. The addition of ZSM-5 enhances the interaction between the PEDOT-PSS and CO gas, a desired characteristic of the

zeolites. However, the composites produce irreversible responses; thus further work is required before it can be used as a CO sensing material. Heat treatment is one possible way to regenerate or to renew the sensing material, but the change in electrical conductivity of the PEDOT-PSS and the stability of the PEDOT-PSS should be taken into consideration

### 3.6 Acknowledgements

The authors are grateful for the financial support from the Conductive and Electroactive Polymers Research Unit of Chulalongkorn University, the Center of Petroleum Petrochemical and Advanced Materials, the Royal Thai Government (Budget of Fiscal Year 2552), and the Thailand Research Fund (PHD/0082/2550, and BRG).

### 3.7 References

- Adhikari, B. and Majumdar, S. (2004) Polymers in sensor applications. Progress in Polymer Science, 29, 699-766.
- Alvaro, M., Cabeza, J.F., Fabuel, D., García, H., Guijarro, E., and de-Juan, J.L.M. (2006) Electrical Conductivity of Zeolite Films: Influence of Charge Balancing Cations and Crystal Structure. Chemistry of Materials, 18, 26-33.
- Auerbach, S.M., Carrado, K.A., and Dutta, P.K. (2003) Handbook of Zeolite Science and Technology, New York: Marcel Dekker.
- Bai, H. And Shi G. (2007) Gas Sensors Based on Conducting Polymers. Sensors, 7, 267-307.
- Bavastrelloa, V., Erokhina, V., Carraraa, S., Sbranab, F., Riccib, D., and Nicolini, C. (2004) Morphology and conductivity in poly(ortho-anisidine)/carbon nanotubes nanocomposite films. Thin Solid Films, 468, 17-22. [14] Y. Chen, Y. Li, H. Wang, M. Yang, Carbon 45 (2007) 357–363.

- Bhambare, K.S., Gupta, S., Mench, M.M., and Ray, A. (2008) A carbon monoxide sensor in polymer electrolyte fuel cells based on symbolic dynamic filtering. Sensors and Actuators B, 134, 803-815.
- Chuapradit, C., Wannatong, L.R., Chotpattananont, D., Hiamtup, P., Sirivat, A., and Schwank, J. (2005) Polyaniline/zeolite LTA composites and electrical conductivity response towards CO. Polymer, 46, 947-953.
- Costa, C., Dzikh, I.P., Lopes, J.M., and Lemos, F. (2000) Activity–acidity relationship in zeolite ZSM-5. Application of Brønsted-type equations. Journal of Molecular Catalysis A, 154, 193-201.
- Densakulprasert, N., Wannatong, L., Chotpattananont, D., Hiamtup, P., Sirivat, A., and Schwank, J. (2005) Electrical conductivity of polyaniline/zeolite composites and synergetic interaction with CO. Materials Science and Engineering B, 117, 276-282.
- Dixit, V., Misra, S.C.K., and Sharma, B.S. (2005) Carbon monoxide sensitivity of vacuum deposited polyaniline semiconducting thin films. Sensors and Actuators B, 104, 90-93.
- Fang, Y. K. and Lee, J. J. (1989) A tin oxide thin film sensor with high ethanol sensitivity. Thin Solid Films, 169, 51-56.
- Guernion, N., de Lacy Costello, B.P.J., and Ratcliffe, N.M. (2002) The synthesis of 3-octadecyl- and 3-docosylpyrrole, their polymerisation and incorporation into novel composite gas sensitive resistors. Synthetic Metals, 128, 139-147.
- Garreau, S., Louarn, G., Buisson, J.P., Froyer, G., and Lefrant, S. (1999) In Situ Spectroelectrochemical Raman Studies of Poly (3, 4 ethylenedioxythiophene)(PEDT). Macromolecules, 32, 6807-6812. [25] L. Chun, T. Imae, Macromolecules 37 (2004) 2411-2416.
- Groenendaal, L., Jonas, F., Freitag, D., Pielartzik, H., and Rynolds, J.R. (2000) Poly(3,4-ethylenedioxythiophene) and Its Derivatives: Past, Present, and Future. Advance Materials, 12, 482-494.
- Han, D., Yang, G., Song, J., Niu, L., and Ivaska, A. (2007) Morphology of electrodeposited poly(3,4-ethylenedioxythiophene)/poly(4-styrene sulfonate) films. Journal of Electroanalytical Chemistry, 602, 24-28.

- Hosseini, S. H. and Entezami, A.A. (2003) Conducting polymer blends of polypyrrole with polyvinyl acetate, polystyrene, and polyvinyl chloride based toxic gas sensors. Journal of Applied Polymer Science, 90, 49-62.
- Jonsson, S.K.M., Birgerson, J., Crispin, X., Greczynski, G., Osikowicz, W., van der Gon, A.W.D., Salaneck, W.R., and Fahlman, M. (2003) The effects of solvents on the morphology and sheet resistance in poly(3,4-ethylenedioxythiophene)-polystyrenesulfonic acid (PEDOT-PSS) films. Synthetic Metals, 139, 1-10.
- Kiebooms, R., Aleshin, A., Hutchison, K., Wudl, F., and Heeger, A. (1999) Doped Poly(3,4-ethylenedioxythiophene) Films: Thermal, Electromagnetical and Morphological Analysis. Synthetic Metals, 101, 436-437.
- Lange, U., Roznyatovskaya, N.V., and Mirsky, V.M. (2008) Conducting polymers in chemical sensors and arrays. Analytica Chimica Acta, 614, 1-26.
- Louwet, F., Groenendaal, L., Dhaen, J., Manca, J., Van, Luppen J., Verdonck, E., and Leenders, L. (2003) PEDOT/PSS: synthesis, characterization, properties and applications. Synthetic Metals, 135-136, 115-117.
- Martin, B.D., Nikolov, N., Pollack, S.K., Saprigin, A., Shashidhar, R., Zhang, F., and Heiney, P.A. (2004) Hydroxylated secondary dopants for surface resistance enhancement in transparent poly(3,4-ethylenedioxythiophene)-poly(styrenesulfonate) thin films. Synthetic Metals, 142, 187-193.
- Mathur, S.C.K., Mathur P., and Srivastava B.K. (2004) Vacuum-deposited nanocrystalline polyaniline thin film sensors for detection of carbon monoxide. Sensors and Actuators A, 114, 30-35.
- Prissanaroon, W., Ruangchuay, L., Sirivat, A., and Schwank, J. (2000) Electrical conductivity response of dodecylbenzene sulfonic acid-doped polypyrrole films to SO<sub>2</sub>-N<sub>2</sub> mixtures. Synthetic Metals, 114, 65-72.
- Ram, M. K., Yavuz, O., and Aldissi, M. (2005) NO<sub>2</sub> gas sensing based on ordered ultrathin films of conducting polymer and its nanocomposite. Synthetic Metals, 151, 77-84.
- Ram, M.K., Yavuz, O., Lahsangah, V., and Aldissi, M. (2005) CO gas sensing from ultrathin nano-composite conducting polymer film. Sensors and Actuators B, 106, 750-757.

- Saxena, V. and Malhotra B.D. (2003) Prospects of conducting polymers in molecular electronics. Current Applied Physics, 3, 293-305.
- Soontornworajit, B., Wannatong, L., Hiamtup, P., Niamlang, S., Chotpattananont, D., Sirivat, A., and Schwank, J. (2007) Induced interaction between polypyrrole and SO<sub>2</sub> via molecular sieve 13X. Materials Science and Engineering B, 136, 78-86.
- Thuwachaowsoan, K., Chotpattananont, D., Sirivat, A., Rujiravanit, R., and Schwank, J.W. (2007) Electrical conductivity responses and interactions of poly(3-thiopheneacetic acid)/zeolites L, mordenite, beta and H<sub>2</sub>. Materials Science and Engineering B, 140, 23-30.
- Vacca, P., Petrosino, M., Miscioscia, R., Nenna, G., Minarini, C., Sala, D.D., and Rubino, A. (2008) Poly(3,4-ethylenedioxythiophene):poly(4-styrenesulfonate) ratio: Structural, physical and hole injection properties in organic light emitting diodes. Thin Solid Films, 516, 4232-4237.
- Watcharaphalakorn, S., Ruangchuay, L., Chotpattananont, D., Srivat, A., and Schwank, J. (2005) Polyaniline/polyimide blends as gas sensors and electrical conductivity response to CO-N<sub>2</sub> mixtures. Polymer International, 54, 1126-1133
- Wichiansee, W. and Sirivat, A. (2009) Electrorheological properties of poly(dimethylsiloxane) and poly(3,4-ethylenedioxy thiophene)/poly(styrene sulfonic acid)/ethylene glycol blends. Materials Science and Engineering C, 29, 78-84.
- Yang, Y., Jiang, Y., Jianhua, X., and Junsheng, Y. (2007) Conducting polymeric nanoparticles synthesized in reverse micelles and their gas sensitivity based on quartz crystal microbalance. Polymer, 48, 4459-4465.



**Table 3.1** The specific surface areas, the pore width, and the pore volume of ZSM-5 (Si/Al = 23, 50, 80 and 280)

Sample	Si/Al mole ratio	Surface area (m <sup>2</sup> /g)	Pore width (Å)	Pore volume (cm <sup>3</sup> /g)	Crystal size μm
ZSM-5(23)	23	329 ± 4.7	5.85 ± 0.013	0.39 ± 0.015	5.61 ± 0.04
ZSM-5(50)	50	336 ± 5.1	5.91 ± 0.021	0.35 ± 0.013	5.69 ± 0.21
ZSM-5(80)	80	347 ± 8.6	6.08 ± 0.017	0.28 ± 0.011	5.78 ± 0.04
ZSM-5(280)	280	355 ± 2.8	6.21 ± 0.048	0.27 ± 0.023	5.94 ± 0.19

**Table 3.2** The specific conductivity (S/cm) of PEDOT-PSS, zeolites ZSM-5, and PEDOT-PSS\_1:1/ZSM-5 composites when exposed to air under chamber temperature ( $T_c$ ) of  $27 \pm 1$  °C

<b>Sample</b>	<b>Specific conductivity (S/cm)</b>
PEDOT-PSS 1:1	$(1.169 \pm 0.003) \times 10^1$
PEDOT-PSS 1:2	$(3.234 \pm 0.008) \times 10^0$
PEDOT-PSS 1:3	$(1.251 \pm 0.001) \times 10^{-1}$
PEDOT-PSS 1:4	$(2.295 \pm 0.004) \times 10^{-2}$
PEDOT-PSS 1:10	$(1.802 \pm 0.612) \times 10^{-3}$
ZSM-5(23)	$(1.257 \pm 0.028) \times 10^{-1}$
ZSM-5(50)	$(3.726 \pm 0.283) \times 10^{-2}$
ZSM-5(80)	$(1.690 \pm 0.223) \times 10^{-2}$
ZSM-5(280)	$(3.957 \pm 1.592) \times 10^{-4}$
PEDOT-PSS 1:1/ ZSM-5(23)	$(7.415 \pm 0.466) \times 10^{-1}$
PEDOT-PSS 1:1/ ZSM-5(50)	$(2.794 \pm 0.085) \times 10^{-1}$
PEDOT-PSS 1:1/ ZSM-5(80)	$(1.333 \pm 0.105) \times 10^{-1}$
PEDOT-PSS 1:1/ ZSM-5(280)	$(8.853 \pm 0.509) \times 10^{-2}$

**Table 3.3** Electrical sensitivity of PEDOT-PSS\_1:1 and its composites when exposed to CO under chamber temperature ( $T_c$ ) of  $27 \pm 1$  °C, asnd at 1 atm,  $K =$  correction factor =  $3.625 \times 10^{-4}$  (probe no. 1) and  $7.759 \times 10^{-4}$  (probe no. 2)

Samples	$\Delta\sigma$ (S/cm)	$\Delta\sigma/\sigma_{N2int}$	$\Delta\sigma_r$ (S/cm)
PEDOT-PSS_1-1	$(-6.41 \pm 1.55) \times 10^{-1}$	$(-5.72 \pm 0.14) \times 10^{-2}$	$(-7.22 \pm 1.39) \times 10^0$
PEDOT-PSS_1:1/ZSM-5 (23)	$(-5.92 \pm 4.05) \times 10^{-3}$	$(-9.47 \pm 0.10) \times 10^{-1}$	$(-1.04 \pm 0.81) \times 10^{-4}$
PEDOT-PSS_1:1/ZSM-5 (50)	$(-4.24 \pm 2.83) \times 10^{-3}$	$(-8.03 \pm 0.12) \times 10^{-1}$	$(-4.34 \pm 1.13) \times 10^{-4}$
PEDOT-PSS_1:1/ZSM-5 (80)	$(-1.24 \pm 0.35) \times 10^{-3}$	$(-5.98 \pm 0.96) \times 10^{-1}$	$(-4.56 \pm 0.26) \times 10^{-4}$
PEDOT-PSS_1:1/ZSM-5 (280)	$(-4.69 \pm 0.16) \times 10^{-4}$	$(-8.45 \pm 1.71) \times 10^{-2}$	$(-3.71 \pm 0.72) \times 10^{-5}$

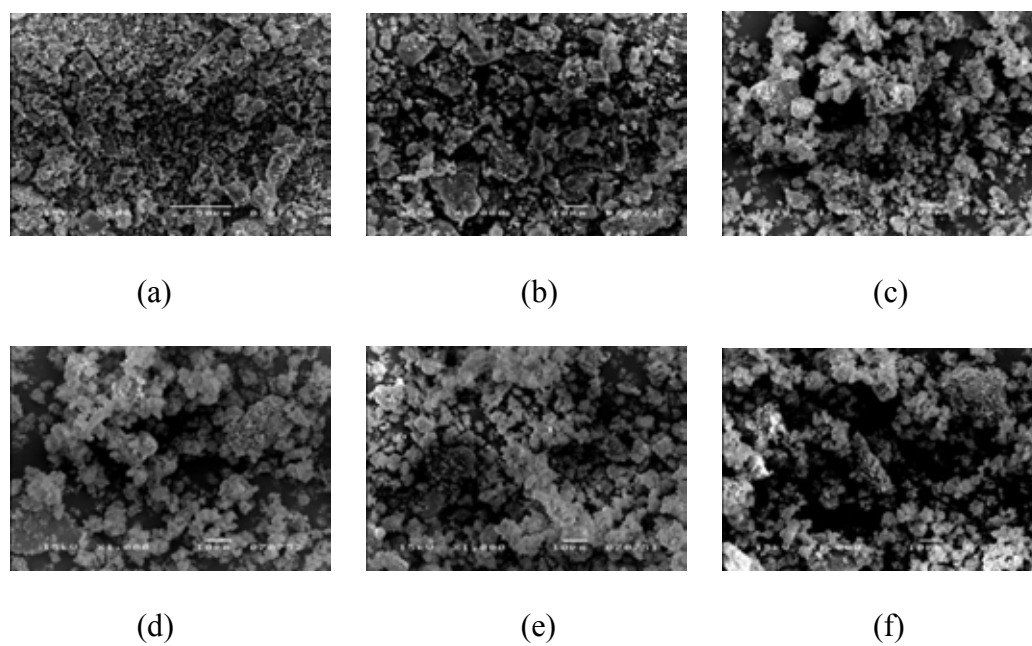
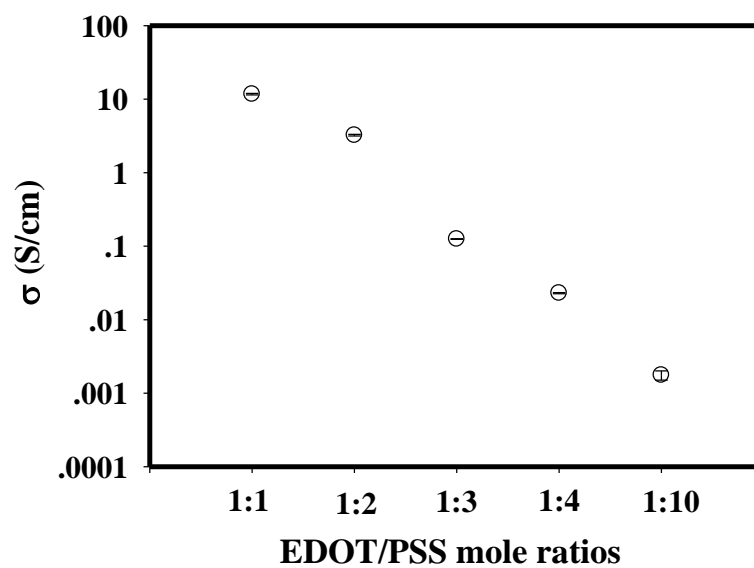
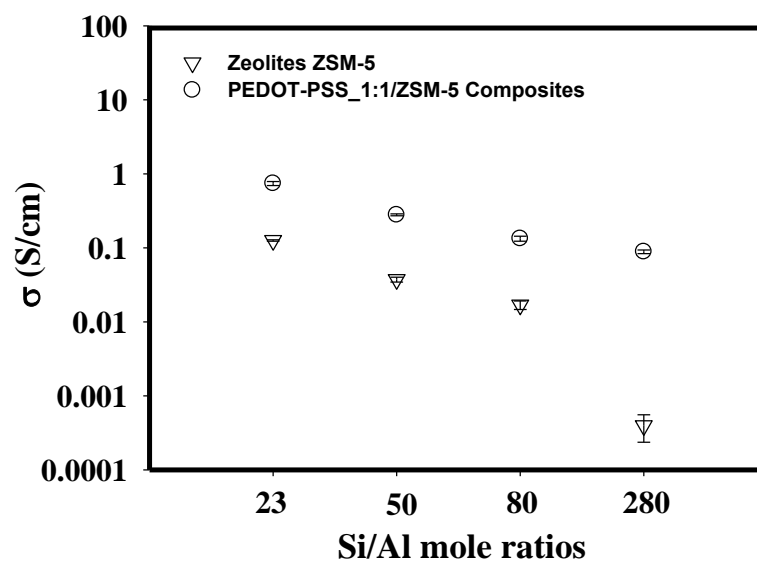


**Figure 3.1** Morphology of PEDOT-PSS<sub>1:1</sub> particles, ZSM-5 powders, and PEDOT-PSS<sub>1:1</sub>/zeolite composites: a) PEDOT-PSS<sub>1:1</sub> at 500x; b) PEDOT-PSS<sub>1:1</sub> at 1000x; c) PEDOT-PSS<sub>1:1</sub>/ ZSM-5(23) at 1000x; d) PEDOT-PSS<sub>1:1</sub>/ ZSM-5(50) at 1000x; e) PEDOT-PSS<sub>1:1</sub>/ ZSM-5(80) at 1000x; and f) PEDOT-PSS<sub>1:1</sub>/ ZSM-5(280) at 1000x.



(a)



(b)

**Figure 3.2** The specific electrical conductivity (S/cm) of: (a) PEDOT-PSS; (b) ZSM-5 and PEDOT-PSS\_1:1/ZSM-5 when exposed to air at temperature ( $T_c$ ) of  $27 \pm 1$  °C.

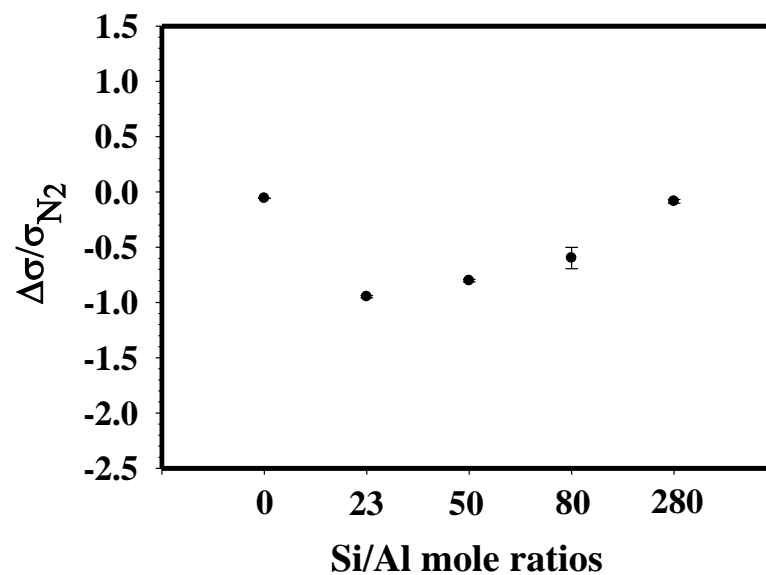


**Figure 3.3** Electrical conductivity sensitivity values of PEDOT-PSS\_1:1 and PEDOT-PSS\_1:1/ZSM-5 composites when exposed to CO (1000 ppm) at temperature ( $T_c$ ) of  $27 \pm 1$  °C, and at 1 atm.

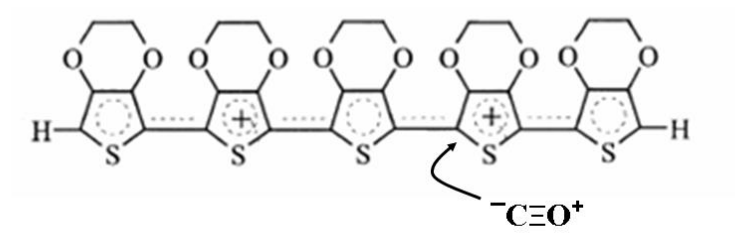


**Figure 3.4** Proposed mechanism of CO-PEDOT interaction.

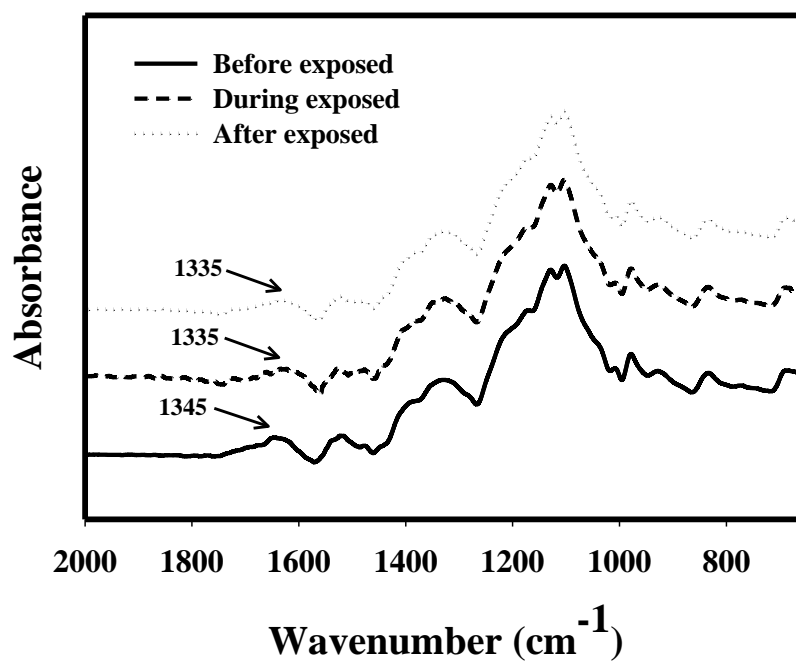


**Figure 3.5** FTIR spectra of PEDOT-PSS: before, during and after exposed to CO.



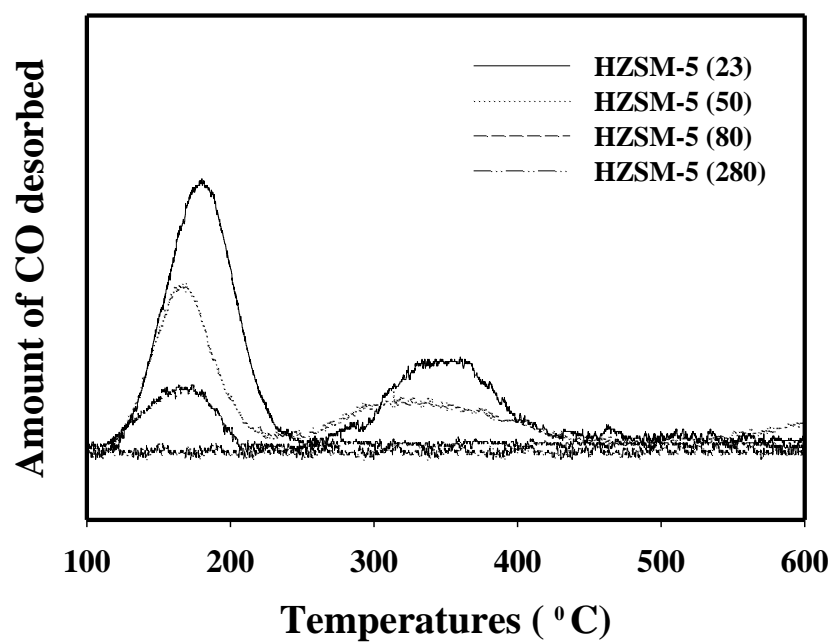


**Figure 3.6** CO-TPD thermograms of HZSM-5 of various Si/Al ratios.

## CHAPTER IV

### EFFECT OF ALKALINE AND ALKALINE EARTH ION-EXCHANGED ZEOLITES Y ON ELECTRICAL CONDUCTIVITY AND RESPONSE OF PEDOT-PSS/ZEOLITE Y COMPOSITES TOWARD SULFUR DIOXIDE

#### 4.1 Abstract

This work reports the association of a conductive polymer and zeolite framework towards SO<sub>2</sub>. Responses and the interaction mechanism of conductive polymer/zeolite composites sensor were investigated. Poly(3,4-ethylenedioxythiophene)(PEDOT)/poly(styrene sulfonic acid) (PSS) complexes were prepared at 1:1 molar ratio of EDOT/PSS. The adsorption properties of the faujasite zeolite type (sodium form) with a Si/Al mole ratio of 5.1 were modified by changing the existing cation with alkaline and alkaline earth metal. Composites with PEDOT-PSS matrix containing faujasite zeolites type Y were fabricated to investigate the effects of zeolite content (v/v%) and cation type (univalent cation: H<sup>+</sup>, Li<sup>+</sup>, Na<sup>+</sup> and K<sup>+</sup>; divalent cation: Mg<sup>2+</sup>, Ca<sup>2+</sup> and Ba<sup>2+</sup>) of faujasite zeolite type Y on the electrical conductivity response when exposed to sulphur dioxide. The highest electrical conductivity response and sensitivity belong to the PEDOT-PSS/KY composite. The types of cation in zeolite Y micropores can tuning adsorption-desorption properties of zeolite Y, which influence the electrical sensitivity of the composite. The composites showed reversibility to detect SO<sub>2</sub>.

**Keywords:** Conducting polymers; Poly (3,4-ethylenedioxythiophene); Faujasite; Zeolite Y; Sulphur dioxide; Gas Sensor

## 4.2 Introduction

Emission of sulfur dioxide (SO<sub>2</sub>) to the atmosphere is of high concern with the primary toxic gas being mainly produced by the use of fossil fuels in the electric power generation industry. Other sources of sulfur dioxide in the air come from heavy industries and heavy vehicles using diesel (Micallef, 2004). Exposure to sulfur dioxide at a certain level by breathing it from the air can cause serious injury to people since it can burn the nose and throat and causing breathing difficulties and obstructing airways. Consequently, the appropriate detection of sulfur dioxide is an issue of major interest in the related gas sensing industry (George *et al.*, 2000).

In recent decades, the study of new materials with unique properties for monitoring SO<sub>2</sub> and other toxic gases has been of interest. Various kinds of gas sensor devices, such as solid electrolyte, oxide semiconductors, zeolite-based gas sensors, mixed sensors, and so on, have been investigated (Srivastava *et al.*, 2006). However, most devices are well suited for use in high temperature and have some limitations such as high cost, low sensitivity, low selectivity, and low reproducibility. Among these materials, the use of conductive polymer as gas sensing materials has been reported on numerous occasions. Due to their properties, they can be operated at room temperature, of low cost, and ease to synthesize (Prissanaroon *et al.*, 2000). Recently, the effective use zeolites for improving sensor responses has been demonstrated (Vilaseca *et al.*, 2006). The aluminosilicate framework structure allows gas molecules to diffuse into the channels and the pores of the zeolite. The electronegative charge of the framework is compensated by the electropositive ion whose ion size and charge depend on the pore geometry of the framework. Charge compensation allows the ion-exchange process with alkaline, alkaline earth, or transition metal cations, resulting in a change of gas adsorption behavior of the zeolite.

A novel strategy in our work is based on the association of a conductive polymer and a zeolite framework. PEDOT-PSS was used as a semiconductor, where its electrical conductivity can be altered when exposed to various gases; the electrical conductivity response depends on the adsorption properties of zeolite microporous material. A faujasite zeolite of type Y with a Si/Al mole ratio of 5.1 was modified by

an ion-exchange process. Sodium form of zeolite Y was subjected to the ion-exchange treatment using chloride solution of alkaline and alkaline earth to produce univalent cation and divalent cation exchange zeolites.

The present work describes the effect of zeolite content (v/v%) and cation type (univalent cation:  $H^+$ ,  $Li^+$ ,  $Na^+$  and  $K^+$ ; divalent cation:  $Mg^{2+}$ ,  $Ca^{2+}$  and  $Ba^{2+}$ ) of faujasite zeolite type Y on the electrical conductivity and sensitivity response of PEDOT-PSS/Zeolite Y composites when exposed to sulphur dioxide. The sensor response behavior was investigated including the mechanism involved between the polymer/zeolite composites and sulfur dioxide.

### 4.3 Experimental

#### 4.3.1 Materials

The 3,4-ethylenedioxythiophene, EDOT (AR grade, Aldrich), was used as the monomer. Poly(styrene sulfonic acid), PSS, was used as the dopant. Sodium persulfate,  $Na_2S_2O_8$  (AR grade, Aldrich), was used as the oxidant. Zeolite Y samples (HY and NaY with Si/Al = 5.1) in powder form were purchased from Zeolyst International. Sulphur dioxide gas (TIG, 1000 ppm in  $N_2$ ) and Nitrogen gas (TIG, 99% purity) were used to investigate the electrical conductivity sensitivity responses of the composites.

#### 4.3.2 Polymerization of Poly(3,4-ethylenedioxythiophene)

The chemical polymerization of PEDOT-PSS was followed from the procedures reported in the literature (Groenendaal *et. al.*, 2000). PEDOT-PSS at 1:1 mole ratios of EDOT:PSS was prepared by adding EDOT monomers to an aqueous solution of PSS, and  $Na_2S_2O_8$ . After initial stirring at room temperature for 10 minutes,  $Fe_2(SO_4)_3$  was added and the mixture was stirred vigorously for 24 hrs. The obtained dark, aqueous PEDOT-PSS mixture was purified by the ion exchanging with Lewatit M600 and Lewatit S100, resulting in dark blue, aqueous PEDOT-PSS solution. PEDOT-PSS film was obtained by casting the aqueous PEDOT-PSS solution at 100°C for 24 hrs in a vacuum oven.

#### 4.3.3 Preparation of Ion-exchange Zeolites

The  $M^{n+}$  zeolites studied in this work are faujasite type Y zeolites (Zeolyst, Si/Al = 5.1) with different compensating cations ( $H^+$ ,  $Li^+$ ,  $Na^+$ ,  $K^+$ ,  $Mg^{2+}$ ,  $Ca^{2+}$  and  $Ba^{2+}$ ). The  $Li^+$ ,  $K^+$ ,  $Mg^{2+}$ ,  $Ca^{2+}$  and  $Ba^{2+}$  -exchanged faujasites were carried out using the conventional ion-exchange procedures (Krista *et. al.*, 2006). Zeolites NaY was used as starting materials for the metal-exchange. For metal-exchanged zeolites, 1 g of the zeolite NaY was added to 25 ml of 0.1 M metal chloride solution at room temperature and stirred for 24 h. The modified zeolite was filtered and washed with distilled water to remove  $Cl^-$  ions followed by drying at 373K in air for 24 h.

#### 4.3.4 Composite Preparation

PEDOT-PSS powder was ground, sieved with 38  $\mu m$  sieve, and then dried prior to mechanically mixed with dried zeolite Y powders at various zeolite amount (v/v%). The mixtures were obtained by compressing with a hydraulic press machine at a pressure of 6 kN into a thin disc with a diameter of 10 mm and a nominal thickness of 1 mm.

#### 4.3.5 Characterization

A Fourier transform infrared spectrometer (FTIR Nicolet, Nexus 670) with a resolution of 4  $cm^{-1}$  and a number of scans of 32 was used to characterize functional groups and the frequency changes before, under, and after the  $SO_2$  exposure. The thermal stability of PEDOT-PSS was investigated by using a thermogravimetric analyzer (Dupont, TGA 2950) with a heating rate 10°C/min under  $O_2$  atmosphere. A scanning electron microscope (SEM JEOL, JSM 5200) was used to observe the morphology of PEDOT-PSS, zeolites, and PEDOT-PSS/zeolite composites in a powder form. An X-ray diffractometer (XRD Phillips, Rigaku) was used to examine the degree of crystallinity of PEDOT-PSS and the crystal order of the zeolites. The surface area, the pore width, and the pore volume of zeolite Y were measured using a surface area analyzer (Sorptomatic-1990). The percentage of ion exchange was measured for each zeolite Y sample by inductively coupled plasma technique (Perkin-Elmer/ Optima 4300DV). Temperature programmed desorption

(Micromeritics, TPD/TPR 2900) were conducted, the zeolite Y were pretreated at 773 K.  $\text{NH}_3$  was adsorbed at room temperature and subsequently flushed with He, TPD was started by increasing the temperature up to 873 K with 10 K/min ramp.

#### 4.3.6 Electrical Conductivity Measurement and Gas Detection

The electrical conductivity values of PEDOT-PSS, zeolites Y, and its composites under exposure to air,  $\text{N}_2$  and,  $\text{SO}_2$  were measured in a special gas cell. It consisted of two stainless steel chambers connected in series. The first chamber and the second chamber were called the mixing and measurement chambers, respectively. The temperature controllers, connecting to both chambers, were used to monitor and control the temperature within the gas chambers. The second chamber contained two custom-built two-point probe meters connected to a voltage supplier (Keithley, 6517A) for applying a constant voltage source and recording a resultant current. The specific conductivity  $\sigma$  (S/cm) values of the pellets were obtained by measuring the bulk pellet resistance  $R$  ( $\Omega$ ). The relation  $\sigma = (1/Rt)(1/K) = (I/Vt)(1/K)$  was used to calculate specific conductivity, where  $t$  is the pellet thickness (cm),  $I$  is the resultant current (A),  $V$  is the applied voltage (V) and  $K$  is the geometric correction factor which is equal to the ratio  $w/l$ , where  $w$  and  $l$  are the probe width and the length, respectively. The geometrical correction factor ( $K$ ) was determined by calibrating the custom-built two-point probe with semi-conducting silicon sheets of known resistivity values. Electrical conductivity values of several samples were first measured at various applied DC voltages to identify their linear Ohmic regimes. The electrical conductivity response ( $\Delta\sigma$ ) and sensitivity ( $S$ ) of the composites are defined by the following equation  $\Delta\sigma = \sigma_{\text{SO}_2} - \sigma_{\text{N}_2}$  and  $= \Delta\sigma / \sigma_{\text{N}_2}$ , respectively. Where  $\sigma_{\text{N}_2}$  and  $\sigma_{\text{SO}_2}$  are the electrical conductivity of the composite in  $\text{N}_2$  and target gas  $\text{SO}_2$ , respectively.

## 4.4 Results and Discussion

### 4.4.1 Characterization of PEDOT-PSS, Y Zeolite and Composites

PEDOT-PSS was synthesized by the polymerization of 3,4-ethylenedioxythiophene (EDOT) in an aqueous solution of PSS using  $S_2O_8^{2-}$  as the oxidant. From the FTIR spectrum of the PEDOT-PSS, the peaks at 1520 and 1339  $cm^{-1}$  can be assigned to the C=C and the C-C stretchings in the thiophene ring (Han *et. al.*, 2007) and the peaks at 929  $cm^{-1}$  and 834  $cm^{-1}$  correspond to the symmetric vibration of C-S bond in the thiophene ring (Chun *et. al.*, 2004). The peaks at 1127 and 1039  $cm^{-1}$  are assigned to the stretching mode of the ethylenedioxy group (Han *et. al.*, 2007), and the peaks at 1198 and 929  $cm^{-1}$  correspond to the  $-SO_3^-$  and the S-OH stretchings of the PSS molecule (Martin *et. al.*, 2004). The vibration of the bending mode of the C-H bond in EDOT monomer ( $\sim 892\text{ cm}^{-1}$ ) is not present. This result confirms the formation of PEDOT molecular chains. The absorption peak at 1645  $cm^{-1}$  can be assigned to the oxidation state of PEDOT which indicates the successful doping of the PEDOT polymer with PSS. In summary, the FTIR spectrum data indicate the successful formation of PEDOT molecular chains doped with PSS counterion. Four transitions were observed in the PEDOT-PSS thermograms: 30-110 °C, 160-380 °C, 380-550 °C, and 560-900 °C; they can be referred to as the loss of water, the side chain degradation, and the polymer backbone degradations of PSS and PEDOT, respectively. From the XRD patterns of the PEDOT-PSS, there is no characteristic peak observed by X-ray diffraction, the broad scattering background indicates the amorphous nature of the materials (Wichiansee *et. al.*, 2009). The mean particle diameter of PEDOT-PSS\_1:1 was determined to be approximately  $34 \pm 0.22\ \mu m$ .

The micrograph in Figure 4.1 of PEDOT-PSS particles shows rough surfaces and irregular shapes; they are moderately dispersed. The density of PEDOT-PSS\_1:1 is  $1.4750 \pm 0.0003\text{ g/cm}^3$ . The electrical conductivity of PEDOT-PSS in air and nitrogen atmosphere are  $(1.169 \pm 0.003) \times 10^1\text{ S/cm}$  and  $(1.123 \pm 0.001) \times 10^1\text{ S/cm}$ , respectively.

Zeolite NaY was ion-exchanged by various alkali and alkaline earth cations ( $Li^+$ ,  $K^+$ ,  $Mg^{2+}$ ,  $Ca^{2+}$  and  $Ba^{2+}$ ) with approximate 90% exchanged (Table 4.1).

Comparison of the scanning electron micrographs (SEM) of starting material zeolite NaY and the zeolite powders obtained by ion-exchange method indicates that for all ion-exchange zeolites remained particles typical of Y zeolite with no change of the particle sizes and morphologies after the ion-exchange process. Zeolite Y particles possess irregular crystal shapes and appear to be inhomogeneously dispersed in the conductive polymer matrix of the composites (Figure 4.3). The X-ray diffractogram of all Y zeolites sample show the characteristic peaks of the faujasite framework that it is highly crystalline in the range 5-70 degrees. Comparison of X-ray diffraction patterns of the metal exchanged zeolite to the starting material NaY shows no significant changes in the crystalline structure of the zeolite during the ion-exchange process (Figure 4.4). There were no significant diffraction lines of any new phase and no peak shift in the peak positions are observed after metal ion-exchange due to its low content and high dispersion through ion exchange [30]. The mean particle diameters of  $H^+$ ,  $Li^+$ ,  $Na^+$ ,  $K^+$ ,  $Mg^{2+}$ ,  $Ca^{2+}$  and  $Ba^{2+}$  -exchanged faujasites (Si/Al mole ratios equal to 5.1) are approximate 200 nm (Table 4.1) ( Yang *et. al.*, 2010). The specific surface areas, the pore width and the pore volume, of Y zeolite (Si/Al = 5.1) of the  $H^+$ ,  $Li^+$ ,  $Na^+$ ,  $K^+$ ,  $Mg^{2+}$ ,  $Ca^{2+}$  and  $Ba^{2+}$  form are tabulated in Table 3.1, and the BET surface area and pore volume was exactly consistent with cationic size; that is, in the order of  $Li > Na > K$  and  $Mg > Ca > Ba$ . The BET surface area and pore volume increase as cation size decrease except zeolite HY. This result indicates that larger ion occupies more pore space, resulting in lesser adsorbable sites. For HY zeolite, the result can be related to the amount of cations increases due to the small size of  $H^+$ , leads to the lower surface area and pore volume (Thomas *et. al.*, 2005).

The exchangeable cation in zeolite micropores can alter the acid-base properties, which play an important role in adsorption-desorption properties, which influence the electrical sensitivity of the sensor. The Temperature Programmed Desorption ( $NH_3$ -TPD) technique was used to express the acid strength. The acidity of all ion-exchange zeolites from  $NH_3$ -temperature desorption program technique are show in Table 4.1. For univalent cation zeolite Y, the acidity increases as cation size in zeolite micropore decrease ( $HY > LiY > NaY > KY$ ). The divalent cation Y zeolites show the same result as univalent cation zeolite Y ( $MgY > CaY > BaY$ ). Comparison of univalent and divalent cation zeolite, the divalent cation zeolite Y have higher



acidity (lower basic strength) than univalent cation Y zeolite. The divalent cation zeolites Y have loss basicity related to the negative charge on framework oxygen decrease (Yaremov *et. al.*, 2007).

The electrical conductivity data in N<sub>2</sub>, for the Y zeolites with different cation types are tabulated in Table 1. The HY zeolite has smallest charge balancing cation (0.30 Å) exhibits the lowest electrical conductivity inversely to KY zeolite has the highest electrical conductivity due to the larger cation size (1.38 Å), which leads to a reduced electrostatic interaction with the anionic framework sites and to the ease in which a cation can move from one site to another (Fonseca *et. al.*, 2010).

#### 4.4.2 Electrical Conductivity Response to SO<sub>2</sub>

##### 4.4.2.1 *Effect of Zeolite Content*

The electrical sensitivity values of PEDOT-PSS\_1:1 and its composites with zeolite Y when exposed to air, N<sub>2</sub>, and SO<sub>2</sub> were measured under chamber temperature (T<sub>c</sub>) of 27 ±1 °C, and at 1 atm. The electrical conductivity sensitivity values of PEDOT-PSS/NaY composites in 1000 ppm SO<sub>2</sub>/N<sub>2</sub> versus molecular sieve Y zeolite content are shown in Figure 4.5.

The composites show a negative response to SO<sub>2</sub>. The sensitivity value of PEDOT-PSS/NaY increases as zeolite NaY content increases from 0 to 20%. Beyond this volume fraction, the sensitivity value decreases as zeolite NaY content increases from 20 and 50%, respectively. A more Y zeolite content is added, its presence also reduces the direct contact area between SO<sub>2</sub> and PEDOT, and hence a lower sensitivity response. This result suggests that the preparation of the composite with appropriate zeolite content would raise the sensitivity of the sensor materials.

##### 4.4.2.1 *Effect of Cation Type*

The electrical sensitivity values of PEDOT-PSS\_1:1 and its composites with Y zeolites when exposed to air, N<sub>2</sub>, and SO<sub>2</sub> were measured under chamber temperature (T<sub>c</sub>) of 27±1 °C, and at 1 atm. The electrical conductivity

sensitivity values of PEDOT-PSS/M<sup>n+</sup>Y composites in 1000 ppm SO<sub>2</sub>/N<sub>2</sub> versus molecular sieve Y zeolite content are shown in Figure 4.6. For the composites of PEDOT-PSS/M<sup>+</sup>Y, the electrical sensitivity to SO<sub>2</sub> increases as cation size of zeolite increases. This result is corresponding to the electrical sensitivity to SO<sub>2</sub> of PEDOT-PSS/M<sup>2+</sup>Y composites. PEDOT-PSS/HY composite shows the lowest sensitivity. The result show that zeolite Y acid-base properties effect to the sensitivity of the PEDOT-PSS/Y composites toward SO<sub>2</sub>. The cation type in zeolite Y; depend on gas adsorption characteristics of cation-exchanged zeolite Y. This is consistent with the acidity of ion-exchanged zeolite Y from NH<sub>3</sub>-temperature desorption program technique (Table 4.1).

In the experiment, observation that the cation type in zeolite Y can alter the electrical conductivity and sensitivity response of the composites toward SO<sub>2</sub> influenced the gas adsorption-desorption characteristics of the composites, where the composites with alkaline cations (Li<sup>+</sup>, Na<sup>+</sup> and K<sup>+</sup>) zeolite Y provided the higher sensitivity to SO<sub>2</sub> more than the composite with alkaline earth cation (Mg<sup>2+</sup>, Ca<sup>2+</sup> and Ba<sup>2+</sup>) zeolite Y and zeolite HY. This result related to the acid-base properties of cation-exchanged zeolite Y that alter by cation-exchanged process. In this work, the acid sites were assigned to the compensate cations and the basic sites to the framework oxygen adjacent to the cation. The adjacent cation mainly influenced the framework basic sites. For the composite of alkaline cation-exchanged zeolite Y, the electrical conductivity sensitivity to SO<sub>2</sub> of the composites increases with increasing cation size (electro negativity value decrease and basic strength increase) of cation in zeolite Y due to a lesser interaction between SO<sub>2</sub> and the zeolite, and hence a greater interaction between SO<sub>2</sub> and the active sites on the PEDOT polymer chain. The stronger bonding between lithium cation and oxygen in zeolite induce a higher reduction in negative charge on the adjacent oxygen, resulted in the lower basic strength than other alkaline cation-exchanged. The PEDOT-PSS/KY has the highest electrical sensitivity due to their highest basic strength.

For the composite of divalent exchange or alkaline earth exchanged zeolites, they loss basic activity toward SO<sub>2</sub> due to the higher acid strength so the basic sites of zeolite framework decrease related to the negative charge on framework oxygen decrease resulted in the lower the electrical

conductivity sensitivity than the composite of alkaline cation zeolite Y. Furthermore, PEDO-PSS/HY composite shows the lowest sensitivity toward SO<sub>2</sub> related to the lower surface area and the lower basic strength of zeolite HY resulted in a lesser degree of interaction between acid gas SO<sub>2</sub> molecules and the active sites of the zeolites. In addition, PEDOT-PSS/HY has poor electrical conductivity and it is more hydrophobic, they do not preferred to adsorb polar molecule like SO<sub>2</sub>.

The temporal response time is the time required for the electrical conductivity value to rise from its initial value in N<sub>2</sub> towards the equilibrium value when exposed to SO<sub>2</sub>. The recovery time is the time is the time required for the electrical conductivity value return to baseline value after the step removal of SO<sub>2</sub>. By adding Y zeolite, a longer response time and recovery time are observed, and the response time and recovery time increase with decreasing cation size of the Y zeolite. The response time of PEDOT-PSS/LiY is longer than PEDOT-PSS and that of the other composites (9.8 minutes), corresponding to the higher density of the adsorption sites available for SO<sub>2</sub> molecules and the greater ion-quadrupole interactions with SO<sub>2</sub>. The shortest temporal response and recovery time is obtain from PEDOT-PSS/KY due to the weaker interaction between SO<sub>2</sub> molecules and zeolite KY (6.1 minutes), which allowed SO<sub>2</sub> molecules to diffused from the composites. The addition of Y zeolite zeolites can thus enhance the interaction between PEDOT-PSS and SO<sub>2</sub> molecules; thus the zeolites can improve the sensitivity of the pristine PEDOT-PSS, but at the expense of a longer response time.

The composite is tested three sensing cycles by repeating sensing and recovery to investigate the reversibility and reproducibility of the composites (Figure 4.5). The conductivity of PEDOT-PSS/KY composite, which showed the highest sensitivity for SO<sub>2</sub> gas, as a function of time when exposed to three cycles of a sequence of SO<sub>2</sub> exposure (sensing), evacuation and kept under N<sub>2</sub> atmosphere (recovery). During the recovery process, the conductivity of the composites does not have much decay, which proves that the sensing characteristics are repeatable.

## 4.5 Conclusions

The electrical sensitivity of pristine PEDOT-PSS can improve by added zeolite Y but provided the longer response time and recovery time. The preparation of the composite with 20% (v/v) of zeolite content gives the highest sensitivity to SO<sub>2</sub>. The highest electrical sensitivity response belongs to the PEDOT-PSS/KY composite. The type of cation in zeolite pores can effect to the sensitivity of the composite and consistent with the acidity of ion-exchanged zeolite Y. The composite showed reversibility almost completely at room temperature. The experimental results show that the zeolite acid-base properties play an important role in the sensitivity response of the composite toward SO<sub>2</sub>. With increasing the basicity of ion-exchanged zeolite Y, the sensitivity of the composites increases.

## 4.6 Acknowledgements

The authors would like to acknowledge the financial supports from the Conductive and Electroactive Research Unit of Chulalongkorn University, the Thailand Research Fund (TRF-RTA and PhD/0082/2550), and the Royal Thai Government.

## 4.7 References

- Adhikari, B. and Majumdar, S. (2004) Polymers in sensor applications. Progress in Polymer Science, 29, 699-766.
- Alvaro, M., Cabeza, J.F., Fabuel, D., García, H., Guijarro, E., and de-Juan, J.L.M. (2006) Electrical Conductivity of Zeolite Films: Influence of Charge Balancing Cations and Crystal Structure. Chemistry of Materials, 18, 26-33.
- Auerbach, S.M., Carrado, K.A., and Dutta, P.K. (2003) Handbook of Zeolite Science and Technology, New York: Marcel Dekker.
- Bai, H. And Shi G. (2007) Gas Sensors Based on Conducting Polymers. Sensors, 7, 267-307.

- Bavastrelloa, V., Erokhina, V., Carrara, S., Sbranab, F., Riccib, D., and Nicolini, C. (2004) Morphology and conductivity in poly(ortho-anisidine)/carbon nanotubes nanocomposite films. Thin Solid Films, 468, 17-22. [14] Y. Chen, Y. Li, H. Wang, M. Yang, Carbon 45 (2007) 357–363.
- Bhambare, K.S., Gupta, S., Mench, M.M., and Ray, A. (2008) A carbon monoxide sensor in polymer electrolyte fuel cells based on symbolic dynamic filtering. Sensors and Actuators B, 134, 803-815.
- Chuapradit, C., Wannatong, L.R., Chotpattananont, D., Hiamtup, P., Sirivat, A., and Schwank, J. (2005) Polyaniline/zeolite LTA composites and electrical conductivity response towards CO. Polymer, 46, 947-953.
- Costa, C., Dzikh, I.P., Lopes, J.M., and Lemos, F. (2000) Activity–acidity relationship in zeolite ZSM-5. Application of Brønsted-type equations. Journal of Molecular Catalysis A, 154, 193-201.
- Densakulprasert, N., Wannatong, L., Chotpattananont, D., Hiamtup, P., Sirivat, A., and Schwank, J. (2005) Electrical conductivity of polyaniline/zeolite composites and synergetic interaction with CO. Materials Science and Engineering B, 117, 276-282.
- Dixit, V., Misra, S.C.K., and Sharma, B.S. (2005) Carbon monoxide sensitivity of vacuum deposited polyaniline semiconducting thin films. Sensors and Actuators B, 104, 90-93.
- Fang, Y. K. and Lee, J. J. (1989) A tin oxide thin film sensor with high ethanol sensitivity. Thin Solid Films, 169, 51-56.
- Guernion, N., de Lacy Costello, B.P.J., and Ratcliffe, N.M. (2002) The synthesis of 3-octadecyl- and 3-docosylpyrrole, their polymerisation and incorporation into novel composite gas sensitive resistors. Synthetic Metals, 128, 139-147.
- Garreau, S., Louarn, G., Buisson, J.P., Froyer, G., and Lefrant, S. (1999) In Situ Spectroelectrochemical Raman Studies of Poly (3, 4 ethylenedioxythiophene)(PEDT). Macromolecules, 32, 6807-6812. [25] L. Chun, T. Imae, Macromolecules 37 (2004) 2411-2416.
- Groenendaal, L., Jonas, F., Freitag, D., Pielartzik, H., and Rynolds, J.R. (2000) Poly(3,4-ethylenedioxythiophene) and Its Derivatives: Past, Present, and Future. Advance Materials, 12, 482-494.

- Han, D., Yang, G., Song, J., Niu, L., and Ivaska, A. (2007) Morphology of electrodeposited poly(3,4-ethylenedioxythiophene)/poly(4-styrene sulfonate) films. Journal of Electroanalytical Chemistry, 602, 24-28.
- Hosseini, S. H. and Entezami, A.A. (2003) Conducting polymer blends of polypyrrole with polyvinyl acetate, polystyrene, and polyvinyl chloride based toxic gas sensors. Journal of Applied Polymer Science, 90, 49-62.
- Jonsson, S.K.M., Birgerson, J., Crispin, X., Greczynski, G., Osikowicz, W., van der Gon, A.W.D., Salaneck, W.R., and Fahlman, M. (2003) The effects of solvents on the morphology and sheet resistance in poly(3,4-ethylenedioxythiophene)-polystyrenesulfonic acid (PEDOT-PSS) films. Synthetic Metals, 139, 1-10.
- Kiebooms, R., Aleshin, A., Hutchison, K., Wudl, F., and Heeger, A. (1999) Doped Poly(3,4-ethylenedioxythiophene) Films: Thermal, Electromagnetical and Morphological Analysis. Synthetic Metals, 101, 436-437.
- Lange, U., Roznyatovskaya, N.V., and Mirsky, V.M. (2008) Conducting polymers in chemical sensors and arrays. Analytica Chimica Acta, 614, 1-26.
- Louwet, F., Groenendaal, L., Dhaen, J., Manca, J., Van, Luppen J., Verdonck, E., and Leenders, L. (2003) PEDOT/PSS: synthesis, characterization, properties and applications. Synthetic Metals, 135-136, 115-117.
- Martin, B.D., Nikolov, N., Pollack, S.K., Saprigin, A., Shashidhar, R., Zhang, F., and Heiney, P.A. (2004) Hydroxylated secondary dopants for surface resistance enhancement in transparent poly(3,4-ethylenedioxythiophene)-poly(styrenesulfonate) thin films. Synthetic Metals, 142, 187-193.
- Mathur, S.C.K., Mathur P., and Srivastava B.K. (2004) Vacuum-deposited nanocrystalline polyaniline thin film sensors for detection of carbon monoxide. Sensors and Actuators A. 114, 30-35.
- Prissanaroon, W., Ruangchuay, L., Sirivat, A., and Schwank, J. (2000) Electrical conductivity response of dodecylbenzene sulfonic acid-doped polypyrrole films to SO<sub>2</sub>-N<sub>2</sub> mixtures. Synthetic Metals, 114, 65-72.
- Ram, M. K., Yavuz, O., and Aldissi, M. (2005) NO<sub>2</sub> gas sensing based on ordered ultrathin films of conducting polymer and its nanocomposite. Synthetic Metals, 151, 77-84.

- Ram, M.K., Yavuz, O., Lahsangah, V., and Aldissi, M. (2005) CO gas sensing from ultrathin nano-composite conducting polymer film. Sensors and Actuators B, 106, 750-757.
- Sakurai, Y., Jung, H-S., Shimanouchi, T., Inoguchi, T., Morita, S., Kuboi, R., and Natsukawa, K. (2002) Novel array-type gas sensors using conducting polymers, and their performance for gas identification. Sensors and Actuators B, 83, 270-275.
- Saxena, V. and Malhotra B.D. (2003) Prospects of conducting polymers in molecular electronics. Current Applied Physics, 3, 293-305.
- Soontornworajit, B., Wannatong, L., Hiamtup, P., Niamlang, S., Chotpattananont, D., Sirivat, A., and Schwank, J. (2007) Induced interaction between polypyrrole and SO<sub>2</sub> via molecular sieve 13X. Materials Science and Engineering B, 136, 78-86.
- Torsi, L., Pezzuto, M., Siciliano, P., Rella, R., Sabbatini, L., Valli, L., and Zambonin, P.G. (1998) Conducting polymers doped with metallic inclusions: New materials for gas sensors. Sensors and Actuators B, 48, 362-367.
- Trivedi, D. C. (1997) Handbook of Organic Conductive Molecules and Polymers, Chichester: Wiley.
- Thuwachaowsoan, K., Chotpattananont, D., Sirivat, A., Rujiravanit, R., and Schwank, J.W. (2007) Electrical conductivity responses and interactions of poly(3-thiopheneacetic acid)/zeolites L, mordenite, beta and H<sub>2</sub>. Materials Science and Engineering B, 140, 23-30.
- Vacca, P., Petrosino, M., Miscioscia, R., Nenna, G., Minarini, C., Sala, D.D., and Rubino, A. (2008) Poly(3,4-ethylenedioxythiophene):poly(4-styrenesulfonate) ratio: Structural, physical and hole injection properties in organic light emitting diodes. Thin Solid Films, 516, 4232-4237.
- Watcharaphalakorn, S., Ruangchuay, L., Chotpattananont, D., Srivat, A., and Schwank, J. (2005) Polyaniline/polyimide blends as gas sensors and electrical conductivity response to CO-N<sub>2</sub> mixtures. Polymer International, 54, 1126-1133

- Wichiansee, W. and Sirivat, A. (2009) Electrorheological properties of poly(dimethylsiloxane) and poly(3,4-ethylenedioxy thiophene)/poly(styrene sulfonic acid)/ethylene glycol blends. Materials Science and Engineering C, 29, 78-84.
- Yang, Y., Jiang, Y., Jianhua, X., and Junsheng, Y. (2007) Conducting polymeric nanoparticles synthesized in reverse micelles and their gas sensitivity based on quartz crystal microbalance. Polymer, 48, 4459-4465.



**Table 4.1** Physicochemical properties of Y zeolites

	<b>HY</b>	<b>LiY</b>	<b>NaY<sup>c</sup></b>	<b>KY</b>	<b>MgY</b>	<b>CaY</b>	<b>BaY</b>
<b>Zeolite structure</b>	FAU	FAU	FAU	FAU	FAU	FAU	FAU
<b>Pore size (nm)</b>	0.74 × 0.74	0.74 × 0.74	0.74 × 0.74	0.74 × 0.74	0.74 × 0.74	0.74 × 0.74	0.74 × 0.74
<b>Surface area (m<sup>2</sup>/g)</b>	630	886	800	772	856	834	847
<b>Pore volume (cm<sup>3</sup>/g)</b>	0.2476	0.2435	0.2463	0.2224	0.2421	0.2428	0.2421
<b>% Cation Exchange</b>	-	91	-	88	93	92	89
<b>Cation radius (Å)</b>	0.30	0.69	1.02	1.38	0.72	1.00	1.35
<b>EN (Pauling)</b>	2.3	0.98	0.93	0.82	1.31	1.00	0.89
<b>Total acidity (mmol/g)<sup>a</sup></b>	2.5000	1.5652	1.3305	0.7903	2.1394	1.8236	1.7349
<b>σ (10<sup>-3</sup> S/cm)<sup>b</sup></b>	1.26 ± 0.035	2.59 ± 0.247	2.69 ± 0.417	2.63 ± 0.035	1.92 ± 0.042	2.11 ± 0.100	1.99 ± 0.035

<sup>a</sup> Calculated from NH<sub>3</sub>-Temperature Program Desorption analysis

<sup>b</sup> DC Electrical Conductivity (σ) calculated from 2-point probe measurement

<sup>c</sup> Zeolite based for cation exchange process

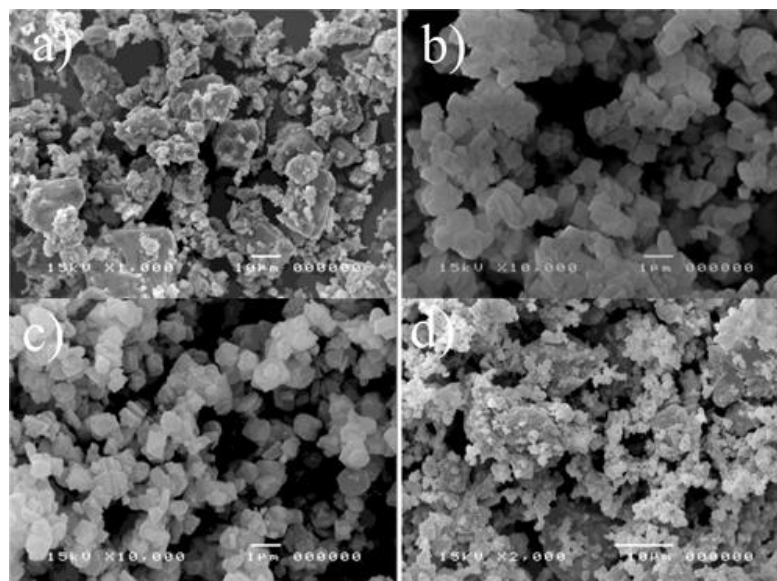


**Figure 4.1** Morphology of PEDOT-PSS particles, Zeolite Y powders and PEDOT-PSS/Zeolite Y composites: a) PEDOT-PSS at 1000x; b) Zeolite NaY at 10000x; c) Zeolite LiY at 10000x; and d) PEDOT-PSS/NaY at 2000x.

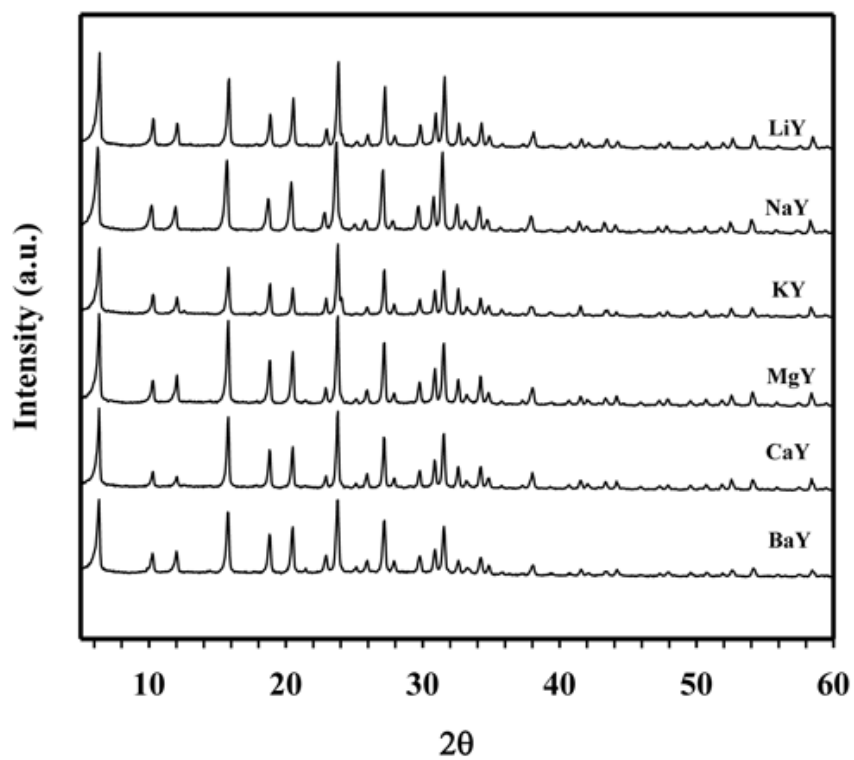


**Figure 4.2** X-ray diffraction patterns of Zeolite LiY, NaY, KY, MgY, CaY and BaY.

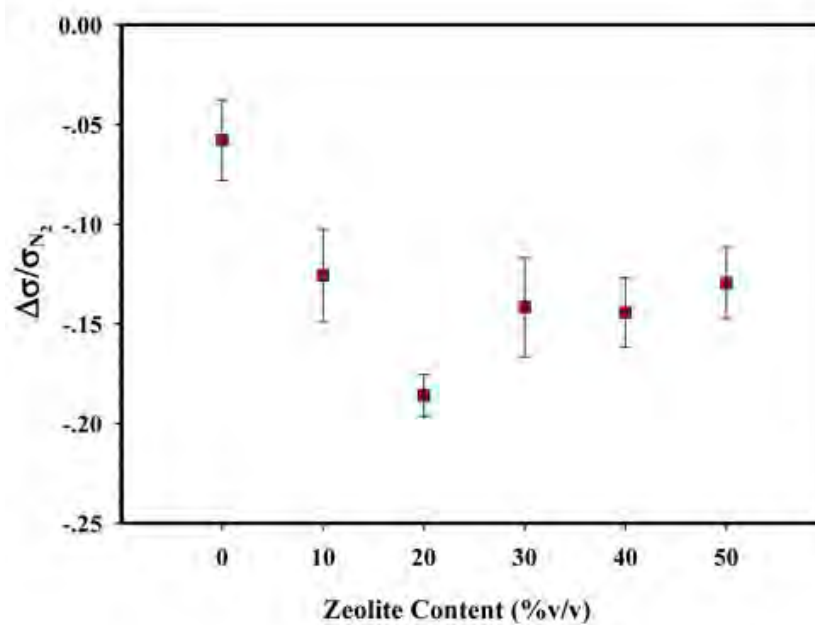


**Figure 4.3** The electrical conductivity sensitivity of PEDOT-PSS\_1:1 and PEDOT-PSS\_1:1/Zeolite NaY composites at various contents: 0, 10, 20, 30, 40 and 50% (v/v) when exposed to SO<sub>2</sub> at 27±1 °C and 1 atm.

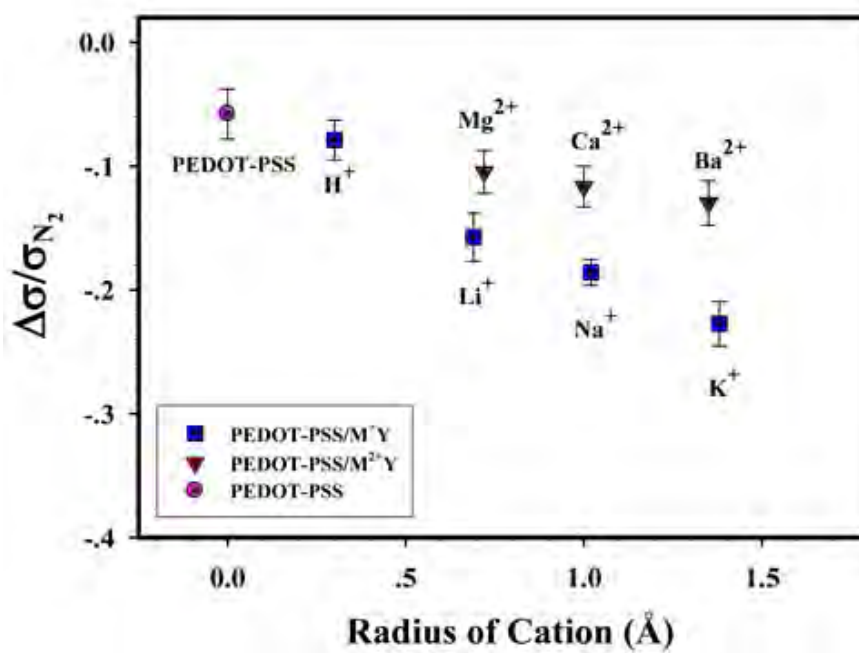


**Figure 4.4** The electrical conductivity sensitivity of PEDOT-PSS and PEDOT-PSS/Zeolite Y composites with various cation type: H<sup>+</sup>, Li<sup>+</sup>, Na<sup>+</sup>, K<sup>+</sup>, Mg<sup>2+</sup>, Ca<sup>2+</sup> and Ba<sup>2+</sup> (20%v/v) when exposed to SO<sub>2</sub> at 27±1 °C and 1 atm.

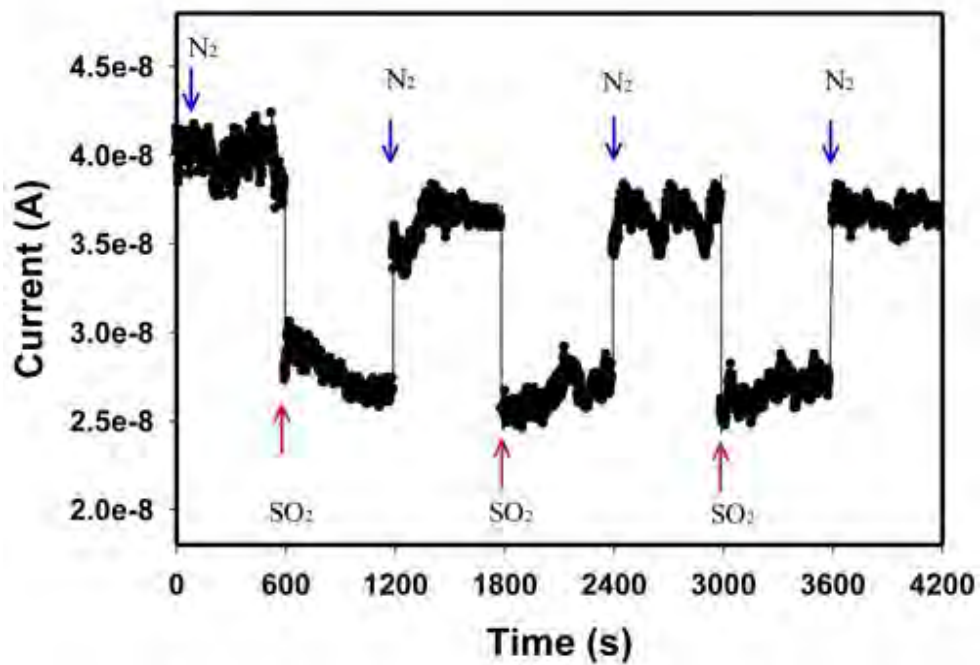


**Figure 4.5** Responses of PEDOT-PSS/KY composite when exposed to  $N_2$  (recovery) and  $SO_2$  (sensing) at  $27 \pm 1$  °C and 1 atm.

**CHAPTER V**  
**EFFECT OF TRANSITION METAL ION-EXCHANGED ZEOLITES Y ON**  
**ELECTRICAL CONDUCTIVITY AND RESPONSE OF PEDOT-**  
**PSS/ZEOLITE Y COMPOSITES TOWARD SULFUR DIOXIDE**

**5.1 Abstract**

This study aims to investigate and to compare the effect of different divalent transition metal cations ( $M^{2+}$ :  $Mn^{2+}$ ,  $Fe^{2+}$ ,  $Co^{2+}$ ,  $Ni^{2+}$ ,  $Cu^{2+}$  and  $Zn^{2+}$ ) exchanged into the hydrated zeolite Y on the electrical conductivity and sensitivity response of Poly(3,4-ethylenedioxythiophene) doped with poly(styrene sulfonic acid), PEDOT-PSS/MY composites when exposed to sulfur dioxide. All composites show higher electrical sensitivity values and significantly longer response times than the pristine conductive polymer matrix. The results obtained can be attributed to the electronegativity of the transition metal cations exchanged into the zeolite Y micropores, which critically affects the adsorption properties of the zeolite Y, and which in turn influences the electrical sensitivity of the composites. The highest electrical conductivity response and sensitivity pertain to the PEDOT-PSS/MnY composite. All composites investigated show nearly reversible responses towards sulfur dioxide

**Keywords:** Conducting polymers; Poly (3,4-ethylenedioxythiophene); Gas sensors; Zeolite Y; Sulfur dioxide

## 5.2 Introduction

The main purposes in improving gas sensors are towards faster response, higher sensitivity, reproducibility, and superior long-term stability. One of possible directions is to combine two or more materials that have distinct but collaborative properties [1-3]. An advantage of this approach is the unique properties obtained from the fabricated composite materials. Gas sensing materials using conductive polymers with or without modifiers are promising as they can be fine tuned for the electrical conductivity response towards particular gases or vapors. The fillers employed may include several metals or metal oxides [4-5], carbon nanotubes [6], graphene [7], insulating polymers [8], clays [9], and zeolites [10-13]. Polymer/zeolites composites with improved sensor responses have been reported for gas detections [10-13]. Sensitivity response and interaction mechanisms between polypyrrole/zeolite 13X composites and CO<sub>2</sub>, CO, and SO<sub>2</sub> were investigated [10]. Zeolite 13 X has been shown to promote the interaction between SO<sub>2</sub> and polypyrrole [10].

The aim of this study to investigate the gas sensing properties and the sensitivity improvement of conductive polymer/zeolite composites as gas sensing materials for sulfur dioxide detection. PEDOT-PSS was utilized as the semiconductor since its electrical conductivity response can be altered and is measurable when exposed to various gases [12]. Zeolite Y microporous material was chosen to improve the sensitivity to sulfur dioxide. Zeolite Y with its exchangeable cations possess more weak bonds to the adjacent atoms than the framework ions, thus enhancing their mobility. Their electrical conductivity is influentially affected by the mobility of existing cations in zeolite micropores [14-15]. The conductivity of zeolite strongly depends on content of water into the channels [16]. Moreover, ionic conduction of zeolite could be considerably enhanced at high-pressure treatment in water medium, and subsequent isolation to preserve the overhydrated structure [17].

In the present work, ion-exchanged zeolite NaY with various transition metal cations were obtained through the ion-exchange process. PEDOT-PSS/zeolite Y composites with different transition-metal ions were fabricated. The electrical conductivity and sensitivity values of PEDOT-PSS, zeolite Y, and their composites



under exposure to sulfur dioxide were measured, analyzed, and compared. Experimental results and discussion are presented here concerning the effects of zeolite content (v/v%) and cation type of zeolite Y on electrical conductivity and sensitivity response of PEDOT-PSS/zeolite Y composites when exposed to sulfur dioxide. The gas sensing mechanisms of the composites with sulfur dioxide is proposed.

### 5.3 Experimental

#### 5.3.1 Materials

The 3,4-ethylenedioxythiophene, EDOT (AR grade, Aldrich), was used as the monomer. Poly(styrene sulfonic acid), PSS, was used as the dopant. Sodium persulfate, Na<sub>2</sub>S<sub>2</sub>O<sub>8</sub> (AR grade, Aldrich), was used as the oxidant. Zeolite Y samples (NaY with Si/Al = 5.1, hydrated form) in a powder form were purchased from Zeolyst International. Sulphur dioxide (TIG, 1000 ppm in N<sub>2</sub>) and Nitrogen (TIG, 99% purity) were used as the target gases.

#### 5.3.2 Polymerization of Poly(3,4-ethylenedioxythiophene)

The chemical polymerization of PEDOT-PSS was followed from the procedures as reported previously [18]. PEDOT-PSS at 1:1 mole ratio of EDOT:PSS was prepared by adding EDOT monomers to an aqueous solution of PSS and Na<sub>2</sub>S<sub>2</sub>O<sub>8</sub>. After an initial stirring at room temperature for 10 minutes, Fe<sub>2</sub>(SO<sub>4</sub>)<sub>3</sub> was added and the mixture and stirred vigorously for 24 hrs. The obtained dark aqueous PEDOT-PSS mixture was purified by the ion exchanging with ion exchange resins (Lewatit, M600 and S100), resulting in a dark blue aqueous PEDOT-PSS solution. PEDOT-PSS film was obtained by casting the aqueous PEDOT-PSS solution at 100 °C for 24 hrs in a vacuum oven.

#### 5.3.3 Preparation of Ion-exchange Zeolites

The M<sup>2+</sup> zeolites studied in this work are zeolite Y (Zeolyst, Si/Al = 5.1, hydrated form) with different compensating cations (Mn<sup>2+</sup>, Fe<sup>2+</sup>, Co<sup>2+</sup>, Ni<sup>2+</sup>, Cu<sup>2+</sup> and Zn<sup>2+</sup>). The Mn<sup>2+</sup>, Fe<sup>2+</sup>, Co<sup>2+</sup>, Ni<sup>2+</sup>, Cu<sup>2+</sup> and Zn<sup>2+</sup> -exchanged zeolite Y were

carried out using the conventional ion-exchange procedures [19]. Zeolites NaY was used as the starting material for the ion-exchange. For ion-exchanged zeolites, 1 g of the zeolite NaY was added to 25 ml of 0.1 M metal chloride solution at room temperature and stirred for 24 h. The modified zeolite was filtered and washed with distilled water to remove Cl<sup>-</sup> ions followed by drying at 100 °C in air for 24 h.

#### 5.3.4 Composite Preparation

PEDOT-PSS powder was ground, sieved with 38 µm sieve, and then dried at 100 °C prior to mechanically mixed with dried zeolite Y powders at various zeolite amount (v/v%). The v/v% means the percentage of the zeolite Y volume over that of the PEDOT-PSS polymer. The weights of the zeolite Y and the PEDOT-PSS were measured before fabrication. The mixtures were obtained by compressing with a hydraulic press machine at a pressure of 6 kN into a thin disc with a diameter of 10 mm and a nominal thickness of 1 mm.

#### 5.3.5 Characterization

A Fourier transform infrared spectrometer (FTIR Nicolet, Nexus 670) with a resolution of 4 cm<sup>-1</sup> and a number of scans of 32 was used to characterize functional groups. The thermal stability of PEDOT-PSS was investigated by using a thermogravimetric analyzer (Dupont, TGA 2950) with a heating rate 10 °C/min under O<sub>2</sub> atmosphere. A scanning electron microscope (SEM JEOL, JSM 5200) was used to observe the morphology of PEDOT-PSS, zeolites, and PEDOT-PSS/zeolite composites in a powder form. An X-ray diffractometer (XRD Phillips, Rigaku) was used to examine the degree of crystallinity of PEDOT-PSS and the crystal order of the zeolites. The surface area, the pore width, and the pore volume of zeolite Y were measured using a surface area analyzer (Sorptomatic-1990). The percentage of ion exchange was measured for each zeolite Y sample by the inductively coupled plasma technique (Perkin-Elmer/ Optima 4300DV).

### 5.3.6 Electrical Conductivity Measurement and Gas Detection

The electrical conductivity values of PEDOT-PSS, zeolite Y, and their composites under exposure to air, N<sub>2</sub> and, SO<sub>2</sub> were measured in a special gas cell. It consisted of two stainless steel chambers connected in series. The first chamber and the second chamber were called the mixing and measurement chambers, respectively. The temperature controllers, connecting to both chambers, were used to monitor and control the temperature within the gas chambers. The second chamber contained two custom-built two-point probe meters connected to a voltage supplier (Keithley, 6517A) for applying a constant voltage source and recording a resultant current. The specific conductivity  $\sigma$  (S/cm) values of the pellets were obtained by measuring the bulk pellet resistance  $R$  ( $\Omega$ ). The relation  $\sigma = (1/Rt)(1/K) = (I/Vt)(1/K)$  was used to calculate the specific electrical conductivity, where  $t$  is the pellet thickness (cm),  $I$  is the resultant current (A),  $V$  is the applied voltage (V) and  $K$  is the geometric correction factor which is equal to the ratio  $w/l$ , where  $w$  and  $l$  are the probe width and the length, respectively. The geometrical correction factor ( $K$ ) was determined by calibrating the custom-built two-point probe with semi-conducting silicon sheets of known resistivity values. Electrical conductivity values of several samples were first measured at various applied DC voltages to identify their linear Ohmic regimes. The electrical conductivity response ( $\Delta\sigma$ ) and sensitivity ( $S$ ) of the composites are defined by the following equation  $\Delta\sigma = \sigma_{SO_2} - \sigma_{N_2}$  and  $S = \Delta\sigma / \sigma_{N_2}$ , respectively.  $\sigma_{N_2}$  and  $\sigma_{SO_2}$  are the electrical conductivity of the composite in N<sub>2</sub> and the target gas SO<sub>2</sub>, respectively.

## 5.4 Results and Discussion

### 5.4.1 Characterization of PEDOT-PSS, Zeolite Y and Composites

PEDOT-PSS was synthesized by the polymerization of 3,4-ethylenedioxythiophene (EDOT) in an aqueous solution of PSS using S<sub>2</sub>O<sub>8</sub><sup>2-</sup> as the oxidant. From the FT-IR spectrum of PEDOT-PSS, the peaks at 1520 and 1339 cm<sup>-1</sup> can be assigned to the C=C and the C-C stretchings of the thiophene ring[20-22,25]; the peaks at 929 cm<sup>-1</sup> and 834 cm<sup>-1</sup> correspond to the symmetric vibration of C-S

bond in the thiophene ring [20,21,25]. The peaks at 1127 and 1039  $\text{cm}^{-1}$  are assigned to the stretching mode of the ethylenedioxy group [20,21,25]. and the peaks at 1198 and 929  $\text{cm}^{-1}$  correspond to the  $-\text{SO}_3^-$  and the S-OH stretchings of the PSS molecule [20,23,25]. The vibration of the bending mode of the C-H bond in EDOT monomer ( $\sim 892 \text{ cm}^{-1}$ ) is not present [20, 25]. This result confirms the formation of PEDOT molecular chains. The absorption peak at 1645  $\text{cm}^{-1}$  can be assigned to the oxidation state of PEDOT which indicates the successful doping of PEDOT polymer with PSS. In summary, the FT-IR spectrum data indicate the successful formation of PEDOT molecular chains doped with the PSS counterion. Four transitions can be observed in the PEDOT-PSS thermograms: 30-110  $^\circ\text{C}$ , 160-380  $^\circ\text{C}$ , 380-550  $^\circ\text{C}$  and 560-900  $^\circ\text{C}$ ; they can be referred to as the loss of water, the side chain degradation, and the polymer backbone degradations of PSS and PEDOT, respectively [18, 25]. From XRD patterns of PEDOT-PSS, there is no characteristic peak observed by X-ray diffraction, the broad scattering background indicates the amorphous nature of the materials [24, 25]. The mean particle diameter of PEDOT-PSS\_1:1 was determined to be approximately  $34 \pm 0.22 \mu\text{m}$ . The micrograph in Figure 1 of PEDOT-PSS particles shows rough surfaces and irregular shapes; they are moderately dispersed. The density of PEDOT-PSS\_1:1 is  $1.4750 \pm 0.0003 \text{ g/cm}^3$ . The electrical conductivity of PEDOT-PSS in air and nitrogen atmosphere are  $(1.169 \pm 0.003) \times 10^1 \text{ S/cm}$  and  $(1.123 \pm 0.001) \times 10^1 \text{ S/cm}$ , respectively.

Zeolite Y was modified by the ion-exchanged process with various divalent transition metal cations ( $\text{Mn}^{2+}$ ,  $\text{Fe}^{2+}$ ,  $\text{Co}^{2+}$ ,  $\text{Ni}^{2+}$ ,  $\text{Cu}^{2+}$  and  $\text{Zn}^{2+}$ ) with approximately 80% exchanged (Table 5.1). Observation of the scanning electron micrographs (SEM) of pure zeolite Y and the modified zeolite Y indicates that the morphology of modified zeolite Y has not changed after modification process. The transition metal cation exchange does not affect markedly the main structure of zeolite Y [26,27]. Zeolite Y particles possess irregular crystal shapes and expose itself to be inhomogeneously dispersed in the conductive polymer matrix of the composites (Figure 5.1).

The X-ray diffractogram of entirely zeolite Y samples exhibits the characteristic peaks of the zeolite Y framework that it is highly crystalline in the range 5-60 degrees. Comparison of X-ray diffraction patterns of the transition metal

cation exchanged zeolite Y to the starting zeolite NaY shows no notable alterations in the crystalline structure of the zeolite during the modification process (Figure 5.2). Due to the low content and high dispersion of transition metal cations exchanged, there is no significant change of diffraction lines observed after modification [28-29]. The mean particle diameters of  $\text{Mn}^{2+}$ ,  $\text{Fe}^{2+}$ ,  $\text{Co}^{2+}$ ,  $\text{Ni}^{2+}$ ,  $\text{Cu}^{2+}$  and  $\text{Zn}^{2+}$  - exchanged zeolite Y (Si/Al mole ratios equal to 5.1) are approximately 500 nm.

The specific surface areas, the pore width, and the pore volume, of zeolite Y (Si/Al = 5.1) of the MnY, FeY, CoY, NiY, CuY and ZnY are tabulated in Table 5.1. Comparison, with the starting zeolite NaY, the transition metal cation exchanged zeolite exhibits a greater pore volume. The BET surface area and pore volume are exactly consistent with the cationic size; that is, in the order of  $\text{MnY} > \text{FeY} > \text{CoY} > \text{ZnY} > \text{NiY} > \text{CuY}$ . The BET surface area and pore volume increase as the transition metal cation size decreases. This result suggests that the smaller ion occupies less pore space, resulting in more available adsorbing sites.

The electrical conductivity data in  $\text{N}_2$ , for the Y zeolites with different cation types are tabulated in Table 1. The CuY zeolite has the smallest charge balancing cation ( $0.69 \text{ \AA}$ ) exhibiting the lowest electrical conductivity. Inversely, the MnY zeolite has the highest electrical conductivity due to the larger cation radius ( $0.91 \text{ \AA}$ ) which induces the reduction of electrostatic interaction with the anionic framework sites and the ease in which a cation can move from one site to another [14,15]. Although, the transition metal cation exchanged zeolite Y has a greater pore volume than starting zeolite NaY (EN=0.93). The higher electronegativity of transition metal cations (EN=1.55-1.91) significantly affects the electrical conductivity of the modified zeolite Y, and the lower the electrical conductivity can be observed.

## 5.4.2 Electrical Conductivity Response to $\text{SO}_2$

### 5.4.2.1 *Effect of Zeolite Content*

The electrical sensitivity values of PEDOT-PSS\_1:1 and its composites with the zeolite Y when exposed to air,  $\text{N}_2$ , and  $\text{SO}_2$  were measured under chamber temperature ( $T_c$ ) of  $27 \pm 1 \text{ }^\circ\text{C}$ , and at 1 atm. The electrical conductivity sensitivity values of the PEDOT-PSS/NaY composites in 1000 ppm

SO<sub>2</sub>/N<sub>2</sub> versus Y zeolite content is shown in Figure 3. All composites exhibit negative responses to SO<sub>2</sub>. The sensitivity value of PEDOT-PSS/NaY increases as zeolite NaY content increases from 0 to 20%, an obvious evidence for the induced interaction. Beyond this volume fraction, the sensitivity value decreases as the zeolite NaY content increases from 20 and 50%, respectively. As more zeolite NaY is added, its presence also prohibits the direct contact area between SO<sub>2</sub> and PEDOT, and consequently a lower response or sensitivity. This result suggests that the composite with a proper zeolite content can be applied as an enhanced sensor material. The addition of a zeolite to a pure polymer at an optimal combination can promote the electrical conductivity response of the composites [10-13].

#### 5.4.2.2 *Effect of Cation Type*

The electrical conductivity sensitivity values of PEDOT-PSS/MY composites in 1000 ppm SO<sub>2</sub>/N<sub>2</sub> versus zeolite Y content are shown in Figure 5.4. In the present work, it is shown that the cation type in the zeolite Y influences the gas adsorption characteristics of the composites and can alter the electrical conductivity and sensitivity response of the composites toward SO<sub>2</sub>. Ion-exchanged transition metal cations in the zeolite Y do not affect the main structure of the zeolite Y framework [14,15]. The presence of the exchanged transition metal cations increases the adsorbing sites in zeolite micropores. Hence, target gases have more available active sites resulting in the more adsorbed target gas molecules to interact with the polymer matrix [10-13]. The electrical sensitivity of PEDOT-PSS/MY can be observed to be consistent with the ionic radii of the transition metal cations on zeolite Y in the order of MnY > FeY > CoY > NiY > CuY < ZnY (the order of transition metals in the sequence is the same as in the periodic table). Thus, the PEDOT-PSS/MnY has the highest electrical sensitivity due to their lesser interaction with SO<sub>2</sub>. These results suggest that the electrostatic interaction exists between the transition metal cations and the target gases and it should be correlated with the ionic potential [14,15]. The exchanged transition metal cation with a radius, the lesser metal-SO<sub>2</sub> interactions, and then the target gas can move more easily and consequently a greater interaction between SO<sub>2</sub> and the active sites on the PEDOT polymer chain. PEDOT-PSS/ZnY composites have the higher the electrical

sensitivity than PEDOT-PSS/NiY and PEDOT-PSS/CuY composites, but lower than others composites. This consequence is not consistent with the sequence in the periodic table. This should be due to the lower electronegativity of  $Zn^{2+}$  than  $Ni^{2+}$  and  $Cu^{2+}$ , respectively. The out-of-line position of the electrical sensitivity of PEDOT-PSS/CuY is a consequence of the fact that  $Cu^{2+}$  often forms a very strong interaction with others molecules, due to its smallest size and with a high electronegativity value (ionic radius = 0.69 Å and EN = 1.90) [30-31].

The temporal response time is the time required for the electrical conductivity value to rise from its initial value in  $N_2$  towards the equilibrium value when exposed to  $SO_2$  [1]. The recovery time is the time required for the electrical conductivity value return to initial value after the step removal of  $SO_2$ . By adding the zeolite Y, a longer response time and recovery time are observed, and the response time and recovery time increase with decreasing cation size of the zeolite Y. The response time of PEDOT-PSS/CuY is longer than that of PEDOT-PSS and those of the other composites (14.1 minutes), corresponding to the higher density of the adsorption sites available for  $SO_2$  molecules and the greater ion-quadrupole interactions with  $SO_2$ . The shortest temporal response and recovery time is obtained from PEDOT-PSS/MnY due to the weaker interaction between  $SO_2$  molecules and the MnY zeolite (8.2 minutes), which allows  $SO_2$  molecules to diffuse away from the composites. The addition of the Y zeolite is thus shown to enhance the interaction between PEDOT-PSS and  $SO_2$  molecules; the zeolite improves the sensitivity of the pristine PEDOT-PSS, but at the expense of a longer response time [10-13].

The PEDOT-PSS/MY composite is examined in three sensing cycles by repeating the sensing and recovery process to examine the reversibility and reproducibility of the composite responses. The conductivity of the PEDOT-PSS/MnY composite, possessing the highest sensitivity for  $SO_2$  gas, is shown in Figure 5 as a function of time when exposed to three cycles of a sequence of the  $SO_2$  exposure (sensing), evacuation and under the  $N_2$  atmosphere (recovery). During the recovery process, the conductivity of the composites nearly recovers the initial value; this suggests that the sensing characteristics are quite reproducible.

## 5.5 Conclusions

An adjusted combination of the composite between PEDOT-PSS and zeolite Y produces some remarkable changes in the composite electrical conductivity response. The composite at 20% (v/v) of the zeolite Y content provides the highest sensitivity to SO<sub>2</sub>. The results suggest that the addition of the zeolite Y to the pristine polymer PEDOT-PSS at the optimized combination can promote the electrical sensitivity response of the composites to SO<sub>2</sub> gas. The metal cation in the zeolite Y intimately induces a synergism to adsorb SO<sub>2</sub>, but at the expense of the longer response time and recovery time. The highest electrical sensitivity response pertains to the PEDOT-PSS/MnY composite. The exchanged of transition metal cations can enlarge the pore volume of zeolites. Therefore, the target gas SO<sub>2</sub> can further introduce to interact with PEDOT-PSS polymer. In the presence of the transition metal cations, with respect to the zeolite micropores, the cations can influence the adsorption properties of the system. The electrical sensitivity of the composite can be correlated with with the electronegativity of the transition metal cations of the cation-exchanged zeolite Y. The reproducibility of the composite response can be observed and the response is nearly reversible at room temperature.

## 5.6 Acknowledgements

The authors would like to acknowledge the financial supports from the Conductive and Electroactive Research Unit of Chulalongkorn University, the 90<sup>th</sup> Anniversary of Chulalongkorn University Fund (Ratchadaphiseksomphot Endowment Fund), the Thailand Research Fund (TRF-RTA and PhD/0082/2550), and the Royal Thai Government.



## 5.7 References

1. Bai, H.; Shi, G. *Sensors* 2007, 7, 267.
2. Adhikari, B.; Majumdar, S. *Prog in Polym Sci* 2004, 29, 699.
3. Rajesh; Ahuja, T.; Kumar, D. *Sensor Actuat B-Chem* 2009, 136, 275.
4. Galdikas, A.; Kancleris, Ž.; Senulien, D.; Šetkus, A. *Sensor Actuat B-Chem* 2003, 95, 244.
5. Ram, M.K.; Yavuz, Ö.; Lahsangah, V.; Aldissi, M. *Sensor Actuat B-Chem* 2005, 106, 750.
6. Chen, Y.; Li, Y.; Wang, H.; Yang, M. *Carbon* 2007, 45, 357.
7. Hu, N.; Wang, Y.; Chai, J.; Gao, R.; Yang, Z.; Kong, E.S.W.; Zhang, Y. *Sensor Actuat B-Chem* 2012, 163, 107.
8. Matsuguchi, M.; Io, J.; Sugiyama, G.; Sakai, Y. *Synthetic Met* 2002, 128, 15.
9. Cosnier, S.; Da Silva, S.; Shan, D.; Gorgy, K. *Bioelectrochemistry*. 2008, 74, 47.
10. Soontornworajit, B.; Wannatong, L.; Hiamtup, P.; Niamlang, S.; Chotpattananont, D.; Sirivat, A.; Schwank, J. *Mat Sci Eng B* 2007, 136, 78.
11. Thuwachaowsoan, K.; Chotpattananont, D.; Sirivat, A.; Rujiravanit, R.; Schwank J.W. *Mat Sci Eng B* 2007, 140, 23.
12. Chuapradit, C.; Wannatong, L.R.; Chotpattananont, D.; Hiamtup, P.; Sirivat, A.; Schwank, J. *Polymer* 2005, 46, 947.
13. Densakulprasert, N.; Wannatong, L.; Chotpattananont, D.; Hiamtup, P.; Sirivat, A.; Schwank, J. *Mat Sci Eng B* 2005, 117, 276.
14. Izni, E.; Izni, A. *Turk J Chem* 2007, 31, 523.
15. Franke, M.E.; Simon, U. *Solid State Ionics* 1999, 118, 311.
16. Goryainov, S.V.; Secco, R.A.; Huang, Y.; Liu, H. *Physica B: Condensed Matter* 2007, 390, 356.
17. Goryainov, S.V.; Secco, R.A.; Huang, Y.; Likhacheva, A.Y. *Micropo Mesopo Mat* 2013, 171, 125.
18. Louwet, F.; Groenendaal, L.; Dhaen, J.; Manca, J.; Van Luppen, J.; Verdonck, E.; Leenders, L. *Synthetic Met* 2003, 135–136, 115.
19. Thomas, B.; Sugunan, S. *Micropo Mesopo Mat* 2004, 72, 227.

20. Han, D.; Yang, G.; Song, J.; Niu, L.; Ivaska, A. *J Electroanal Chem* 2007, 602, 24.
21. Garreau, S.; Louarn, G.; Buisson, J. P.; Froyer, G.; Lefrant, S. *Macromolecules* 1999, 32, 6807.
22. Li, C.; Imae, T. *Macromolecules* 2004, 37, 2411.
23. Martin, B.D.; Nikolov, N.; Pollack, S.K.; Saprigin, A.; Shashidhar, R.; Zhang, F.; Heiney, P.A. *Synthetic Met* 2004, 142, 187.
24. Wichiansee, W.; Sirivat, A. *Mat Sci Eng C* 2009, 29, 78.
25. Chanthanont, P.; Sirivat, A. *e-Polymers*, 2012, 10, 1.
26. Bendenia, S.; Marouf-Khelifa, K.; Batonneau-Gener, I.; Derriche, Z.; Khelifa, A. *Adsorption* 2001, 17, 361.
27. Maurin, G.; Llewellyn, P.L.; Poyet, T.; Kuchta, B. *Micropo Mesopo Mat* 2005, 79, 53.
28. Nam, S.S.; Kim, H.; Kishan, G.; Choi, M.J.; Lee, K.W. *Appl Cat A-Gen* 1999, 179, 155.
29. Castaldi, P.; Santona, L.; Enzo, S.; Melis, P. *J Hazard Mater* 2008, 156, 428.
30. Mews, R.; Lork, E.; Watson, P.G.; Görtler, B. *Coordin Chem Rev* 2000, 197, 277.
31. Matsuguchi, M.; Tamai, K.; Sakai, Y. *Sensor Actuat B-Chem* 2001, 77, 363.
32. Nasluzov, V.A.; Shor, A.M.; Nörtemann, F.; Staufer, M.; Yudanov, I.V.; Rösch, N. *J Mol Struc-Theochem*. 1999, 466, 235.

**Table 5.1** Physicochemical properties of zeolite Y

	<b>NaY<sup>a</sup></b>	<b>MnY</b>	<b>FeY</b>	<b>CoY</b>	<b>NiY</b>	<b>CuY</b>	<b>ZnY</b>
<b>Zeolite structure</b>	FAU	FAU	FAU	FAU	FAU	FAU	FAU
<b>Pore size<sup>c</sup> (nm)</b>	0.74 × 0.74	0.74 × 0.74	0.74 × 0.74	0.74 × 0.74	0.74 × 0.74	0.74 × 0.74	0.74 × 0.74
<b>Surface area (m<sup>2</sup>/g)</b>	800	811	833	819	836	867	842
<b>Pore volume (cm<sup>3</sup>/g)</b>	0.2476	0.2645	0.2694	0.2689	0.2706	0.2856	0.2761
<b>% Cation Exchange</b>	-	84	85	83	84	85	86
<b>Cation ionic radius (Å)</b>	0.97	0.91	0.83	0.82	0.78	0.69	0.74
<b>EN of Cation (Pauling)</b>	0.93	1.55	1.83	1.88	1.91	1.90	1.65
<b>Atomic Number</b>	11	25	26	27	28	29	30
<b>σ (10<sup>-3</sup> S/cm)<sup>b</sup></b>	2.69 ± 0.417	2.30 ± 0.428	2.18 ± 0.378	2.01 ± 0.765	1.77 ± 0.567	1.59 ± 0.146	1.83 ± 0.186

<sup>a</sup> Zeolite based for cation exchange process

<sup>b</sup> DC Electrical Conductivity (σ) calculated from 2-point probe measurement

<sup>c</sup> Data from Zeolyst

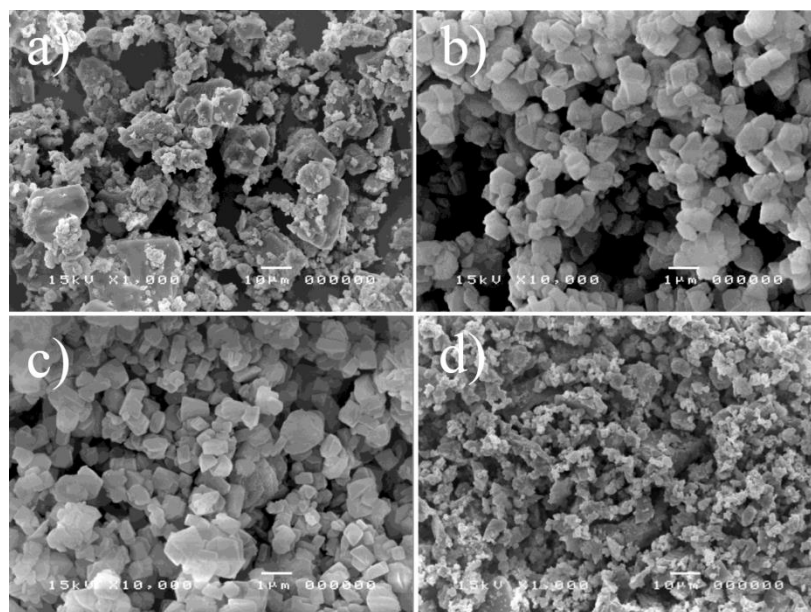


**Figure 5.1** Morphology of PEDOT-PSS particles, Zeolite Y powders and PEDOT-PSS/Zeolite Y composites: a) PEDOT-PSS at 1000x; b) Zeolite MnY at 10000x; c) Zeolite CuY at 10000x; and d) PEDOT-PSS/MnY at 1000x.

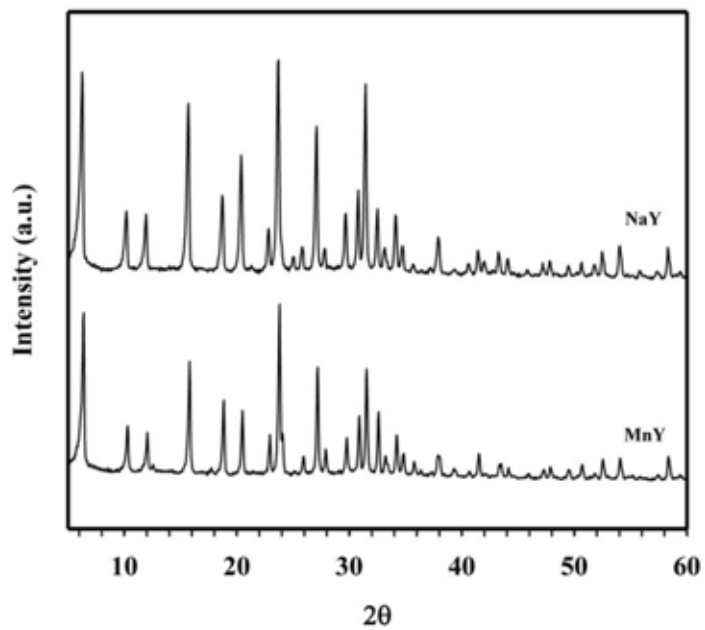


**Figure 5.2** X-ray diffraction patterns of Zeolite NaY and MnY.

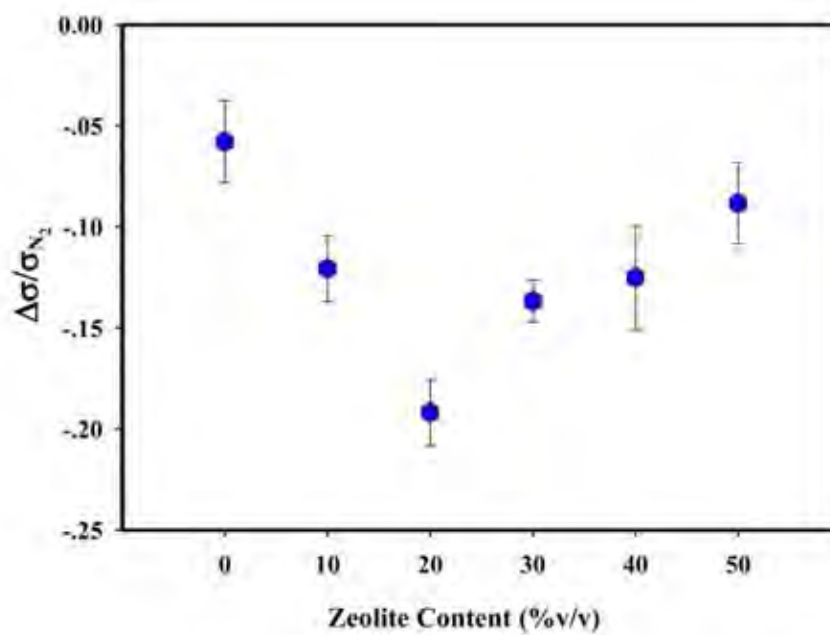


**Figure 5.3** The electrical conductivity sensitivity of PEDOT-PSS\_1:1 and PEDOT-PSS\_1:1/Zeolite NaY composites at various contents: 0, 10, 20, 30, 40 and 50% (v/v) when exposed to SO<sub>2</sub> at 27±1 °C and 1 atm.

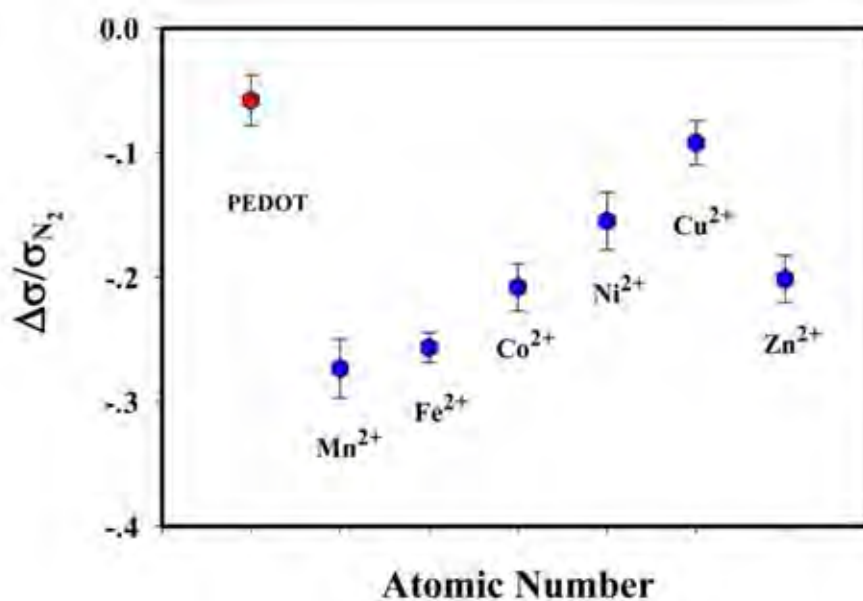


**Figure 5.4** The electrical conductivity sensitivity of PEDOT-PSS and PEDOT-PSS/Zeolite Y composites with various transition metal cation type:  $Mn^{2+}$ ,  $Fe^{2+}$ ,  $Co^{2+}$ ,  $Ni^{2+}$ ,  $Cu^{2+}$  and  $Zn^{2+}$  (20%v/v) when exposed to  $SO_2$  at  $27\pm 1$  °C and 1 atm.

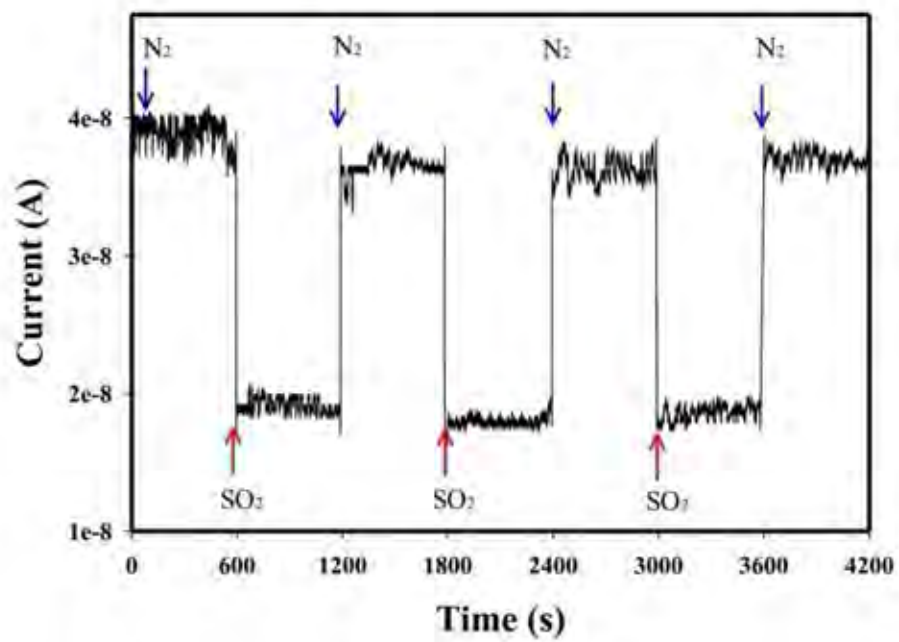


**Figure 5.5** Responses of PEDOT-PSS/MnY composite when exposed to  $N_2$  (recovery) and  $SO_2$  (sensing) at  $27 \pm 1$  °C and 1 atm.



**CHAPTER VI**  
**EFFECT OF METAL EXCHANGED ZEOLITE Y COVER LAYER ON**  
**ELECTRICAL CONDUCTIVITY RESPONSE OF PEDOT-PSS AND THEIR**  
**SULFUR DIOXIDE SENSING PROPERTIES**

**6.1 Abstract**

This work reports the electrical sensitivity response of conductive polymer, poly(3,4-ethylenedioxythiophene) doped with poly(styrenesulfonate), PEDOT-PSS, as the active layer of gas sensing materials for sulfur dioxide detection. The metal exchanged zeolite Y was applied as a cover layer, to study the influence of the zeolite Y cover layer on the sensing response of PEDOT-PSS toward sulfur dioxide. The effective of the thickness of the metal exchanged zeolite Y also related to the metal content that can induce the gas molecule to interact with PEDOT-PSS. The zeolites Y cover layer have been employed as physical and chemical filters, which used to improve the gas sensing response of PEDOT-PSS polymer. The thickness of the zeolite Y layer is one of the most influential parameter that has to optimize and this also associated to the metal exchanged content in the zeolite Y. The sensitivity response of PEDOT-PSS toward sulfur dioxide was enhanced when they are covered with the metal exchanged zeolite Y layer. Nevertheless, the response time of PEDOT-PSS covered by the zeolite Y layer toward sulfur dioxide was increases when compare with PEDOT-PSS pristine. Theirs response time also increase simultaneously with the thickness of zeolite Y cover layer. This related to the zeolite porous material cover layer acts as a diffusion barrier.

**Keywords:** Conducting polymers; Poly (3,4-ethylenedioxythiophene); Gas sensors; Zeolite Y; Zeolite cover layer; Sulfur dioxide

## 6.2 Introduction

Conductive polymer gas sensors have attracted much attention due to their excellent properties, usage and the variation of electrical characteristics [1-3]. Conductive polymers are inexpensive, highly sensitive and can be operate at room temperature [4-6]. Gas sensing materials base on conductive polymer rely on the interaction occurring between gas molecules and conductive polymer and their response can be translated into an electrical output [7-8]. In the presence of a gas, conductive polymers respond with a change in electrical conductivity due to the change of electron density [9-10]. Most of The widely studied conductive polymers in sensor application are polythiophene, polypyrrole, polyaniline, theirs derivatives and theirs composites [1-3].

Signal or sensitivity enhancement is an importance feature for sensor application. One of the approaches for improving the sensing performance of conductive polymer is the addition of another material [11]. Due to the use of the zeolites in several ways for sensor application as previous reported: a zeolite layer can be added to the sensor structure as filter layer to enhance the adsorption of analyze gas, and changes in conductivity of the zeolite itself [12]. In order to enhance the gas sensitivity of conductive polymer, zeolite microporous material is the most promising material for this approach.

Zeolites are aluminosilicates with highly porous crystallite structure, large surface area and their pore/channel have the ability to hold and exchange cations [13-14]. The use of the zeolite as cover layer on the top of sensing layer is the strategy way to enhance the interaction between gas molecules and conductive polymer sensing materials, which may improve their sensitivity response. The pore system, the ability to exchanged cations, adsorption and diffusion properties of zeolites are the useful properties that may enhance the gas molecules adsorption [15]. Due to these properties, zeolite cover layer will preconcentrate the analyte gas and increase the probability of the gas molecules that diffuse to the sensing layer. Future more, some of the interference

molecules also blocked completely from entering the zeolite pores or favor the adsorption of one molecule over another, which may be a key for improving the selectivity of the sensors [16].

In the previous work, we studied the effect of cation type (alkaline, alkaline earth, and transition metal cations) of the zeolite Y on electrical conductivity response of PEDOT-PSS toward sulfur dioxide. The sodium form of the zeolite Y with a Si/Al mole ratio of 5.1 was modified by a solution ion-exchange process. The sensing composite materials between PEDOT-PSS and the zeolite Y were prepared, by mechanically mixed of PEDOT-PSS and the zeolite Y powders. The mixed powders were compressed, with a hydraulic press machine to form the pellet. In the presence of the metal cations, with respect to the zeolite micropores, the cations can influence the adsorption properties of the system, and which in turn influences the electrical sensitivity of the composites.

In this study, we attempt to investigate the effect of metal exchanged zeolite Y cover layer and the thickness of cover layers on electrical conductivity response of PEDOT-PSS and their sulfur dioxide sensing properties. Their gas sensing response; sensitivity, response time, recovering time and complication of fabrication were compared with PEDOT-PSS/MY zeolite composites in powder mixing compress form.

## **6.3 Experimental**

### **6.3.1 Materials**

The 3,4-ethylenedioxythiophene, EDOT (AR grade, Aldrich), was used as the monomer. Poly(styrene sulfonic acid), PSS, was used as the dopant. Sodium persulfate,  $\text{Na}_2\text{S}_2\text{O}_8$  (AR grade, Aldrich), was used as the oxidant. Zeolite Y samples (NaY with Si/Al = 5.1, hydrated form) in a powder form were purchased from Zeolyst International. Sulphur dioxide (TIG, 1000 ppm in  $\text{N}_2$ ) and Nitrogen (TIG, 99% purity) were used as the target gases.

### 6.3.2 Polymerization of Poly(3,4-ethylenedioxythiophene)

The chemical polymerization of PEDOT-PSS was followed from the procedures as reported previously [17]. PEDOT-PSS at 1:1 mole ratio of EDOT:PSS was prepared by adding EDOT monomers to an aqueous solution of PSS and  $\text{Na}_2\text{S}_2\text{O}_8$ . After an initial stirring at room temperature for 10 minutes,  $\text{Fe}_2(\text{SO}_4)_3$  was added and the mixture and stirred vigorously for 24 hrs. The obtained dark aqueous PEDOT-PSS mixture was purified by the ion exchanging with ion exchange resins (Lewatit, M600 and S100), resulting in a dark blue aqueous PEDOT-PSS solution. PEDOT-PSS film was obtained by casting the aqueous PEDOT-PSS solution at 100 °C for 24 hrs in a vacuum oven.

### 6.3.3 Preparation of Ion-exchange Zeolites

The metal in exchanged zeolites studied in this work are zeolite Y (Zeolyst, Si/Al = 5.1, hydrated form) with different compensating cations ( $\text{K}^+$ ,  $\text{Ba}^{2+}$  and  $\text{Mn}^{2+}$ ). The  $\text{K}^+$ ,  $\text{Ba}^{2+}$  and  $\text{Mn}^{2+}$  -exchanged zeolite Y were carried out using the conventional ion-exchange procedures [18]. Zeolites NaY was used as the starting material for the ion-exchange. For ion-exchanged zeolites, 1 g of the zeolite NaY was added to 25 ml of 0.1 M metal chloride solution at room temperature and stirred for 24 h. The modified zeolite was filtered and washed with distilled water to remove  $\text{Cl}^-$  ions followed by drying at 100 °C in air for 24 h.

### 6.3.4 Sensing materials Preparation

PEDOT-PSS powder was ground, sieved with 38  $\mu\text{m}$  sieve, and then dried at 100 °C prior to mechanically mixed with dried zeolite Y powders at various zeolite amount (v/v%). The v/v% means the percentage of the zeolite Y volume over that of the PEDOT-PSS polymer. The weights of the zeolite Y and the PEDOT-PSS were measured before fabrication. The mixtures were obtained by compressing with a hydraulic press machine at a pressure of 6 kN into a thin disc with a diameter of 10 mm and a nominal thickness of 1 mm. The pellet of PEDOT-PSS and MY zeolites were

prepared by direct compression at 6 kN into a thin disc. The metal zeolite pellet was placed on the top of PEDOT-PSS pellet, then compressing again to form the tablet by varying the thickness of zeolite pellet (zeolite cover layer).

### 6.3.5 Characterization

A Fourier transform infrared spectrometer (FTIR Nicolet, Nexus 670) with a resolution of  $4\text{ cm}^{-1}$  and a number of scans of 32 was used to characterize functional groups. The thermal stability of PEDOT-PSS was investigated by using a thermogravimetric analyzer (Dupont, TGA 2950) with a heating rate  $10\text{ }^{\circ}\text{C}/\text{min}$  under  $\text{O}_2$  atmosphere. A scanning electron microscope (SEM JEOL, JSM 5200) was used to observe the morphology of PEDOT-PSS, zeolites, and PEDOT-PSS/zeolite composites in a powder form. An X-ray diffractometer (XRD Phillips, Rigaku) was used to examine the degree of crystallinity of PEDOT-PSS and the crystal order of the zeolites. The surface area, the pore width, and the pore volume of zeolite Y were measured using a surface area analyzer (Sorptomatic-1990). The percentage of ion exchange was measured for each zeolite Y sample by the inductively coupled plasma technique (Perkin-Elmer/ Optima 4300DV).

### 6.3.6 Electrical Conductivity Measurement and Gas Detection

The electrical conductivity values of PEDOT-PSS, zeolite Y, and their composites under exposure to air,  $\text{N}_2$  and,  $\text{SO}_2$  were measured in a special gas cell. It consisted of two stainless steel chambers connected in series. The first chamber and the second chamber were called the mixing and measurement chambers, respectively. The temperature controllers, connecting to both chambers, were used to monitor and control the temperature within the gas chambers. The second chamber contained two custom-built two-point probe meters connected to a voltage supplier (Keithley, 6517A) for applying a constant voltage source and recording a resultant current. The specific conductivity  $\sigma$  (S/cm) values of the pellets were obtained by measuring the bulk pellet resistance  $R$  ( $\Omega$ ). The relation  $\sigma = (1/Rt)(1/K) = (I/Vt)(1/K)$  was used to calculate the

specific electrical conductivity, where  $t$  is the pellet thickness (cm),  $I$  is the resultant current (A),  $V$  is the applied voltage (V) and  $K$  is the geometric correction factor which is equal to the ratio  $w/l$ , where  $w$  and  $l$  are the probe width and the length, respectively. The geometrical correction factor ( $K$ ) was determined by calibrating the custom-built two-point probe with semi-conducting silicon sheets of known resistivity values. Electrical conductivity values of several samples were first measured at various applied DC voltages to identify their linear Ohmic regimes. The electrical conductivity response ( $\Delta\sigma$ ) and sensitivity ( $S$ ) of the composites are defined by the following equation  $\Delta\sigma = \sigma_{SO_2} - \sigma_{N_2}$  and  $S = \Delta\sigma / \sigma_{N_2}$ , respectively.  $\sigma_{N_2}$  and  $\sigma_{SO_2}$  are the electrical conductivity of the composite in  $N_2$  and the target gas  $SO_2$ , respectively. Electrical conductivity responses were measured at  $SO_2$  concentrations of 1000, 500, 250, 125, 62.5, 31.25, 15.63, and 7.86 ppm through successive serial dilutions.  $SO_2$  concentration was successively reduced in half from 1000 to 7.8 ppm. A 1000 ppm  $SO_2/N_2$  mixture was injected into the mixing chamber until the pressure reached 2 atm and at 27 °C. The half of the gas mixture was then allowed to escape into the working chamber where now the pressures in both chambers were reduced to 1 atm. Then the gas mixture in the working chamber was evacuated.  $N_2$  was injected into the mixing chamber until its pressure reached 2 atm, and therefore the  $SO_2$  concentration was reduced to 500 ppm. Half of the gas mixture was allowed to escape into the working chamber. The procedure was repeated 7 times where the final  $SO_2$  concentration was 7.8 ppm.

## 6.4 Results and Discussion

### 6.4.1 Characterization of PEDOT-PSS, Zeolite Y and Composites

Poly(3,4-ethylenedioxythiophene) doped with poly(styrenesulfonate), PEDOT-PSS, PEDOT-PSS, with at 1:1 mole ratio of EDOT:PSS was synthesized by the polymerization of 3,4-ethylenedioxythiophene (EDOT) in an aqueous solution of PSS in a similar method that reported in the previous research conducted in our group [10]. From XRD patterns of PEDOT-PSS, there is no characteristic peak observed by X-ray

diffraction, the broad scattering background indicates the amorphous nature of the materials [19-20]. The mean particle diameter of PEDOT-PSS\_1:1 was determined to be approximately  $34 \pm 0.22 \mu\text{m}$ . The micrograph of PEDOT-PSS particles shows rough surfaces and irregular shapes; they are moderately dispersed. The density of PEDOT-PSS\_1:1 is  $1.4750 \pm 0.0003 \text{ g/cm}^3$ . The electrical conductivity of PEDOT-PSS in air and nitrogen atmosphere are  $(1.169 \pm 0.003) \times 10^1 \text{ S/cm}$  and  $(1.123 \pm 0.001) \times 10^1 \text{ S/cm}$ , respectively [10].

Zeolite Y was modified by the ion-exchanged process with various metal cations ( $\text{K}^+$ ,  $\text{Ba}^{2+}$  and  $\text{Mn}^{2+}$ ) with approximately 80% exchanged. Observation of the scanning electron micrographs (SEM) of pure zeolite Y and the modified zeolite Y indicates that the morphology of modified zeolite Y has not changed after modification process. The transition metal cation exchange does not affect markedly the main structure of zeolite Y [21]. Zeolite Y particles possess irregular crystal shapes and expose itself to be inhomogeneously dispersed in the conductive polymer matrix of the composites.

The X-ray diffractogram of entirely zeolite Y samples exhibits the characteristic peaks of the zeolite Y framework that it is highly crystalline in the range 5-60 degrees. Comparison of X-ray diffraction patterns of the transition metal cation exchanged zeolite Y to the starting zeolite NaY shows no notable alterations in the crystalline structure of the zeolite during the modification process. Due to the low content and high dispersion of transition metal cations exchanged, there is no significant changed of diffraction lines observed after modification [22]. The mean particle diameters of  $\text{K}^+$ ,  $\text{Ba}^{2+}$  and  $\text{Mn}^{2+}$ -exchanged zeolite Y (Si/Al mole ratios equal to 5.1) are approximate 500 nm.

## 6.4.2 Electrical Conductivity Response to SO<sub>2</sub>

### 6.4.2.1 *Effect of sulfur dioxide concentration*

The dependence of electrical conductivity change of PEDOT-PSS with KY zeolite cover layers and PEDOT-PSS/KY zeolite composites with 20% v/v zeolite content versus SO<sub>2</sub> concentration (7.8 - 1000 ppm) at 1 atm and at 27 ± 1 °C was shown in Figure 1. The lowest concentration level of SO<sub>2</sub> exposure gas limited by the measuring equipment is equal to 7.8 ppm. The change in electrical conductivity of both sensing materials varies linearly with the SO<sub>2</sub> concentration. The more SO<sub>2</sub> molecules promote the SO<sub>2</sub> interaction with PEDOT -PSS. The response time of both sensing materials also decreases with an increase in the SO<sub>2</sub> concentration. The both sensor materials were not capable of measuring concentrations of SO<sub>2</sub> concentration less than 125 ppm. No electrical conductivity changes were observed when concentration level of SO<sub>2</sub> exposure lower than 125 ppm. PEDOT-PSS with KY zeolite cover layers provide the larger conductivity change than the powder PEDOT-PSS/KY zeolite composites. The result suggests that the zeolite cover layers have more ability to attracting and releasing SO<sub>2</sub> molecules to interact with PEDOT-PSS than zeolite powder dispersed in PEDOT-PSS matrix.

### 6.4.2.2 *Effect of sulfur dioxide concentration*

The electrical sensitivity values of PEDOT-PSS<sub>1:1</sub> and its composites with the zeolite Y when exposed to air, N<sub>2</sub>, and SO<sub>2</sub> were measured under chamber temperature (T<sub>c</sub>) of 27 ± 1 °C, and at 1 atm. The electrical conductivity sensitivity values of the PEDOT-PSS with metal zeolite cover layer versus zeolite cover layer thickness in 1000 ppm SO<sub>2</sub>/N<sub>2</sub> are shown in Figure 2. All sensing materials exhibit negative responses to SO<sub>2</sub>. The thicknesses of zeolite cover layers for the best sensitivity have been optimized in the range of 0.1 – 0.5 mm. The sensitivity value of the PEDOT-PSS with metal zeolite cover layer is increases as the zeolite cover layer thickness decrease in the range of 0.1 – 0.25 mm. The thin of zeolite cover layer thickness increase



the possibilities of sulfur dioxide gas molecules to preconcentrate, result in the more gas molecules that moving to the PEDOT-PSS sensing layer. Despite that the sensitivity value decreases as the thickness of zeolite cover layer increases from 0.3 and 0.5 mm respectively. The more thickness of zeolite cover layers is applied; the diffusion barrier is present for gas molecule to moving to the PEDOT-PSS sensing layer. The results suggest that the PEDOT-PSS with a proper zeolite cover layer thickness can be used to promote the sensitivity response of PEDOT-PSS [12, 23-24].

The sensitivities response of PEDOT-PSS with metal zeolite Y cover layers were compared with PEDOT-PSS/MY zeolite composites in powder mixing compress form (KY, BaY and MnY). In order to compare their sensitivity response, we use the same amount of PEDOT-PSS and metal zeolite Y in each sample. In previous work, the results suggest that the addition of the zeolite Y to the pristine polymer PEDOT-PSS at the optimized combination (20% v/v zeolite Y content) can promote the electrical sensitivity response of the composites to SO<sub>2</sub> gas. The PEDOT-PSS with metal zeolite Y cover layers provide the higher sensitivities response than powder PEDOT-PSS/MY zeolite composites. The metal zeolite cover layers can induce and preconcentrate the gas molecule result in the more interaction between sulfur dioxide gas molecules and PEDOT-PSS. This result can be related to the more surface area of zeolite cover layer; this leads to a higher number of active sites available on the surface for the target gas molecules to diffuse deeper into the PEDOT-PSS sensing layer and this enhances the more interaction between the PEDOT-PSS and the SO<sub>2</sub> gas; the sensitivity increases more than the powder PEDOT-PSS/MY zeolite composites.

The response time and recovery time of sensing material sample were shown in Table 2. The temporal response time is the time required for the electrical conductivity value to rise from its initial value in N<sub>2</sub> towards the equilibrium value when exposed to SO<sub>2</sub>. The recovery time is the time required for the electrical conductivity value return to the initial value after the step removal of SO<sub>2</sub> [4-6]. The response and recovery times exhibited to increase with of the zeolite cover layer thickness. The zeolite

cover layer act as the diffusion barrier for sulfur dioxide gas molecule to diffuse to the PEDOT-PSS sensing layer [25-27]. The uses of zeolite cover layers produce a very longer recovery time responses; thus heat treatment is one possible way to recover the sensing material, but the change in electrical conductivity of the PEDOT-PSS and the stability of the PEDOT-PSS should be taken into consideration. Applied heat is lead to impractical for the fabrication and design of the sensor.

#### *6.4.2.3 The Proposed Mechanism of SO<sub>2</sub> Adsorption in PEDOT-PSS and Zeolite Y*

An observed electrical conductivity decrease can be attributed to the charge transfer due to the chemical nature of SO<sub>2</sub> gas. The conductivity of the conductive polymer is known to be due to the product between the charge carrier concentration and the charge carrier mobility along the polymer backbone. The reduction in the charge carrier concentration on the backbone of p-type PEDOT polymer occurs upon the electron transfer from SO<sub>2</sub> to the positive charged sulfur site on the polymer backbone. Therefore, the charge carrier concentration along the polymer backbone decreases resulting in the electrical conductivity decrease (Figure 5.6). The electrical conductivity of all composites return almost completely to their baselines after SO<sub>2</sub> is evacuated and replaced by N<sub>2</sub>. This result suggests that the weak interaction between SO<sub>2</sub> and the composites occurs. This also suggests that the interaction between SO<sub>2</sub> and MnY is not permanent. Most importantly, the interaction between SO<sub>2</sub> and the zeolite Y take place through the basic oxygen centers of the Si-O-Al fragment. An oxygen atom can form a bond with the sulfur atom of an SO<sub>2</sub> molecule via the donor-acceptor interaction. In addition to the charges on oxygen, other zeolite sites also interact with SO<sub>2</sub>, namely the bridging metal center via the ion-dipole interaction [28].

## 6.5 Conclusions

The metal zeolite Y layer can enhance the sensitivity response of PEDOT-PSS when exposed to sulfur dioxide gas. The PEDOT-PSS with zeolite cover layer provided the higher sensitivity response than the pristine PEDOT-PSS. The use of zeolite cover layer with 0.25 mm thickness provided the highest sensitivity response. The zeolite cover layer can preconcentrate the sulfur dioxide gas and this increase the probability of sulfur dioxide molecules that moving from zeolite layer to interact with the PEDOT-PSS sensing layer. Despite that the zeolite cover layer act as a diffusion barrier for gas molecules for moving to the PEDOT-PSS sensing layer typically led to increased response and recovery times as compared to the pristine PEDOT-PSS. The zeolite cover layer provided the longer recovery time than PEDOT-PSS/MY zeolite composites in powder mixing compress form and therefore, the sensing materials need for heat during recovery will add complication in device fabrication. Ongoing studied are there for aiming at investigating the selectivity improving of PEDOT-PSS by using the zeolite cover layer toward mixed gases in more deal with respect the different response to each type of gas.

## 6.6 Acknowledgements

The authors would like to acknowledge the financial supports from the Conductive and Electroactive Polymers Research Unit of Chulalongkorn University, the Thailand Research Fund (TRF-RTA and PhD/0082/2550), and the Royal Thai Government.

## 6.7 References

1. Adhikari, B. and Majumdar, S. (2004) Polymers in sensor applications. Progress in Polymer Science, 29, 699-766.
2. Bai, H. and Shi G. (2007) Gas sensors based on conducting polymers. Sensors, 7, 267-307.
3. Chandrasekhar, P. (2002) Conducting Polymers, Fundamentals and Applications: A practical Approach, Boston: Kluwer Academic Publishers.
4. Chuapradit, C., Wannatong, L.R., Chotpattananont, D., Hiamtup, P., Sirivat, A., and Schwank, J. (2005) Polyaniline/zeolite LTA composites and electrical conductivity response towards CO. Polymer, 46, 947-953.
5. Prissanaroon, W., Ruangchuay, L., Sirivat, A., and Schwank, J. (2000) Electrical conductivity response of dodecylbenzene sulfonic acid-doped polypyrrole films to SO<sub>2</sub>-N<sub>2</sub> mixtures. Synthetic Metals, 114, 65-72.
6. Soontornworajit, B., Wannatong, L., Hiamtup, P., Niamlang, S., Chotpattananont, D., Sirivat, A., and Schwank, J. (2007) Induced interaction between polypyrrole and SO<sub>2</sub> via molecular sieve 13X. Materials Science and Engineering B, 136, 78-86.
7. Watcharaphalakorn, S., Ruangchuay, L., Chotpattananont, D., Sirivat, A., and Schwank, J. (2005) Polyaniline/polyimide blends as gas sensors and electrical conductivity response to CO-N<sub>2</sub> mixtures. Polymer International, 54, 1126-1133.
8. Thuwachaowsoan, K., Chotpattananont, D., Sirivat, A., Rujiravanit, R., and Schwank, J.W. (2007) Electrical conductivity responses and interactions of poly(3-thiopheneacetic acid)/zeolites L, mordenite, beta and H<sub>2</sub>. Materials Science and Engineering B, 140, 23-30.
9. Densakulprasert, N., Wannatong, L., Chotpattananont, D., Hiamtup, P., Sirivat, A., and Schwank, J. (2005) Electrical conductivity of polyaniline/zeolite composites and synergetic interaction with CO. Materials Science and Engineering B, 117, 276-282.

10. Chanthaanont, P., and Sirivat, A. (2012) Interaction of carbon monoxide with PEDOT-PSS/Zeolite composite: Effect of Si/Al ratio of ZSM-5 zeolite. e-Polymers, 10, 1-11.
11. Gangopadhyay, R. and De, A. (2001) Conducting polymer composites: novel materials for gas sensing. Sensors and Actuators B, 77, 326-329.
12. Sahner, K., Schonauer, D., Moos, R., Matam, M., and Post, M.L. (2006) Effect of electrodes and zeolite cover layer on hydrocarbon sensing with *p*-type perovskite SrTi<sub>0.8</sub>Fe<sub>0.2</sub>O<sub>3</sub> thick and thin films. Journal of Materials Science, 41, 5828-5835.
13. Auerbach, S.M., Carrado, K.A., and Dutta, P.K. (2003) Handbook of Zeolite Science and Technology, New York: Marcel Dekker.
14. Dyer, A. (1988) An Introduction to Zeolite Molecular Sieves, Chichester: John Wiley & Son Ltd.
15. Breck, D.W. (1974) Zeolite Molecular Sieves: Structure, Chemistry, and Use, New York: Wiley.
16. Alvaro, M., Cabeza, J.F., Fabuel, D., García, H., Guijarro, E., and de-Juan, J.L.M. (2006) Electrical Conductivity of Zeolite Films: Influence of Charge Balancing Cations and Crystal Structure. Chemistry of Materials, 18, 26-33.
17. Louwet, F., Groenendaal, L., Dhaen, J., Manca, J., Van, Luppen J., Verdonck, E., and Leenders, L. (2003) PEDOT/PSS: synthesis, characterization, properties and applications. Synthetic Metals, 135-136, 115-117.
18. Thomas, B. and Sugunan, S. (2004) Influence of residual cations (Na<sup>+</sup>, K<sup>+</sup> and Mg<sup>2+</sup>) in the alkylation activity of benzene with 1-octene over rare earth metal ion exchanged FAU–Y zeolite. Microporous and Mesoporous Materials, 72, 227-238.
19. Martin, B.D., Nikolov, N., Pollack, S.K., Sapirgin, A., Shashidhar, R., Zhang, F., and Heiney, P.A. (2004) Hydroxylated secondary dopants for surface resistance enhancement in transparent poly(3,4-ethylenedioxythiophene)-poly(styrenesulfonate) thin films. Synthetic Metals, 142, 187-193.

20. Wichiansee, W. and Sirivat, A. (2009) Electrorheological properties of poly(dimethylsiloxane) and poly(3,4-ethylenedioxy thiophene)/poly(styrene sulfonic acid)/ethylene glycol blends. Materials Science and Engineering C, 29, 78-84.
21. Maurin, G., Llewellyn, P.L., Poyet, T., Kuchta, B. (2005) Adsorption of argon and nitrogen in X-faujasites: relationships for understanding the interactions with monovalent and divalent cations. Microporous and Mesoporous Materials, 79, 53-59.
22. Castaldi, P., Santona, L., Enzo, S., and Melis, P. (2008) Sorption processes and XRD analysis of a natural zeolite exchanged with Pb(2+), Cd(2+) and Zn(2+) cations. Journal of Hazardous Material, 156, 428-434.
23. Hugon, O., Sauvan, M., Benech, P., Pijolat, C., and Lefebvre, F. (2000) Gas separation with a zeolite filter, application to the selectivity enhancement of chemical sensors. Sensors and Actuators B, 67, 235-243.
24. Limtrakul, J., Khongpracha, P., Jungsuttiwong, S., and Truong, T. (2000) Adsorption of carbon monoxide in H-ZSM-5 and Li-ZSM-5 zeolites: an embedded cluster study. Journal of Molecular Catalysis A, 153, 155-163.
25. Vilaseca, M., Coronas, J., Cirera, A., Cornet, A., Morante, J.R., and Santamaria, J. (2003) Use of zeolite films to improve sensitivity of reactive gas sensors. Catalysis Today, 82, 179-185.
26. Xu, X.W., Wang, J., and Long, Y.C. (2005) Nano-tin dioxide/NaY zeolite composite material: Preparation, morphology, adsorption and hydrogen sensitivity. Microporous Mesoporous Material, 83, 60-66.
27. Xu, X., Wang, J., and Long, Y. (2006) Zeolite-based materials for gas sensors. Sensors, 6, 1751-1764.

**Table 6.1** Physicochemical properties of zeolite Y

	<b>NaY<sup>a</sup></b>	<b>KY</b>	<b>BaY</b>	<b>MnY</b>
<b>Zeolite structure</b>	FAU	FAU	FAU	FAU
<b>Pore size (nm)</b>	0.74 × 0.74	0.74 × 0.74	0.74 × 0.74	0.74 × 0.74
<b>Surface area (m<sup>2</sup>/g)</b>	800	772	847	811
<b>Pore volume (cm<sup>3</sup>/g)</b>	0.2476	0.2224	0.2421	0.2645
<b>% Cation Exchange</b>	-	88	89	84
<b>Cation ionic radius (Å)</b>	0.97	1.38	1.35	0.91
<b>EN of Cation (Pauling)</b>	0.93	0.82	0.89	1.55
<b>σ (10<sup>-3</sup> S/cm)<sup>b</sup></b>	2.69 ± 0.417	2.18 ± 0.378	1.99 ± 0.035	2.30 ± 0.428

<sup>a</sup> Zeolite based for cation exchange process

**Table 6.2** Response time and Recovery time of PEDOT-PSS, PEDOT-PSS with MY zeolite cover layer and PEDOT-PSS/MY composite (20% v/v zeolite content) when exposed to SO<sub>2</sub> at 27±1 °C and 1 atm.

Time (min)	PEDOT-PSS	KY		BaY		MnY	
		Layer	Mixed	Layer	Mixed	Layer	Mixed
Response	4.5	8.3	6.1	9.1	7.3	9.3	8.2
Recovery	9.2	16.4	11.2	15.2	12.5	17.8	12.8



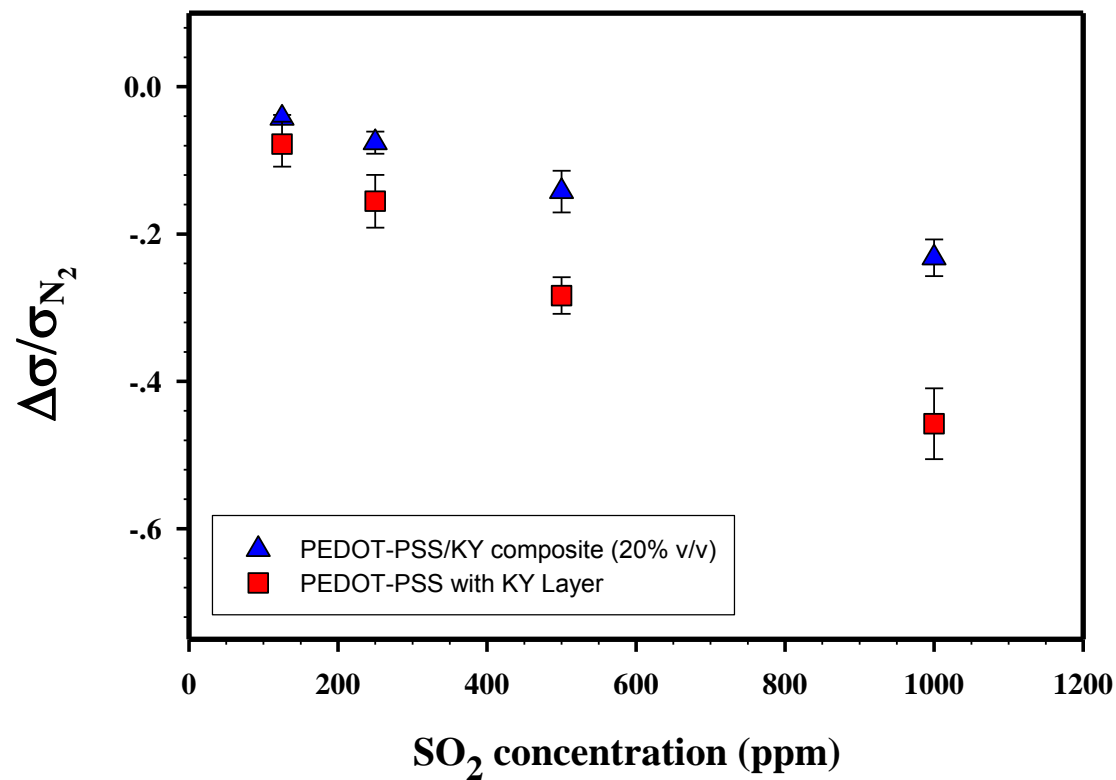


**Figure 6.1** Dependence of conductivity change on SO<sub>2</sub> concentration of PEDOT-PSS with KY zeolite cover layer and PEDOT-PSS/KY composite (20% v/v zeolite content) at temperature (T<sub>c</sub>) of 27 ± 1 °C, and at 1 atm.

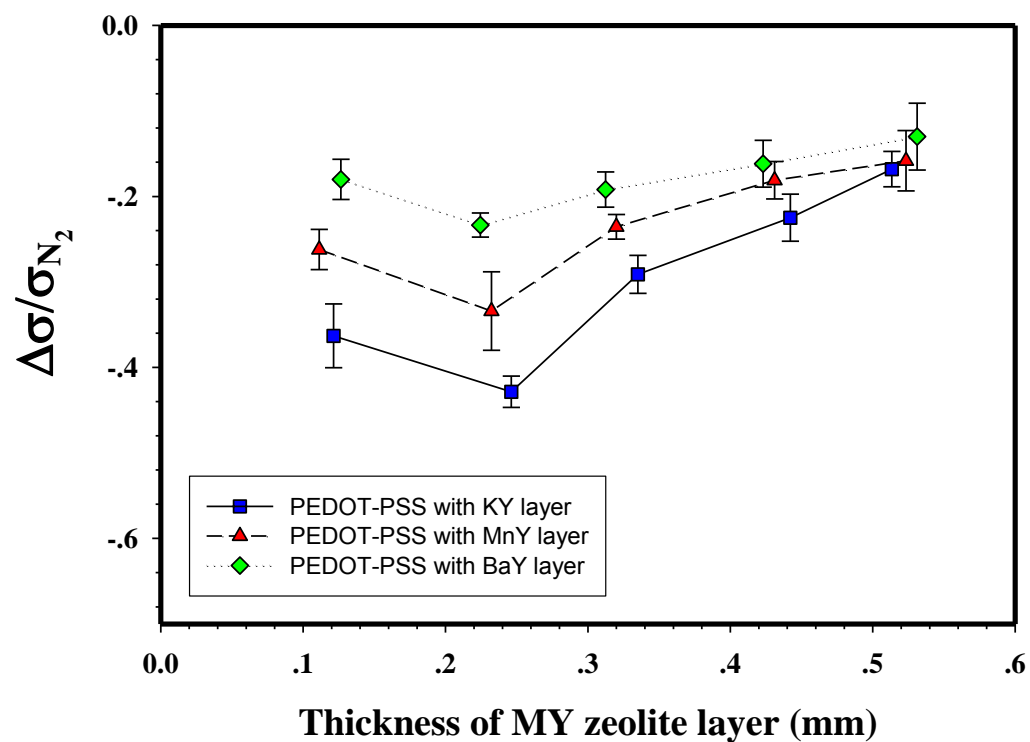


**Figure 6.2** The electrical conductivity sensitivity of PEDOT-PSS and PEDOT-PSS with MY zeolite cover layer at various zeolite cover layer thickness when exposed to  $SO_2$  at  $27\pm 1$  °C and 1 atm.

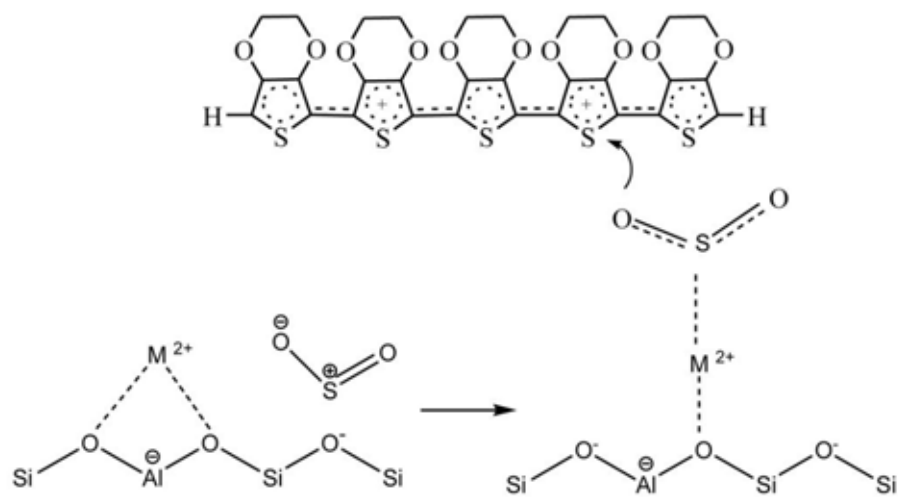


**Figure 6.3** A schematic diagram indicates possibility of electrostatic interactions between  $SO_2$ , Zeolite Y and PEDOT-PSS.

## CHAPTER VII

### CONCLUSIONS AND RECOMMENDATIONS

#### 7.1 Conclusions

The present work investigated the potential of PEDOT-PSS/zeolite composites as gas sensing material to be used for sensor applications. Poly(3,4-ethylenedioxythiophene) doped with poly(styrene sulfonic acid), PEDOT-PSS, was successfully synthesized via oxidative polymerization at various EDOT to PSS mole ratios. The specific electrical conductivity of the PEDOT-PSS increases with EDOT:PSS mole ratio due to the reduction of the insulating PSS shell surrounding the conducting PEDOT-PSS grains, which improves the pathways for charge transport. The concentration of zeolite component was investigated because it can be influential in the electrical conductivity of conducting polymer composites. The preparations of the composite with 20% (v/v) of zeolite content (zeolite ZSM-5 or zeolite Y) give the highest sensitivity to both analyte gases (CO or SO<sub>2</sub>). The composites with PEDOT-PSS as the matrix containing ZSM-5 zeolites of various Si/Al ratios (23-280) at 20% (v/v) were used to investigate the electrical conductivity sensitivity responses towards CO. The specific electrical conductivity of ZSM-5 increases with decreasing Si/Al mole ratios. The electrical conductivity sensitivity of PEDOT-PSS\_1:1/zeolite ZSM-5 composites towards CO negatively increases with decreasing Si/Al mole ratio of the ZSM-5 zeolite. PEDOT-PSS\_1:1/ZSM-5(Si/Al = 23) has the highest electrical conductivity sensitivity response. The addition of ZSM-5 enhances the interaction between the PEDOT-PSS and CO gas, a desired characteristic of the zeolites. However, the composites produce irreversible responses; thus further work is required before it can be used as a CO sensing material. Heat treatment is one possible way to regenerate or to renew the sensing material, but the change in electrical conductivity of the PEDOT-PSS and the stability of the PEDOT-PSS should be taken into consideration.

The electrical sensitivity of pristine PEDOT-PSS can be improved by adding zeolite Y but provided the longer response time and recovery time. The type of

cation in zeolite pores can effect to the sensitivity of the composite and consistent with the acidity of ion-exchanged zeolite Y. The composite showed reversibility almost completely at room temperature. The experimental results show that the zeolite acid-base properties play an important role in the sensitivity response of the composite toward SO<sub>2</sub>. With increasing the basicity of ion-exchanged zeolite Y, the sensitivity of the composites increase

An adjusted combination of the composite between PEDOT-PSS and Zeolite Y produces some remarkable changes in the composite electrical conductivity response. The results suggest that the addition of Zeolite Y to the pristine polymer PEDOT-PSS at the optimized combination can promote the electrical sensitivity response of the composites to SO<sub>2</sub> gas. The metal cation in zeolite Y intimately induces a synergism to adsorb SO<sub>2</sub>, but at the expense of the longer response time and recovery time. The exchanged of transition metal cations can enlarge the pore volume of zeolites. Therefore, the target gas SO<sub>2</sub> can further introduce to interact with PEDOT-PSS polymer. In the presence of the transition metal cations, with respect to the zeolite micropores, the cations can influence the adsorption properties of the system. The electrical sensitivity of the composite can be correlated with with the electronegativity of the transition metal cations of the-exchanged zeolite Y. The reproducibility of the composite response can be observed and the response is nearly reversible at room temperature.

The metal zeolite Y layer can enhance the sensitivity response of PEDOT-PSS when exposed to sulfur dioxide gas. The PEDOT-PSS with zeolite cover layer provided the higher sensitivity response than the pristine PEDOT-PSS. The use of zeolite cover layer with 0.25 mm thickness provided the highest sensitivity response. The zeolite cover layer can preconcentrate the sulfur dioxide gas and this increase the probability of sulfur dioxide molecules that moving from zeolite layer to interact with the PEDOT-PSS sensing layer. Despite that the zeolite cover layer act as a diffusion barrier for gas molecules for moving to the PEDOT-PSS sensing layer typically led to increased response and recovery times as compared to the pristine PEDOT-PSS.

## **7.2 Recommendations**

In this work, the gas sensing properties has been carried out in nitrogen atmosphere. In regular condition, there are many effective factors which can affect the sensitivity response of gas sensor material. The atmospheric gases and humidity variations are the important factors which may distort the expected reaction of sensor materials toward the target gas. The effect of atmospheric gases and humidity on the sensing performance of conductive polymer/zeolite composites based gas sensor is interesting for further investigation. Future more, the selectivity of sensing material is one of the interesting approaches which may improve by zeolite microporous material. The more experiment have to investigate to achieved this goal.

## REFERENCES

- Adhikari, B. and Majumdar, S. (2004) Polymers in sensor applications. Progress in Polymer Science, 29, 699-766.
- Alvaro, M., Cabeza, J.F., Fabuel, D., García, H., Guijarro, E., and de-Juan, J.L.M. (2006) Electrical Conductivity of Zeolite Films: Influence of Charge Balancing Cations and Crystal Structure. Chemistry of Materials, 18, 26-33.
- Auerbach, S.M., Carrado, K.A., and Dutta, P.K. (2003) Handbook of Zeolite Science and Technology, New York: Marcel Dekker.
- Bai, H. and Shi G. (2007) Gas sensors based on conducting polymers. Sensors, 7, 267-307.
- Bavastrelloa, V., Erokhina, V., Carraraa, S., Sbranab, F., Riccib, D., and Nicolini, C. (2004) Morphology and conductivity in poly(ortho-anisidine)/carbon nanotubes nanocomposite films. Thin Solid Films, 468, 17-22.
- Bhambare, K.S., Gupta, S., Mench, M.M., and Ray, A. (2008) A carbon monoxide sensor in polymer electrolyte fuel cells based on symbolic dynamic filtering. Sensors and Actuators B, 134, 803-815.
- Bhat, N.V., Gadre, A.P., and Bambole, V.A. (2003) Investigation of electropolymerized polypyrrole composite film: Characterization and application to gas Sensors. Journal of Applied Polymer Science, 88, 22-29.
- Breck, D.W. (1974) Zeolite Molecular Sieves: Structure, Chemistry, and Use, New York: Wiley.
- Chandrasekhar, P. (2002) Conducting Polymers, Fundamentals and Applications: A practical Approach, Boston: Kluwer Academic Publishers.
- Chanthaanont, P., and Sirivat, A. (2012) Interaction of carbon monoxide with PEDOT-PSS/Zeolite composite: Effect of Si/Al ratio of ZSM-5 zeolite. e-Polymers, 10, 1-11.
- Chen, Y., Li Y., Wang, H., and Yang, M. (2007) Gas sensitivity of a composite of multi-walled carbon nanotubes and polypyrrole prepared by vapor phase polymerization. Carbon, 45, 357-363.

- Chuapradit, C., Wannatong, L.R., Chotpattananont, D., Hiamtup, P., Sirivat, A., and Schwank, J. (2005) Polyaniline/zeolite LTA composites and electrical conductivity response towards CO. Polymer, 46, 947-953.
- Chun, L. and Imae, T. (2004) Electrochemical and Optical Properties of the Poly(3,4-ethylenedioxythiophene) Film Electropolymerized in an Aqueous Sodium Dodecyl Sulfate and Lithium Tetrafluoroborate Medium. Macromolecules, 37, 2411-2416.
- Conn, C., Sestak, S., Baker, A.T., and Unsworth, J. (1998) A polyaniline-based selective hydrogen sensors. Electroanalysis, 10, 1735-1738.
- Costa, C., Dzikh, I.P., Lopes, J.M., and Lemos, F. (2000) Activity-acidity relationship in zeolite ZSM-5. Application of Brønsted-type equations. Journal of Molecular Catalysis A, 154, 193-201.
- Densakulprasert, N., Wannatong, L., Chotpattananont, D., Hiamtup, P., Sirivat, A., and Schwank, J. (2005) Electrical conductivity of polyaniline/zeolite composites and synergetic interaction with CO. Materials Science and Engineering B, 117, 276-282.
- Dixit, V., Misra, S.C.K., and Sharma, B.S. (2005) Carbon monoxide sensitivity of vacuum deposited polyaniline semiconducting thin films. Sensors and Actuators B, 104, 90-93.
- Dyer, A. (1988) An Introduction to Zeolite Molecular Sieves, Chichester: John Wiley & Son Ltd.
- Enzel, P. and Bein, T. (1989) Inclusion of polyaniline filaments in zeolite molecular sieves. The Journal of Physical Chemistry, 93, 6270-6272.
- Fang, Y. K. and Lee, J. J. (1989) A tin oxide thin film sensor with high ethanol sensitivity. Thin Solid Films, 169, 51-56.
- Farkas, A.P., and Solymosi, F. (2007) Adsorption and reactions of ethanol on Mo<sub>2</sub>C/Mo (100). Surface Science, 601, 193-200.
- Gangopadhyay, R. and De, A. (2001) Conducting polymer composites: novel materials for gas sensing. Sensors and Actuators B, 77, 326-329.
- Garreau, S., Louarn, G., Buisson, J.P., Froyer, G., and Lefrant, S. (1999) In Situ Spectroelectrochemical Raman Studies of Poly (3,4-ethylenedioxythiophene)(PEDT). Macromolecules, 32, 6807-6812.



- Groenendaal, L., Jonas, F., Freitag, D., Pielartzik, H., and Rynolds, J.R. (2000) Poly(3,4-ethylenedioxythiophene) and its derivatives: Past, present, and future. Advance Materials, 12, 482-494.
- Guernion, N., de Lacy Costello, B.P.J., and Ratcliffe, N.M. (2002) The synthesis of 3-octadecyl- and 3-docosylpyrrole, their polymerisation and incorporation into novel composite gas sensitive resistors. Synthetic Metals, 128, 139-147.
- Gustafsson, G. and Lundstrom, I. (1987) The effect of ammonia on the physical properties of polypyrrole. Synthetic Metals, 21, 203-208.
- Han, D., Yang, G., Song, J., Niu, L., and Ivaska, A. (2007) Morphology of electrodeposited poly(3,4-ethylenedioxythiophene)/poly(4-styrene sulfonate) films. Journal of Electroanalytical Chemistry, 602, 24-28.
- Hanawa, T. and Yoneyama, H. (1989) Gas sensitiveness of polypyrrole films doped chemically in the gas phase. Synthetic Metals, 30, 341-350.
- Hanawa, T., Kuwabata, S., Hashimoto, H., and Yoneyama, H. (1989) Gas sensitivities of electropolymerized polythiophene films. Synthetic Metals, 30, 173-181.
- Hong, K.H., Oh, K.W., and Kang, T.J. (2004) Polyaniline-Nylon 6 composite fabric for ammonia gas sensor. Journal of Applied Polymer Science, 92, 37-42.
- Hosseini, S. H. and Entezami, A.A. (2003) Conducting polymer blends of polypyrrole with polyvinyl acetate, polystyrene, and polyvinyl chloride based toxic gas sensors. Journal of Applied Polymer Science, 90, 49-62.
- Huang, H., Zhou, J., Chen, S., Zeng, L., and Huang, Y. (2004) A highly sensitive QCM sensor coated with Ag<sup>+</sup>-ZSM-5 film for medical diagnosis. Sensors and Actuators B, 101, 316-321.
- Jang, J. and Bae, J. (2006) Carbon nanofiber/polypyrrole nanocable as toxic gas sensor. Sensors and Actuators B, 122, 7-13.
- Jonsson, S.K.M., Birgeron, J., Crispin, X., Greczynski, G., Osikowicz, W., van der Gon, A.W.D., Salaneck, W.R., and Fahlman, M. (2003) The effects of solvents on the morphology and sheet resistance in poly(3,4-ethylenedioxythiophene)-polystyrenesulfonic acid (PEDOT-PSS) films. Synthetic Metals, 139, 1-10.

- Kiebooms, R., Aleshin, A., Hutchison, K., Wudl, F., and Heeger, A. (1999) Doped Poly(3,4-ethylenedioxythiophene) Films: Thermal, Electromagnetical and Morphological Analysis. Synthetic Metals, 101, 436-437.
- Kumar, D. and Sharma, R.C. (1998) Advance in conductive polymers. European Polymer Journal, 34, 1053-1060.
- Lange, U., Roznyatovskaya, N.V., and Mirsky, V.M. (2008) Conducting polymers in chemical sensors and arrays. Analytica Chimica Acta, 614, 1-26.
- Limtrakul, J., Khongpracha, P., Jungstittiwong, S., and Truong, T. (2000) Adsorption of carbon monoxide in H-ZSM-5 and Li-ZSM-5 zeolites: an embedded cluster study. Journal of Molecular Catalysis A, 153, 155-163.
- Louwet, F., Groenendaal, L., Dhaen, J., Manca, J., Van, Luppen J., Verdonck, E., and Leenders, L. (2003) PEDOT/PSS: synthesis, characterization, properties and applications. Synthetic Metals, 135-136, 115-117.
- Martin, B.D., Nikolov, N., Pollack, S.K., Saprigin, A., Shashidhar, R., Zhang, F., and Heiney, P.A. (2004) Hydroxylated secondary dopants for surface resistance enhancement in transparent poly(3,4-ethylenedioxythiophene)-poly(styrenesulfonate) thin films. Synthetic Metals, 142, 187-193.
- Mathur, S.C.K., Mathur P., and Srivastava B.K. (2004) Vacuum-deposited nanocrystalline polyaniline thin film sensors for detection of carbon monoxide. Sensors and Actuators A. 114, 30-35.
- McCullough, R. D. (1998) The Chemistry of conducting polythiophenes, Advanced Materials, 10, 93-116.
- Miasik, J., Hooper, A., and Tofield, B. (1986) Conducting polymer gas sensors. Journal of Chemistry Society, 82, 1117-1126.
- Mohammad, F. (1998) Compensation behaviour of electrically conductive polythiophene and polypyrrole. Journal of Physics D: Applied Physics, 31, 951-959.
- Niu, X., Zhong, H., Wang, X., and Jiang, K. (2006) Sensing properties of rare earth oxide doped In<sub>2</sub>O<sub>3</sub> by a sol-gel method. Sensors and Actuators B, 115, 434-438.

- Pijolat, C., Pupier, C., Sauvan, M., Tournier, G., and Lalauze, R. (1999) Gas detection for automotive pollution control. Sensors and Actuators B, 59, 195-202.
- Prissanaroon, W., Ruangchuay, L., Sirivat, A., and Schwank, J. (2000) Electrical conductivity response of dodecylbenzene sulfonic acid-doped polypyrrole films to SO<sub>2</sub>-N<sub>2</sub> mixtures. Synthetic Metals, 114, 65-72.
- Rajesh, Ahuja, T., and Kumar, D., (2009) Recent progress in the development of nano-structured conducting polymers/nanocomposites for sensor applications. Sensors and Actuators B, 136, 275-286.
- Ram, M. K., Yavuz, O., and Aldissi, M. (2005) NO<sub>2</sub> gas sensing based on ordered ultrathin films of conducting polymer and its nanocomposite. Synthetic Metals, 151, 77-84.
- Ram, M.K., Yavuz, O., Lahsangah, V., and Aldissi, M. (2005) CO gas sensing from ultrathin nano-composite conducting polymer film. Sensors and Actuators B, 106, 750-757.
- Rauch, W.L., and Liu, M. (2003) Development of a selective gas sensor utilizing a perm-selective zeolite membrane. Journal of Materials Science, 38, 4307-4317.
- Reemts, J., Parisi, J., and Schlettwein, D. (2004) Electrochemical growth of gas-sensitive polyaniline thin films across an insulating gap. Thin Solid Films, 466, 320-325.
- Rosa, R.M., Szulc, R.L., Li, R.W.C., and Gruber, J. (2005) Conducting polymer-based chemiresistive sensor for organic vapours. Die Makromolekulare Chemie: Macromolecular Symposia, 229, 138-142.
- Sahner, K., Schonauer, D., Moos, R., Matam, M., and Post, M.L. (2006) Effect of electrodes and zeolite cover layer on hydrocarbon sensing with *p*-type perovskite SrTi<sub>0.8</sub>Fe<sub>0.2</sub>O<sub>3</sub> thick and thin films. Journal of Materials Science, 41, 5828-5835.
- Sakurai, Y., Jung, H-S., Shimanouchi, T., Inoguchi, T., Morita, S., Kuboi, R., and Natsukawa, K. (2002) Novel array-type gas sensors using conducting

- polymers, and their performance for gas identification. Sensors and Actuators B, 83, 270-275.
- Saxena, V. and Malhotra B.D. (2003) Prospects of conducting polymers in molecular electronics. Current Applied Physics, 3, 293-305.
- Schaf, O., Wernert, V., Ghobarkar, H., and Knauth, P. (2006) Microporous stilbite single crystals for alcohol sensing. Journal of Electroceramics, 16, 93-98.
- Shirakawa, H., Louis, E.J., MacDiarmid, A.G., Chiang, C.K., and Heeger, A.J. (1977) Synthesis of electrically conducting organic polymers: Halogen derivatives of polyacetylene,(CH)<sub>x</sub>. Journal of the Chemical Society, Chemical Communications, 578-580.
- Soontornworajit, B., Wannatong, L., Hiamtup, P., Niamlang, S., Chotpattananont, D., Sirivat, A., and Schwank, J. (2007) Induced interaction between polypyrrole and SO<sub>2</sub> via molecular sieve 13X. Materials Science and Engineering B, 136, 78-86.
- Srivastava, A., Jain, K., Rashmi, Srivastava, A.K., and Lakshmikumar, S.T. (2006) Study of structural and microstructural properties of SnO<sub>2</sub> powder for LPG and CNG gas sensors. Materials Chemistry and Physics, 97, 85-90.
- Stankova, M., Vilanova, X., Llobet, E., Calderer, J., Vinaixa, M., Gracia, I., Cane, C., and Correig, X. (2006) On-line monitoring of CO<sub>2</sub> quality using doped WO<sub>3</sub> thin film sensors. Thin Solid Films, 500, 302-308.
- Thuwachaowsoan, K., Chotpattananont, D., Sirivat, A., Rujiravanit, R., and Schwank, J.W. (2007) Electrical conductivity responses and interactions of poly(3-thiopheneacetic acid)/zeolites L, mordenite, beta and H<sub>2</sub>. Materials Science and Engineering B, 140, 23-30.
- Torsi, L., Pezzuto, M., Siciliano, P., Rella, R., Sabbatini, L., Valli, L., and Zambonin, P.G. (1998) Conducting polymers doped with metallic inclusions: New materials for gas sensors. Sensors and Actuators B, 48, 362-367.
- Trivedi, D. C. (1997) Handbook of Organic Conductive Molecules and Polymers, Chichester: Wiley.
- Vacca, P., Petrosino, M., Miscioscia, R., Nenna, G., Minarini, C., Sala, D.D., and Rubino, A. (2008) Poly(3,4-ethylenedioxythiophene): poly(4-

- styrenesulfonate) ratio: Structural, physical and hole injection properties in organic light emitting diodes. Thin Solid Films, 516, 4232-4237.
- Vilaseca, M., Yague, C., Coronas, J., and Santamaria, J. (2006) Development of QCM sensors modified by  $\text{AlPO}_4$ -18 films, Sensors and Actuators B, 117, 143-150.
- Vilaseca, M., Coronas, J., Cirera, A., Cornet, A., Morante, J.R., and Santamaria, J. (2003) Use of zeolite films to improve sensitivity of reactive gas sensors. Catalysis Today, 82, 179-185.
- Wagh, M.S., Jain, G.H., Patil, D.R., Patil, S.A., and Patil, L.A. (2006) Modified zinc oxide thick film resistors as  $\text{NH}_3$  gas sensor. Sensors and Actuators B, 115, 128-133.
- Warnken, M., Lazar, K., and Wark, M. (2001) Redox behaviour of  $\text{SnO}_2$  nanoparticles encapsulated in the pores of zeolites towards reductive gas atmospheres studied by in situ diffuse reflectance UV/Vis and Mossbauer spectroscopy. Physical Chemistry Chemical Physics, 3, 1870-1876.
- Watcharaphalakorn, S., Ruangchuay, L., Chotpattananont, D., Srivat, A., and Schwank, J. (2005) Polyaniline/polyimide blends as gas sensors and electrical conductivity response to  $\text{CO-N}_2$  mixtures. Polymer International, 54, 1126-1133
- Wichiansee, W. and Srivat, A. (2009) Electrorheological properties of poly(dimethylsiloxane) and poly(3,4-ethylenedioxy thiophene)/poly(styrene sulfonic acid)/ethylene glycol blends. Materials Science and Engineering C, 29, 78-84.
- Wu, C.G. and Bein, T. (1994) Conducting polyaniline filaments in mesoporous channel host. Science, 264, 1757-1759.
- Xie, D., Jiang, Y., Pan, W., Li, D., Wu, Z., and Li, Y. (2002) Fabrication and characterization of polyaniline-based gas sensor by ultra-thin film technology. Sensors and Actuators B, 81, 158-164.
- Xu, X.W., Wang, J., and Long, Y.C. (2005) Nano-tin dioxide/ $\text{NaY}$  zeolite composite material: Preparation, morphology, adsorption and hydrogen sensitivity. Microporous Mesoporous Material, 83, 60-66.

- Xu, X., Wang, J., and Long, Y. (2006) Zeolite-based materials for gas sensors. Sensors, 6, 1751-1764.
- Yang, Y., Jiang, Y., Jianhua, X., and Junsheng, Y. (2007) Conducting polymeric nanoparticles synthesized in reverse micelles and their gas sensitivity based on quartz crystal microbalance. Polymer, 48, 4459-4465.
- Zhu, W., Tan, O.K., Yan, Q., and Oh, J.T. (2000) Microstructure and hydrogen gas sensitivity of amorphous (Ba,Sr)TiO<sub>3</sub> thin film sensors. Sensors and Actuators B, 65, 366-370.
- Zhou, J., Li, P., Zhang, S., Long, Y., Zhou, F., Huang, Y., Yang, P., and Bao, M., (2003) Zeolite-modified microcantilever gas sensor for air indoor quality control. Sensors and Actuators B, 94, 337-342.

## CURRICULUM VITAE

**Name:** Ms. Pojjawan Chanthaanont

**Date of Birth:** January 19, 1982

**Nationality:** Thai

**University Education:**

2002–2005 Bachelor Degree of Chemistry, Faculty of Science, Srinakarinwirot University, Bangkok, Thailand

**Publications:**

1. Chanthaanont, P.; and Sirivat, A. (2012) Interaction of carbon monoxide with PEDOT-PSS/Zeolite composite: Effect of Si/Al ratio of ZSM-5 zeolite, *Polymers*.
2. Yimlamai, I.; Niamlang, S.; Chanthaanont, P.; Kunanuraksapong, R.; Changkhamchom, S.; and Sirivat, (2011) A. Electrical Conductivity Response and Sensitivity of ZSM-5, Y, and Mordenite Zeolites towards Ethanol Vapor, *Ionics*.
3. Konkayan S.; Chanthaanont, P.; Prissanaroon, W.; Hormnirun, P.; and Sirivat, A. (2013) Ammonia sensing and electrical properties based on composite of poly(3-thiopheneacetic acid) and zeolite Y, *Materials Technology: Advanced Performance Materials*.
4. Chanthaanont, P.; and Sirivat, A. Effect of Transition Metal Ion-exchanged into the Zeolite Y on Electrical Conductivity and Response of PEDOT-PSS/MY Composites toward SO<sub>2</sub>". Revisions Being Processed, *Advances in Polymer Technology*.
5. Chanthaanont, P.; and Sirivat, A. Effect of Alkaline and Alkaline Earth Ion-exchanged Zeolites Y on Electrical Conductivity and Response of PEDOT-PSS/Zeolite Y Composites toward SO<sub>2</sub>. Submission Being Processed.
6. Chanthaanont, P.; and Sirivat, Effect of Metal Exchanged Zeolite Y Cover Layer on Electrical Conductivity Response of PEDOT-PSS and Their Sulfur Dioxide Sensing Properties. Submission Being Processed.

**Proceedings:**

1. Chanthanont, P., Sirivat, A. (2009, March 8-12) Carbon monoxide sensitivity detection by PEDOT-PSS/zeolite composites gas sensing materials. SPIE Smart Sensor Phenomena, Technology, Networks, and Systems, San Diego, CA, USA.

**Presentations:**

1. Chanthanont, P.; and Sirivat, A. (2010, April 1-3) Electrical Conductivity Response of PEDOT-PSS/Zeolite to SO<sub>2</sub>. Oral presented at the RGJ-Ph.D. Congress XI, Pattaya, Chonburi, Thailand.
2. Chanthanont, P.; and Sirivat, A. (2008, March 10-14) Development of PEDOT-PSS/Zeolite Composites as a Gas Sensor. Poster presented at the 2008 APS March Meeting, New Orleans, Louisiana, USA.
3. Chanthanont, P.; and Sirivat, A. (2008, April 22-25) Preparation of PEDOT-PSS/Zeolite Composite as a Gas Sensor. Poster presented at the Smart/Intelligent Materials And Nano Technology 2008 & 2<sup>nd</sup> International workshop on Functional Materials and nanomaterials (SmartMat'08-IWOFM-2), Chiang Mai, Thailand.
4. Chanthanont, P.; and Sirivat, A. (2008, August 19-20) PEDOT-PSS/zeolite ZSM-5 composites as gas sensing materials. Poster presented at the Thai-Japan Joint Symposium on Advances in Materials Science and Environmental Technology, Bangkok, Thailand.
5. Chanthanont, P.; and Sirivat, A. (2008, November 6-8) Gas sensing property of PEDOT-PSS-Zeolite composites. Poster presented at the Nano Thailand Symposium 2008 (NTS 2008) International Conference & Exhibition, Bangkok, Thailand.
6. Chanthanont, P.; and Sirivat, A. (2009, March 16-20) Sensitivity Enhancement of PEDOT-PSS towards CO by Zeolite ZSM-5 Additive. Poster presented at the APS March Meeting 2009, Pittsburgh, Pennsylvania, USA.
7. Chanthanont, P.; and Sirivat, A. (2009, August 7) PEDOT-PSS/zeolite ZSM-5 composites and electrical conductivity response towards CO, Poster presented at the RGJ Seminar Series LXII Advanced Materials, Bangkok, Thailand.



8. Chanthanont, P.; and Sirivat, A. (2009, June 7-9) Electrical conductivity responses of PEDOT- PSS/zeolite composites towards CO. Poster presented at International Symposium Frontier in Polymer Science 2009, Mainz, Germany.
9. Chanthanont, P.; and Sirivat, A. (2011, May 29-31) Effect of Univalent Cation Exchanged Zeolites Y on Electrical Conductivity and Response of PEDOT- PSS/Zeolite Y Composites toward SO<sub>2</sub>. Poster presented at the Second International Symposium Frontier in Polymer Science 2011, Lyon, France.
10. Chanthanont, P.; and Sirivat, A. (2012, June 10-14) Electrical Conductivity and Response of PEDOT-PSS/Ion-Exchanged Zeolite Y Composites toward SO<sub>2</sub>. Poster presented at the 4<sup>th</sup> International Conference "Smart Materials, Structures and Systems CIMTEC 2012, Montecatini Terme, Italy.